‘Two-Phase Continuum Models for Geophysical Particle-Fluid Flows (Geoflo16)’, The Max Planck Institute for the Physics of Complex Systems, Dresden, Germany, March-April 2016

Mixing dynamics of turbidity currents interacting with complex seafloor topography

Mohamad M. Nasr-Azadani
Department of Mechanical Engineering

University of California, Santa Barbara

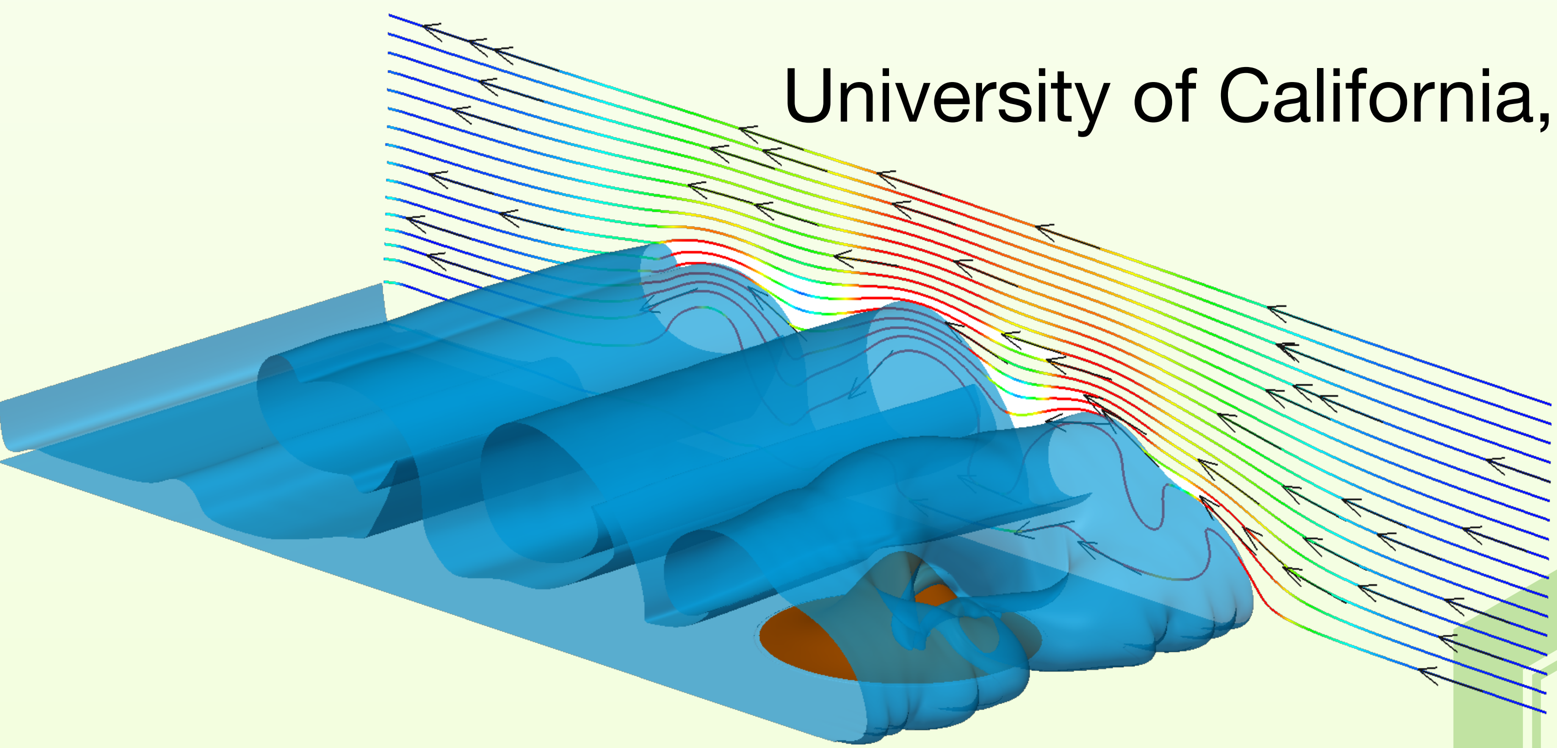

UC SANTA BARBARA engineering

Acknowledgment

C. Cenedese[5], K. Bhaganagar[1], R. Nokes[2] , J. Hyatt[3], M. Nayamatullah[1]
F. Testik[7]
E. Meiburg[4], S. Radhakrishnan[4], and B. Kneller[6]

[1] University of Texas at San Antonio, [2] University of Canterbury, [3] Massachusetts Maritime Academy,
[4] University of California at Santa Barbara, [5] Woods Hole Oceanographic Institute
[6] University of Aberdeen, [7] Clemson University

Introduction: Gravity currents

- Gravity currents form in nature and industrial settings
- Horizontal flows driven by hydrostatic horizontal density differences and the associated hydrostatic pressure gradients
- Encompass atmospheric and oceanic flows: sandstorms, powdersnow avalanches, pyroclastic flows, thunderstorm outflows, and turbidity currents

Sandstorm (haboob)

Sandstorm in Phoenix AZ. Courtesy of Andrew Pielage (http://apizm.com/)

Sandstorm (haboob)

Sandstorm in Phoenix AZ (2011). Courtesy of Mike Olbinski (http://www.mikeolbinski.com/)

Powdersnow avalanche

Avalanche in Mt. Logan in Canada. Courtesy of Jeffrey Levison

Pyroclastic flows

Left: Mount Pinatubo's eruption (Philippines) in 1991 (Photo by Alberto Garcia/Corbis available at http://www.guardian.co.uk/)

Right: Mount Merapi in central Java, Indonesia (AP Photo, available at http://www.commercialappeal.com/)

Pyroclastic flows

Mount Unzen, Japan (1991).

Turbidity currents

Los Cabos in Baja California, Mexico.
Movie by Andre Frota available at http://www.youtube.com/watch?v=ruC77oiGIiE

Turbidity currents: the Grand Banks landslide

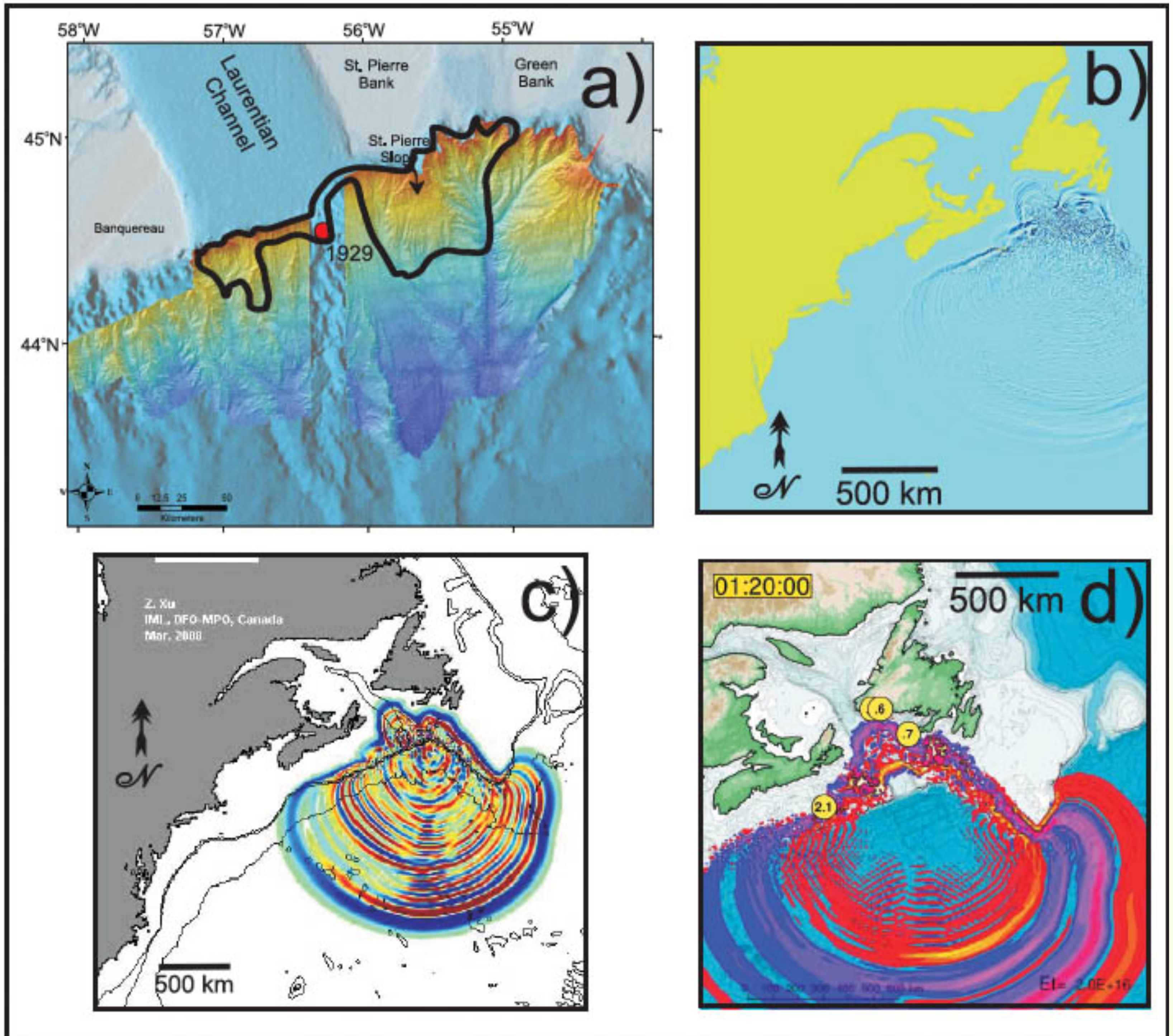

In 1929: 7.2 scale earthquake triggered a landslide. Transported O(200) km^3 sediment into deep-sea regions (≈ 800 km)

http://journals.hil.unb.ca/ocean

Turbidity currents: the Grand Banks landslide

Estimated velocity ≈ 15 – 50 mph (Heezen & Ewing (1952))

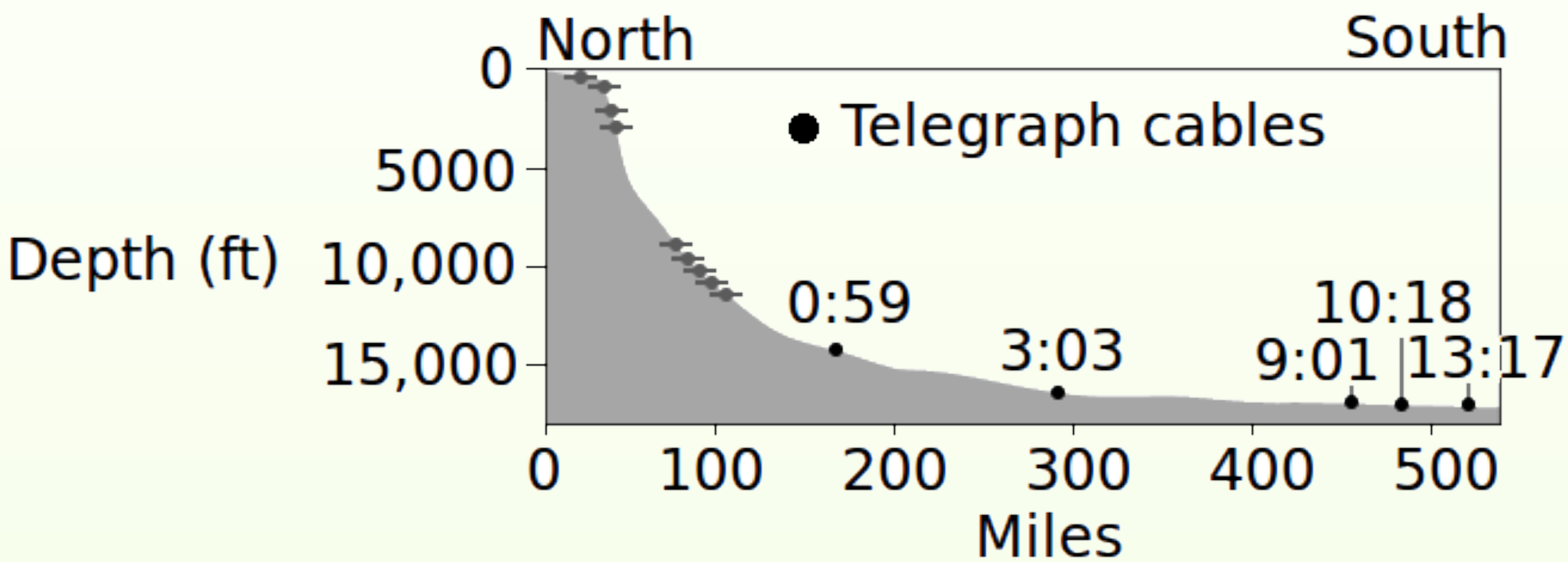

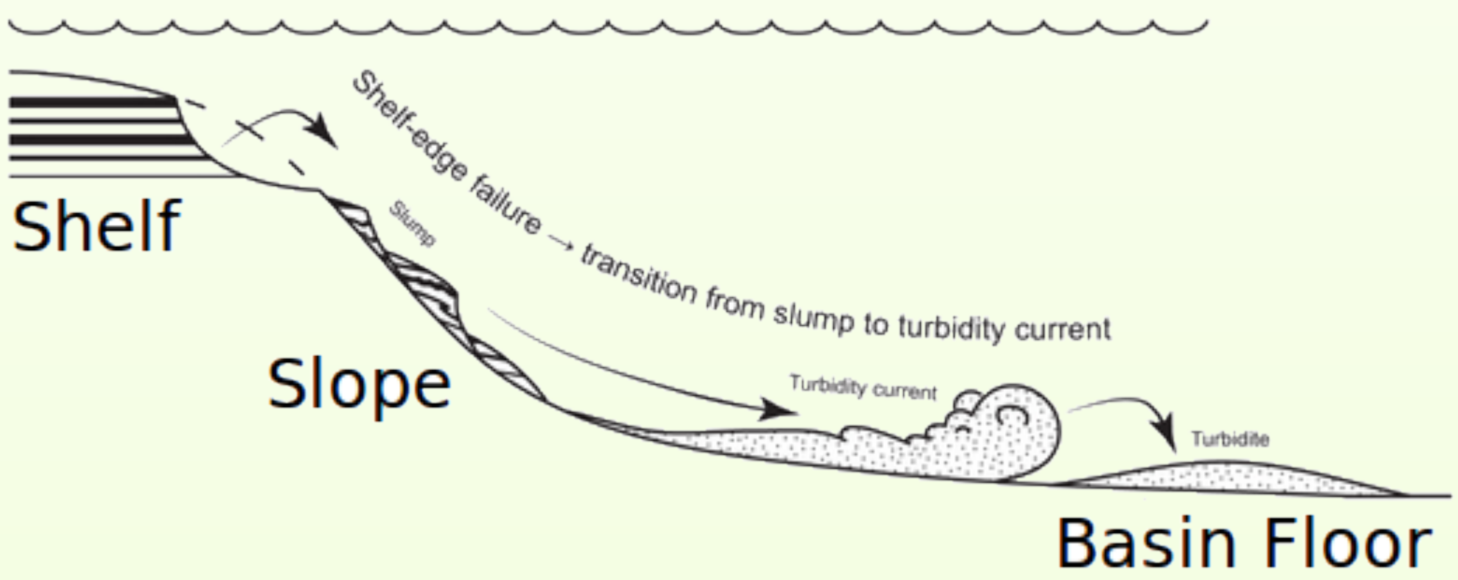

Top: Recorded times (hr:min) of disrupted telegraphs after the 1929 Grand Banks landslide (http://www.geol.lsu.edu/jlorenzo/
Bottom: Configuration of a turbidity current caused by a landslide (Covaul (2011), Nature)

Outline

- Direct Numerical Simulation of turbidity currents
- Investigate the mixing and 'unmixing' dynamics
- Evolution of interstitial fluid as current interacts with a seamount

- And more…

Problem setup

- Suspension : ‘lock-exchange’ configuration
- Complex topography: a Gaussian bump
- Two different particle sizes with identical densities

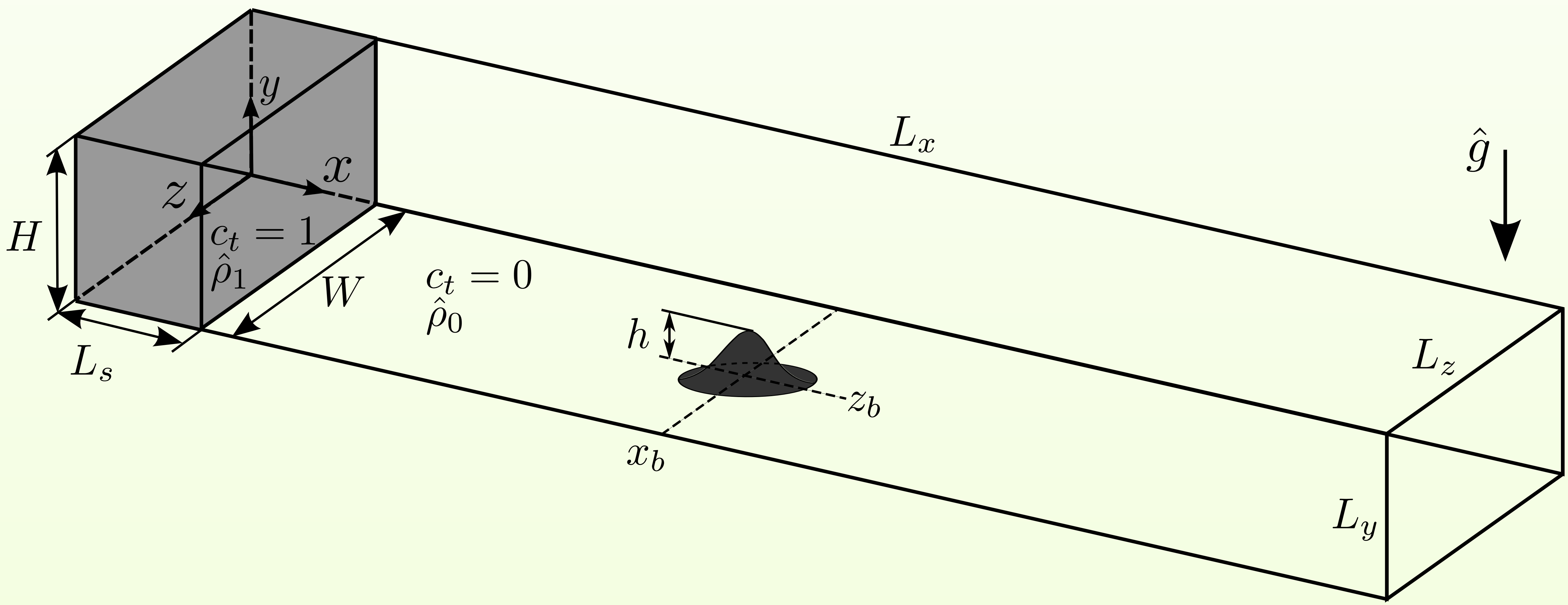

Basic assumptions

- Dilute suspension of particles: $\mathcal{O}(1)\%$ volume fractions
- No particle-particle interaction
- Incompressible flow with Boussinesq approximations
- No change in bottom bed height as particles settle out
- No erosion and/or bedload transport

Governing equations

Continuity:

$$\boldsymbol{\nabla} \cdot \mathbf{u} = 0$$

Momentum: Navier-Stokes equations with Boussinesq approximations

$$\frac{\partial \mathbf{u}}{\partial t} + \mathbf{u} \cdot \boldsymbol{\nabla} \mathbf{u} = -\boldsymbol{\nabla} p + \frac{1}{Re} \nabla^2 \mathbf{u} + \underbrace{c\mathbf{e}^g}_{\text{effective density}}$$

Particle transport: Small particles, neglect inertia

$$\frac{\partial c}{\partial t} + (\mathbf{u} + u_s \mathbf{e}^g) \cdot \boldsymbol{\nabla} c = \frac{1}{ScRe} \nabla^2 c$$

Important numbers

Reynolds number:

$$Re = \frac{u_b H/2}{\nu}$$

Particle settling speed:

$$u_s = \frac{U_s}{u_b}$$

Buoyancy velocity:

$$u_b = \sqrt{g \frac{\Delta \rho}{\rho_0} H/2}$$

Software code: TURBINS

- Viscous terms: Implicit second-order finite difference scheme
- Convective terms: Third-order ENO
- Time integration: Third-order TVD Runge-Kutta method
- To impose a divergence-free velocity field: Fractional projection method
- Complex topography: Immersed boundary method with direct forcing
- Domain decomposition approach using MPI
- Parallel Krylov iterative solvers: PETSc
- Algebraic Multigrid preconditioning for the solution of Poisson equation: BoomerAMG provided by *hypre*

Nasr-Azadani, M. M., & Meiburg, E. (2011). TURBINS: an immersed boundary, Navier–Stokes code for the simulation of gravity and turbidity currents interacting with complex topographies. ***Computers & Fluids***.

Problem setup

Sim.	h	(x_b, z_b)	Re	(L_x, L_y, L_z)
FL	0.0	N/A	2000	(38,2,3)
B1	0.25	(5.5,1.5)	2000	(38,2,3)
B2	0.5	(5.5,1.5)	2000	(38,2,3)

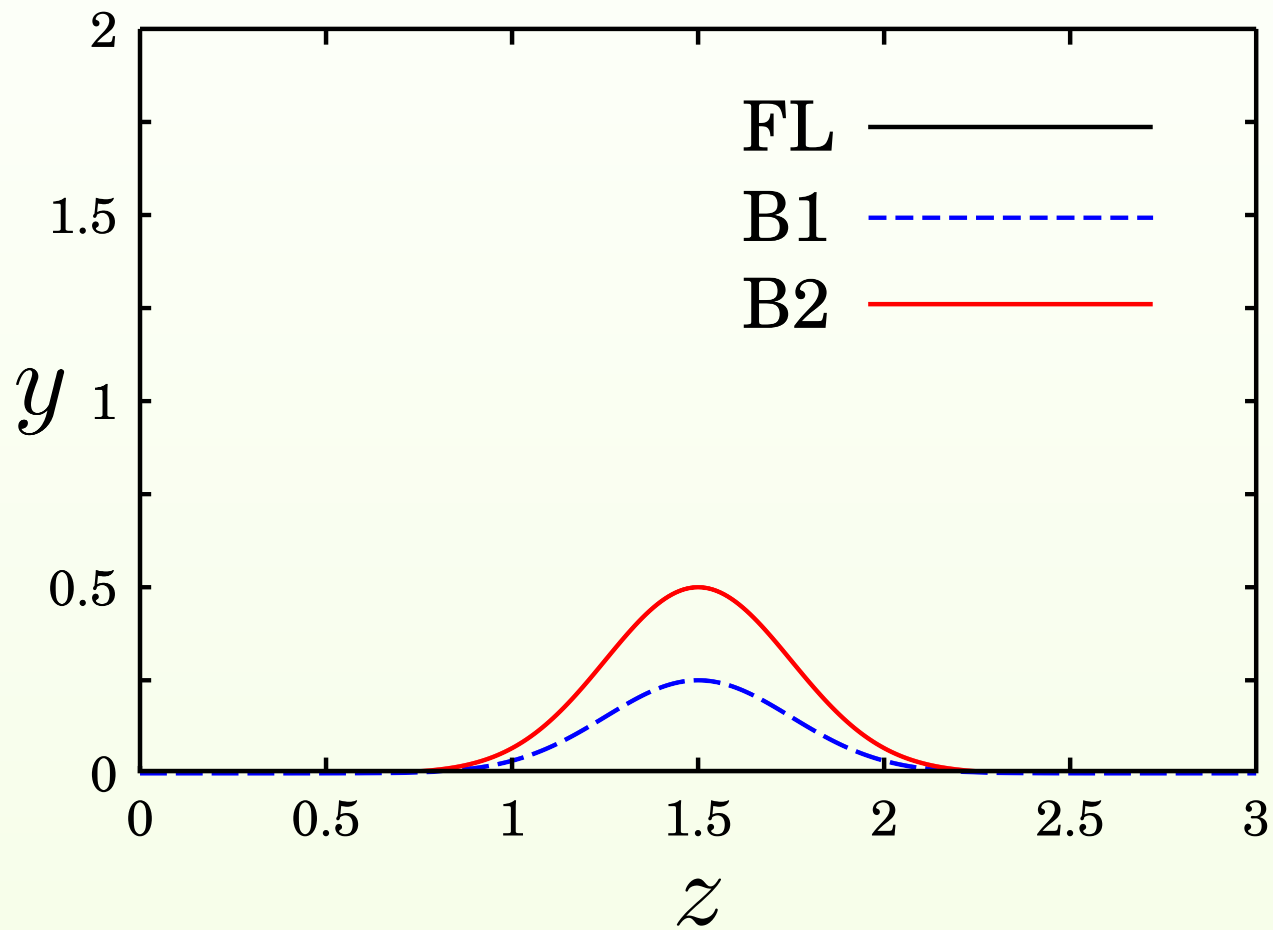

Two particle sizes:

1. Coarse particles (50%):
$$u_s^c = 0.03$$
2. Fine particles (50%):
$$u_s^f = 0.006$$

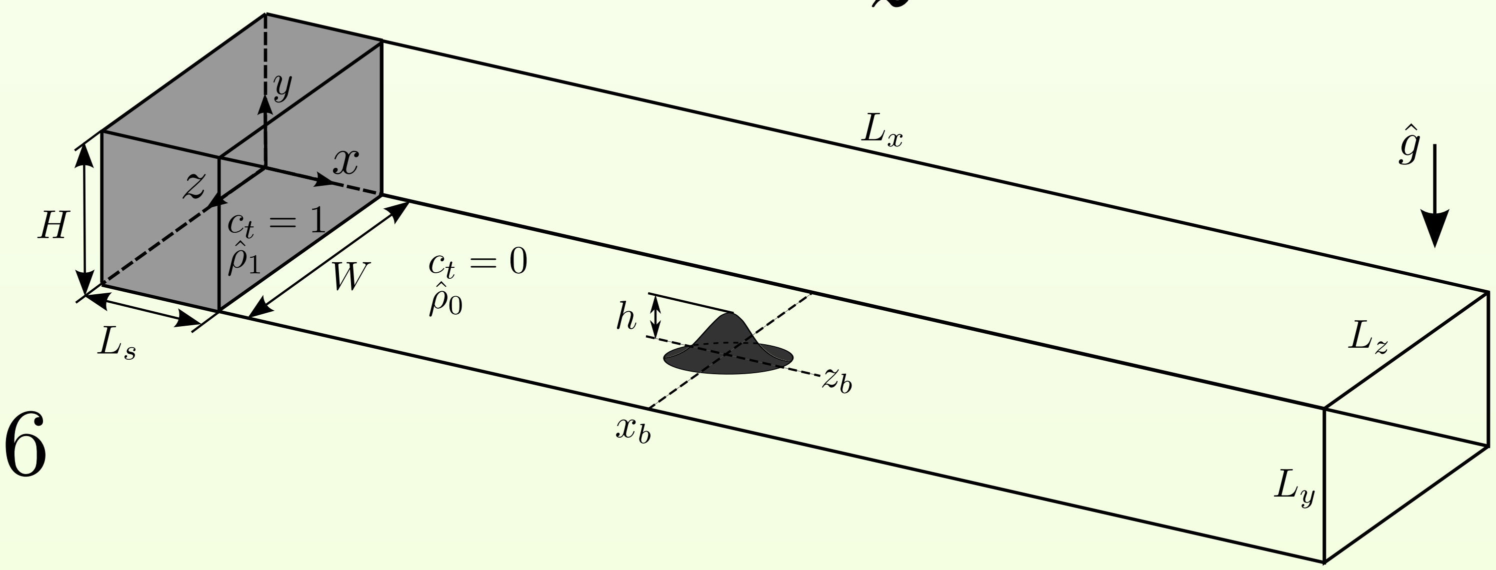

Flow evolution

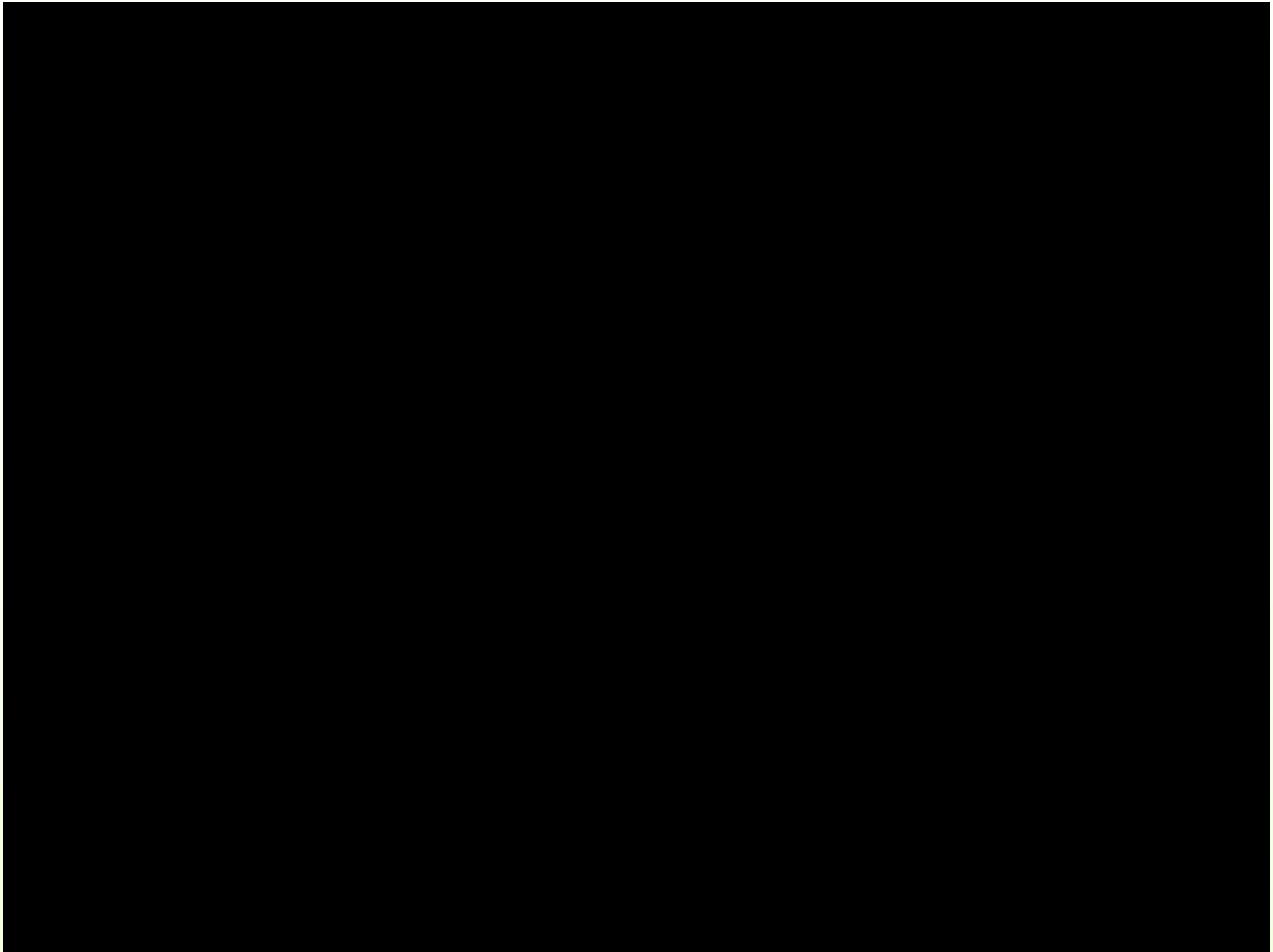

Frontal structure

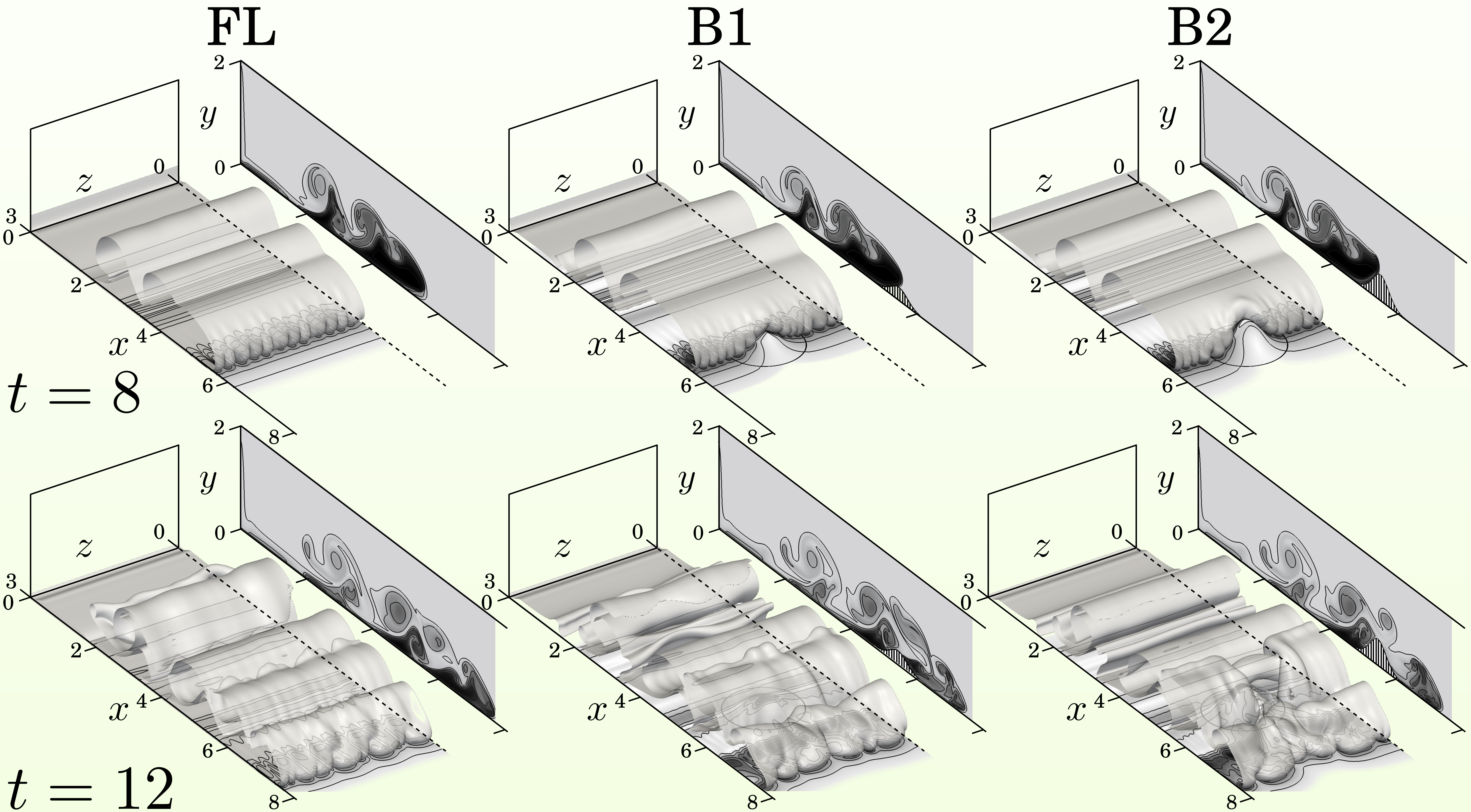

Frontal structure

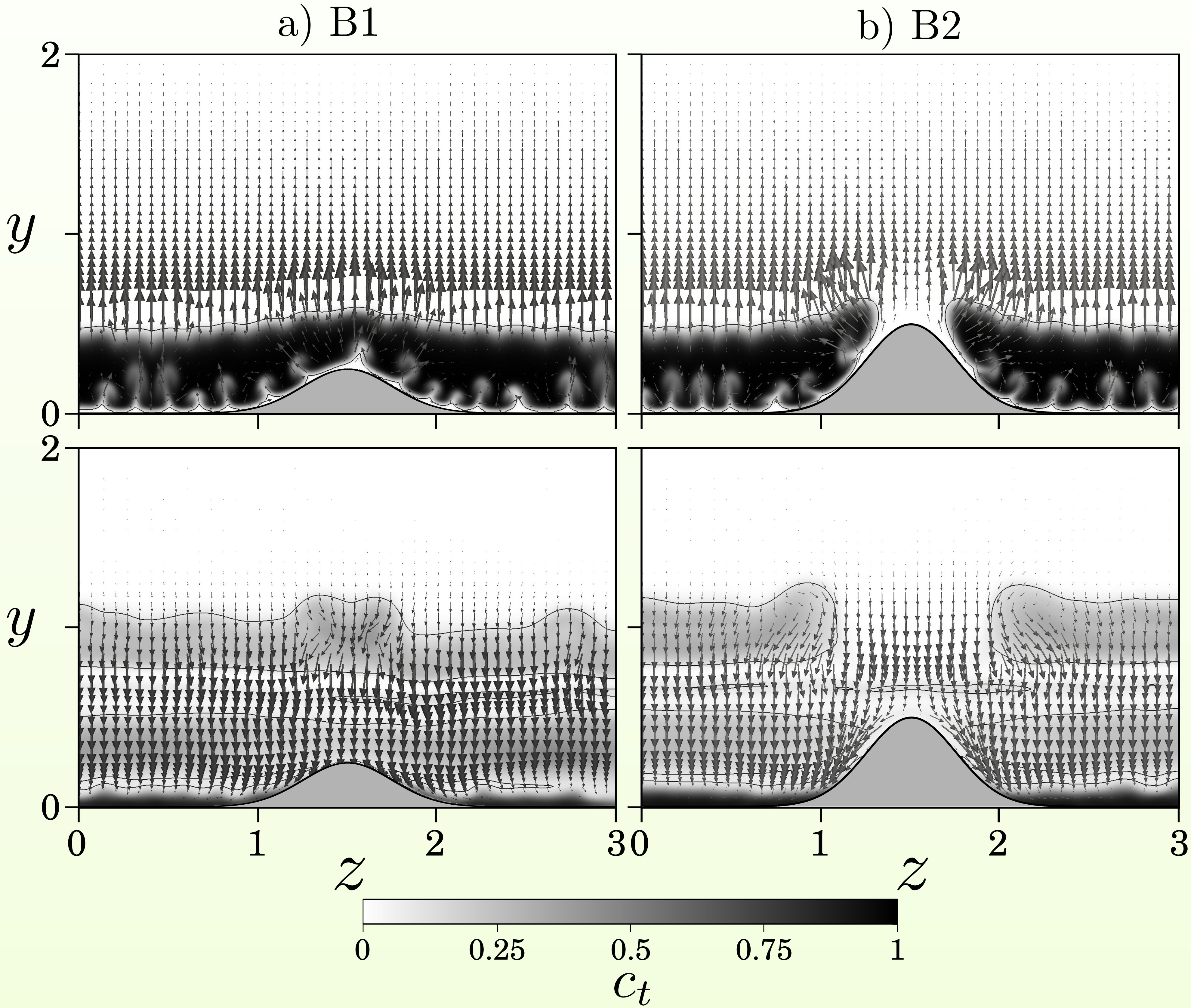

Three-dimensional structures

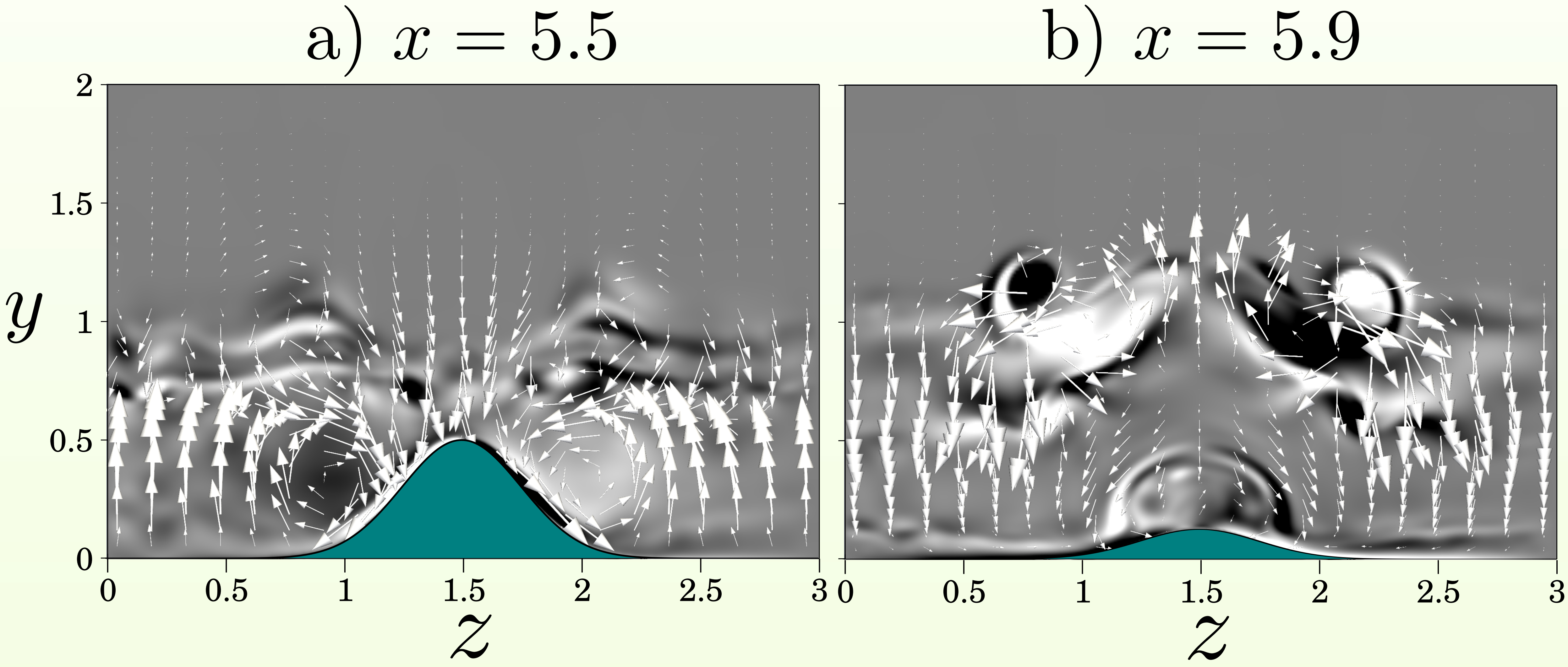

Three-dimensional structures

Horse-shoe vortices in case B2

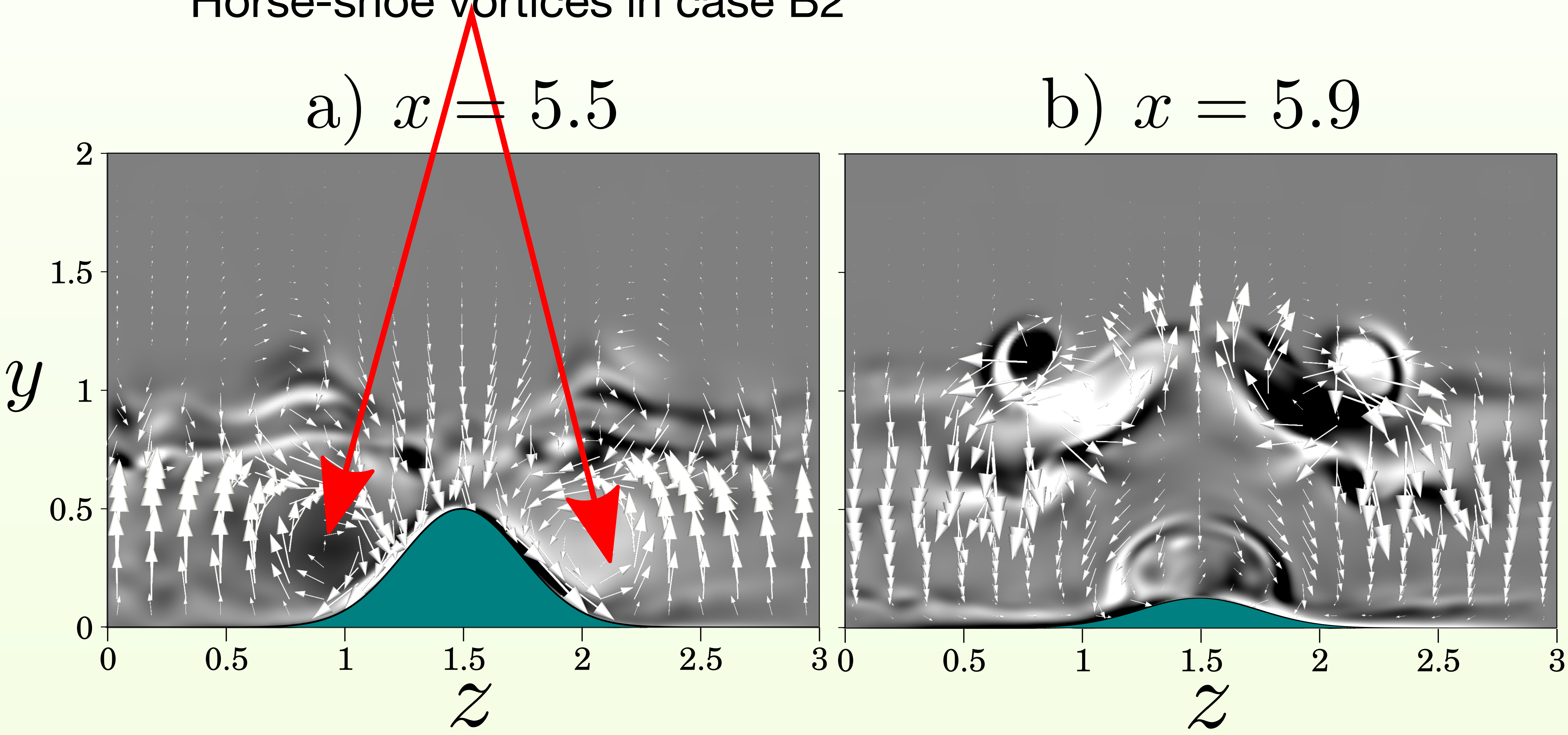

Three-dimensional structures

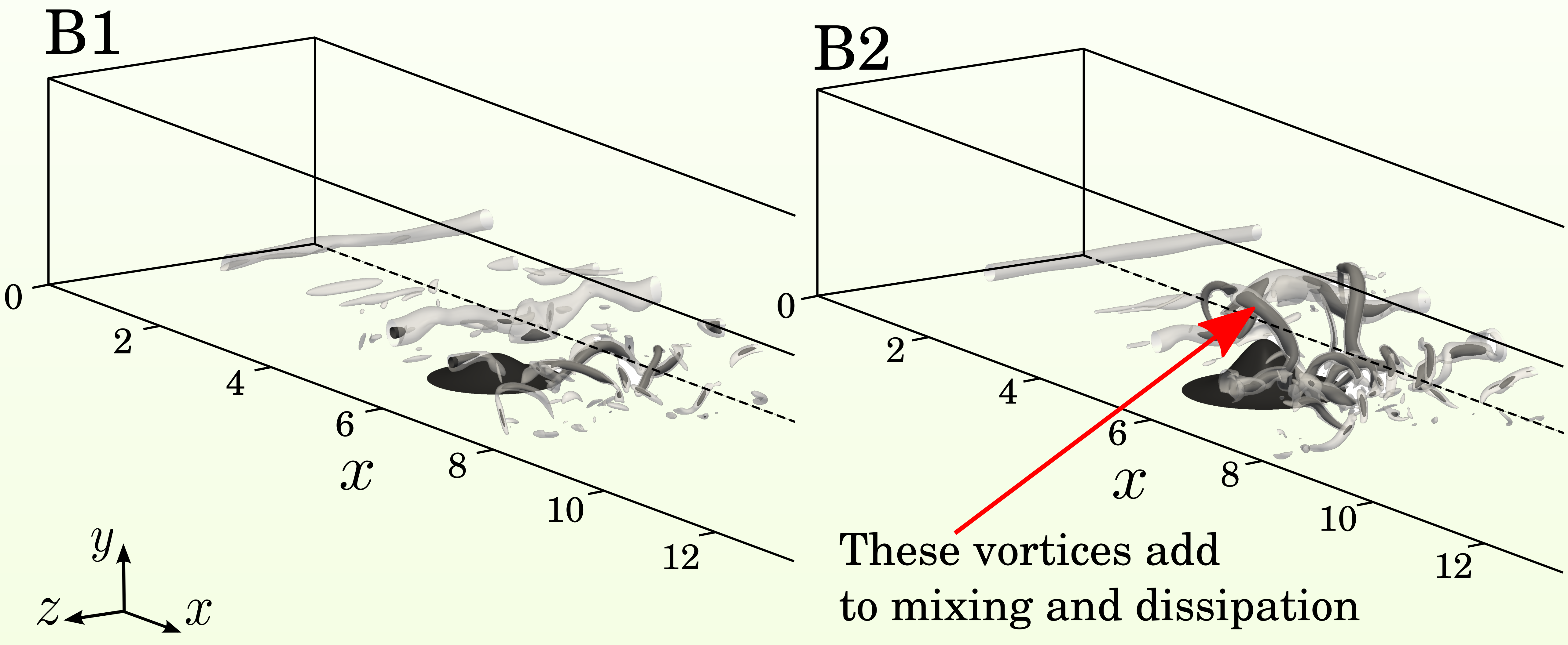

Q-criterion

Experiments

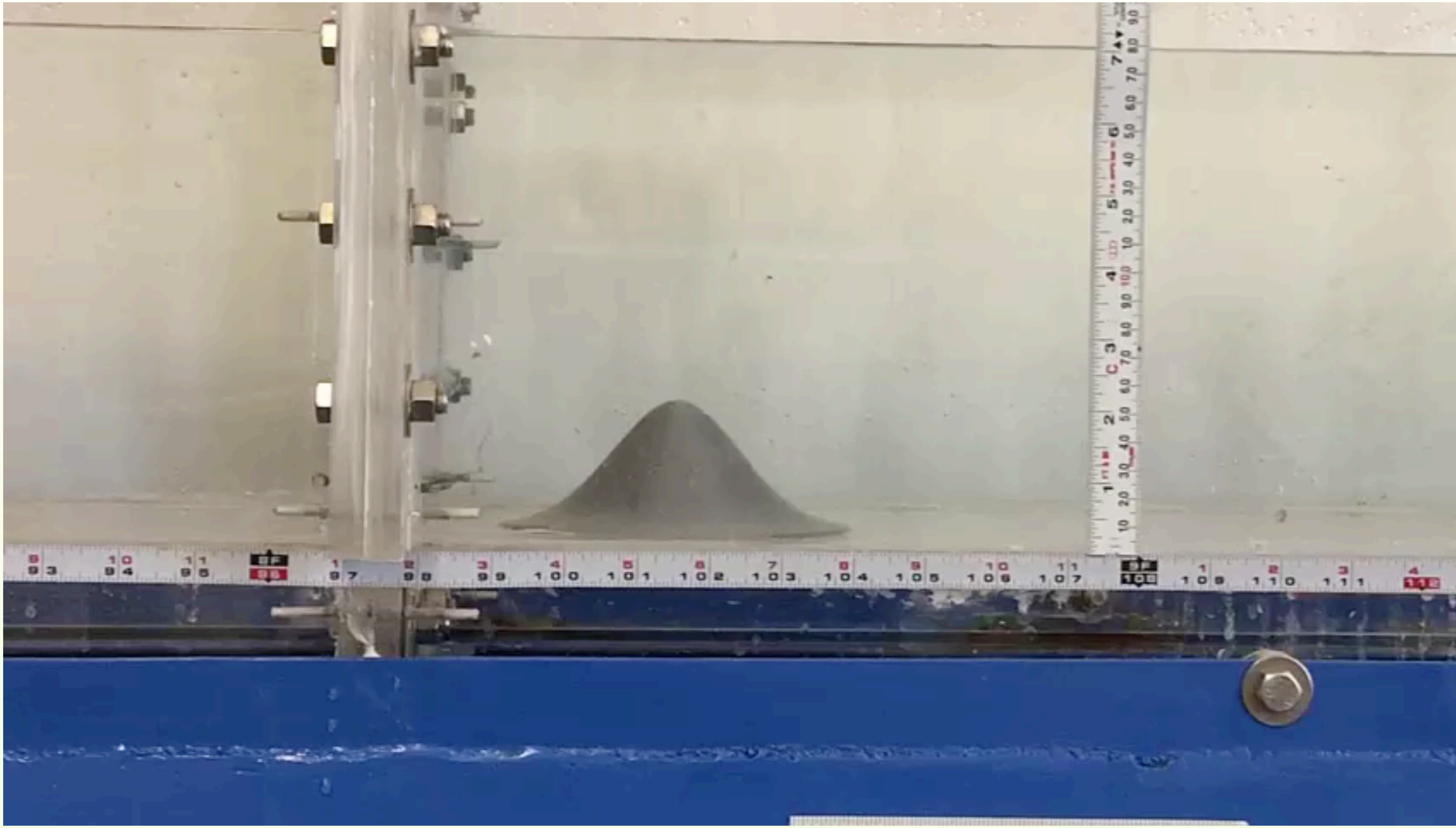

Case B2. Gravity current. Experiments by Dr. Firat Y. Testik, Clemson University

Experiments

Case B2. Gravity current. Experiments by Dr. Firat Y. Testik, Clemson University

Front location & suspended mass

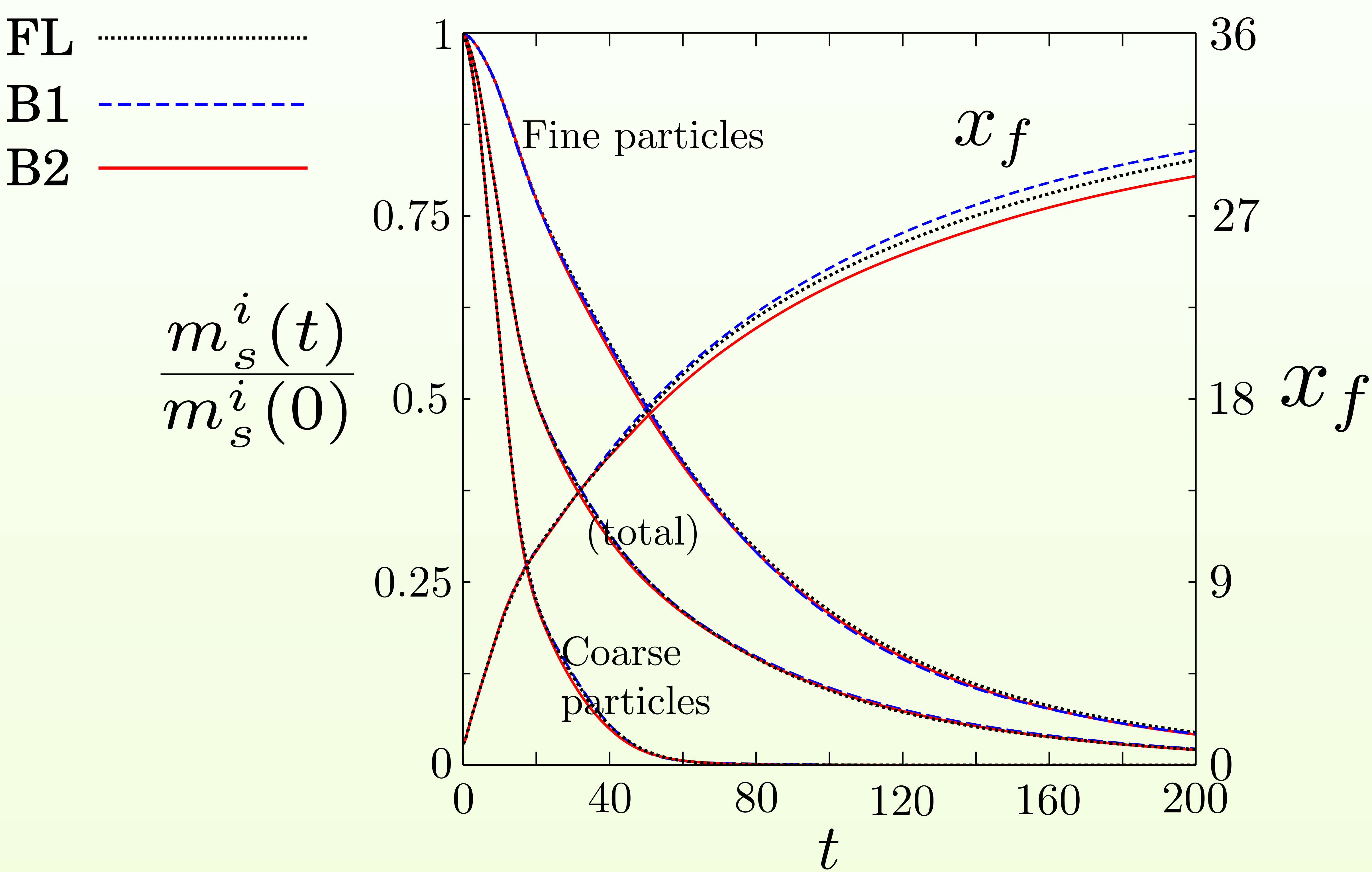

Front location

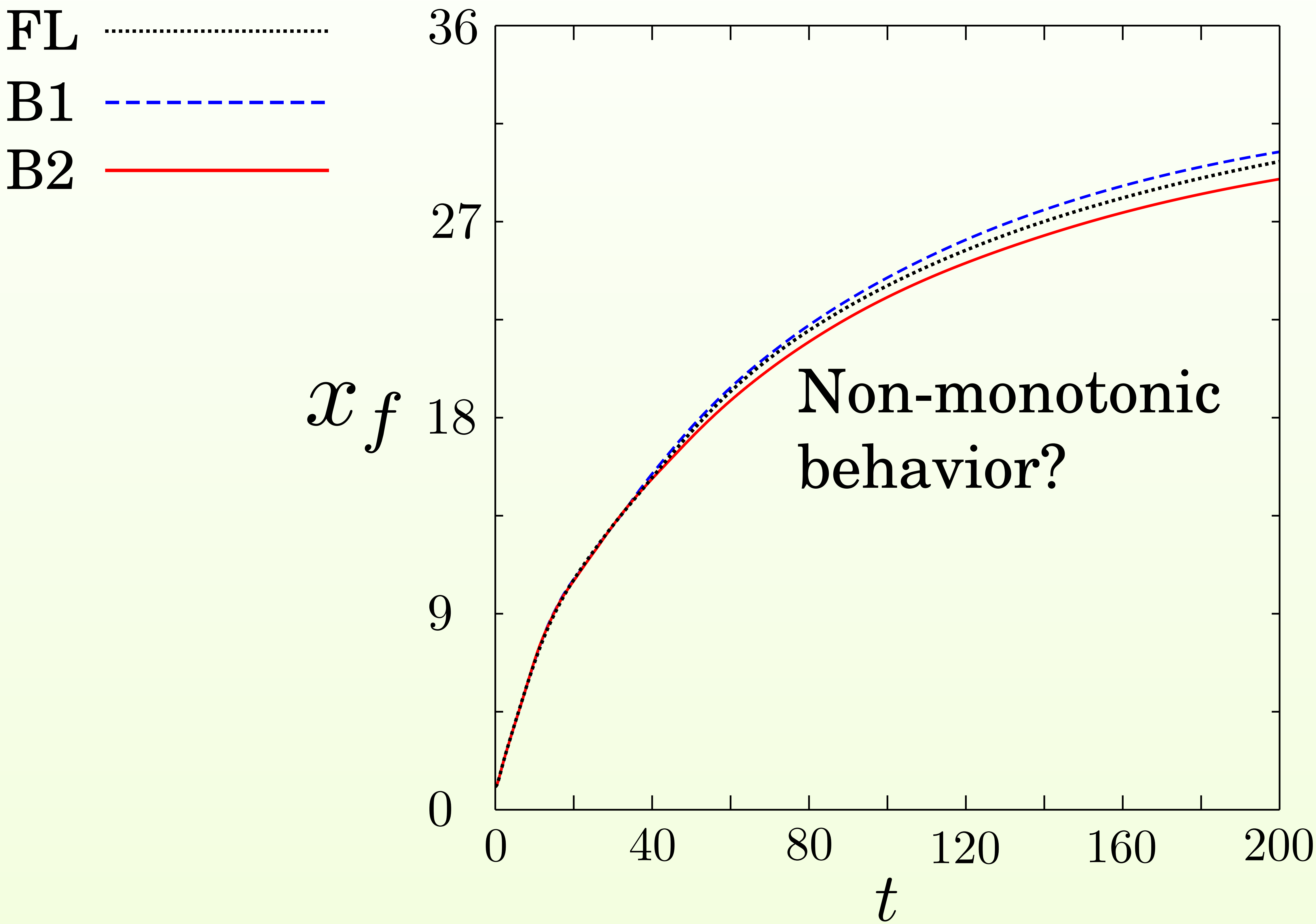

Viscous dissipation

Case B2 (taller bump):
Demonstrates further enhancement in viscous dissipation

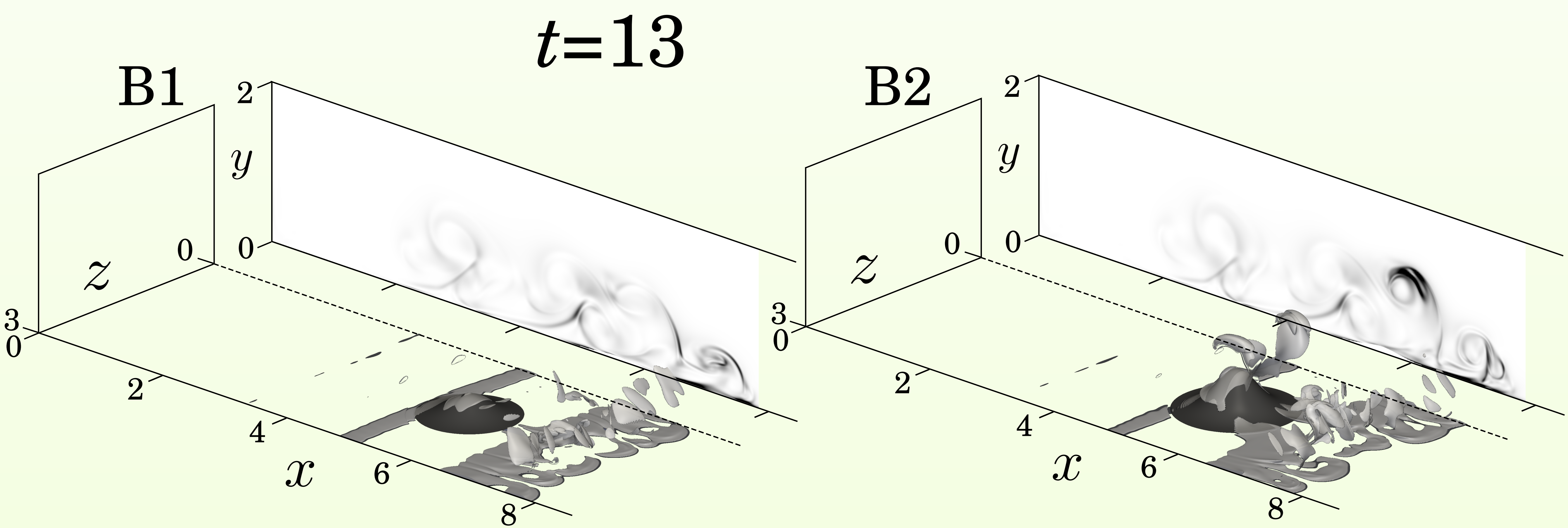

Current height and front velocity

Case B2 (taller bump):

Current thickens, front velocity increases

Front velocity

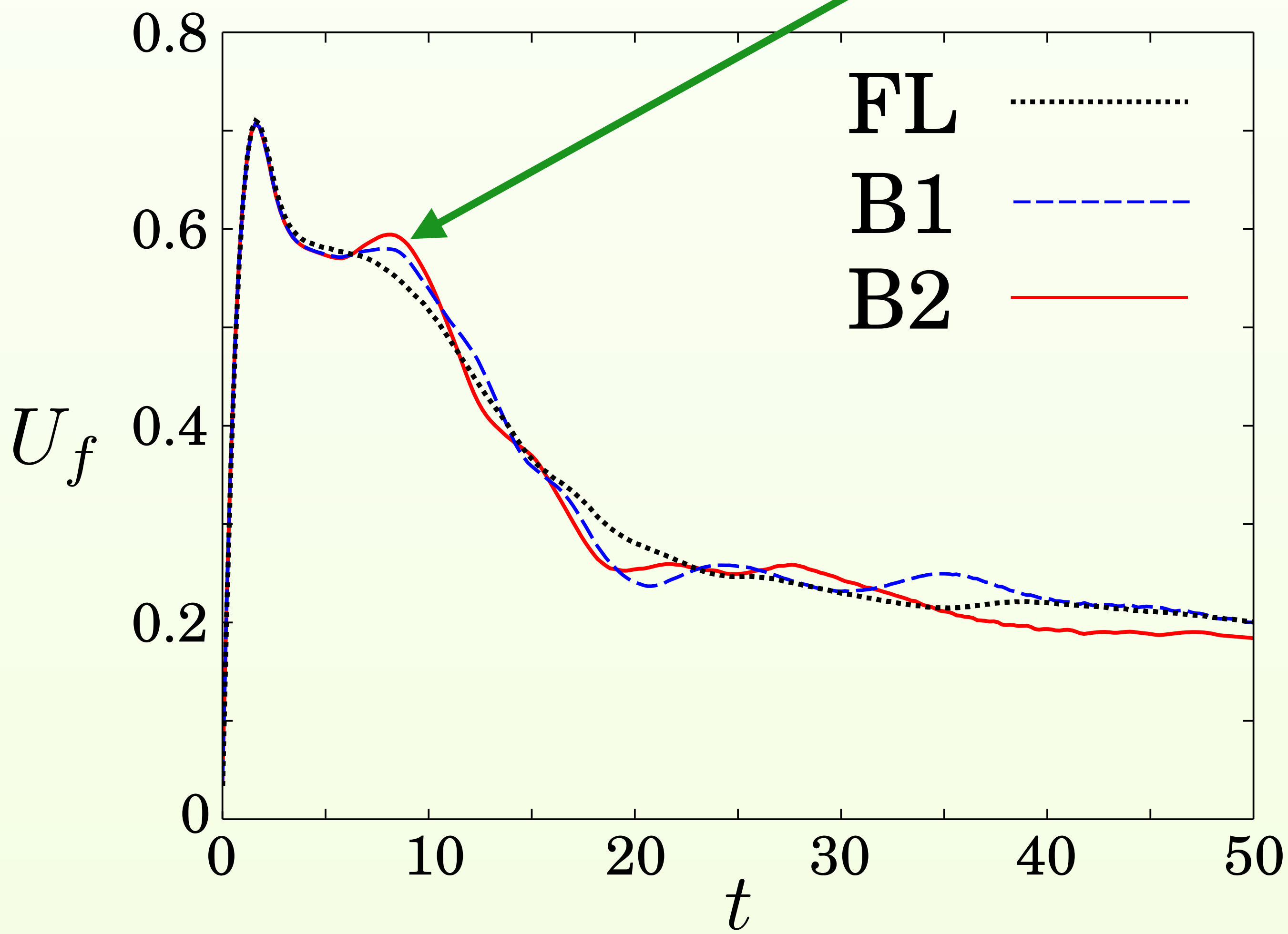

Current height at t=8

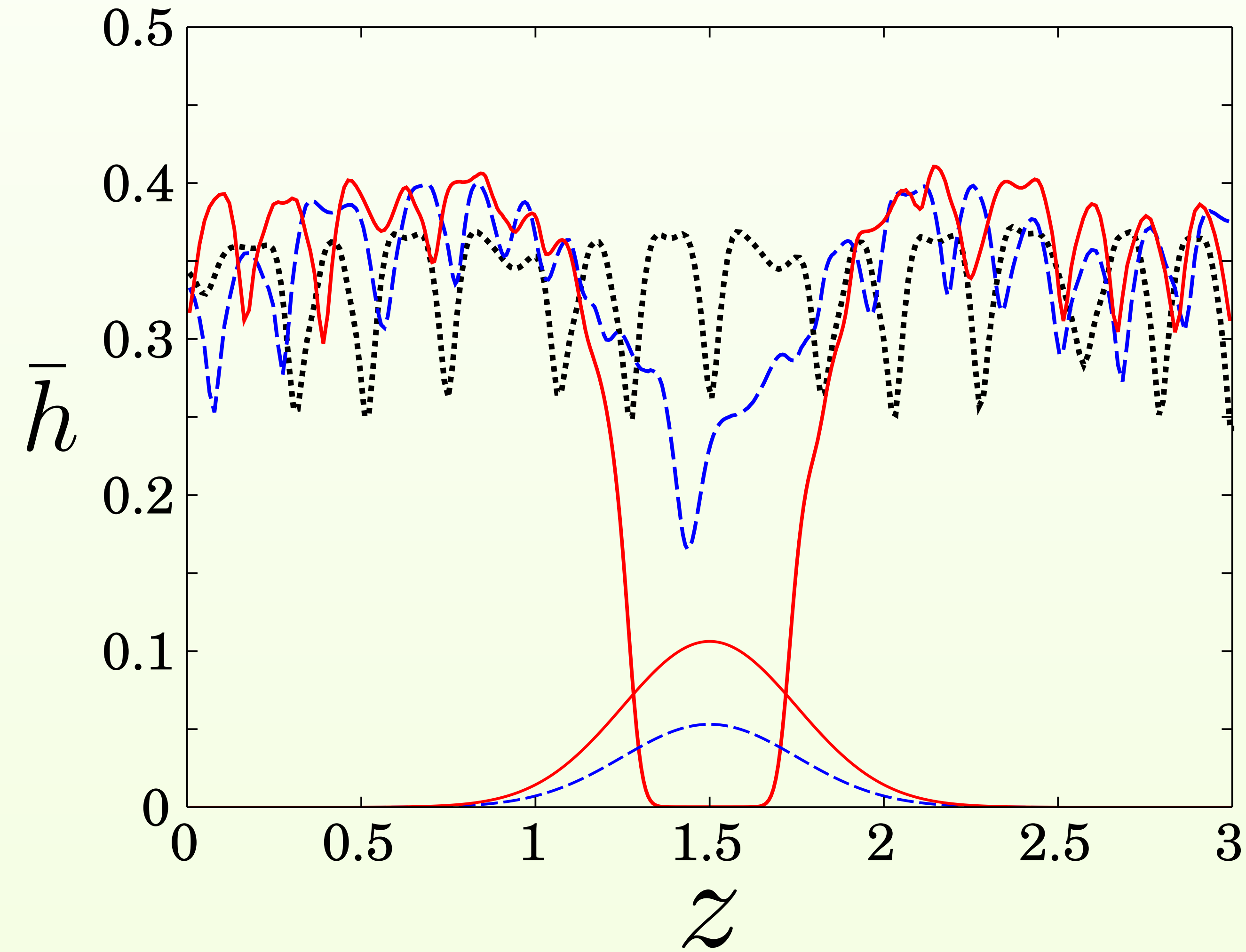

Discussion: Bump height & non-monotonic effect

- With the increase in bump height, there are two competing effects
  - Enhanced viscous dissipation due to three-dimensional vortical structures
  - Increase in front velocity due to a higher effective current height
  - Existence of a critical bump height which indicates the current traveling faster or slower than the flat bottom case

Mixing: Interstitial fluid

- Lock-fluid (interstitial fluid) is tracked via a continuous concentration field:

$$c_l(x, y, z, t)$$

- It is advected along the fluid velocity (minimal diffusion, *Sc* = 6)

$$\Phi^\theta = \frac{1}{\underbrace{H \times L_s \times W}_{\text{Lock volume}}} \int_V G(c_l; c_\theta)\ \mathrm{d}V$$

- With

$$G(c_l; c_\theta) = \begin{cases} 1 & \text{if} \quad c_l \geq c_\theta \\ 0 & \text{if} \quad c_l < c_\theta \end{cases}$$

c_θ: Mixing concentration threshold

Mixing: Interstitial fluid

- Evolution of interstitial fluid concentration field
- Cross sections of incoming flow downstream of the bump

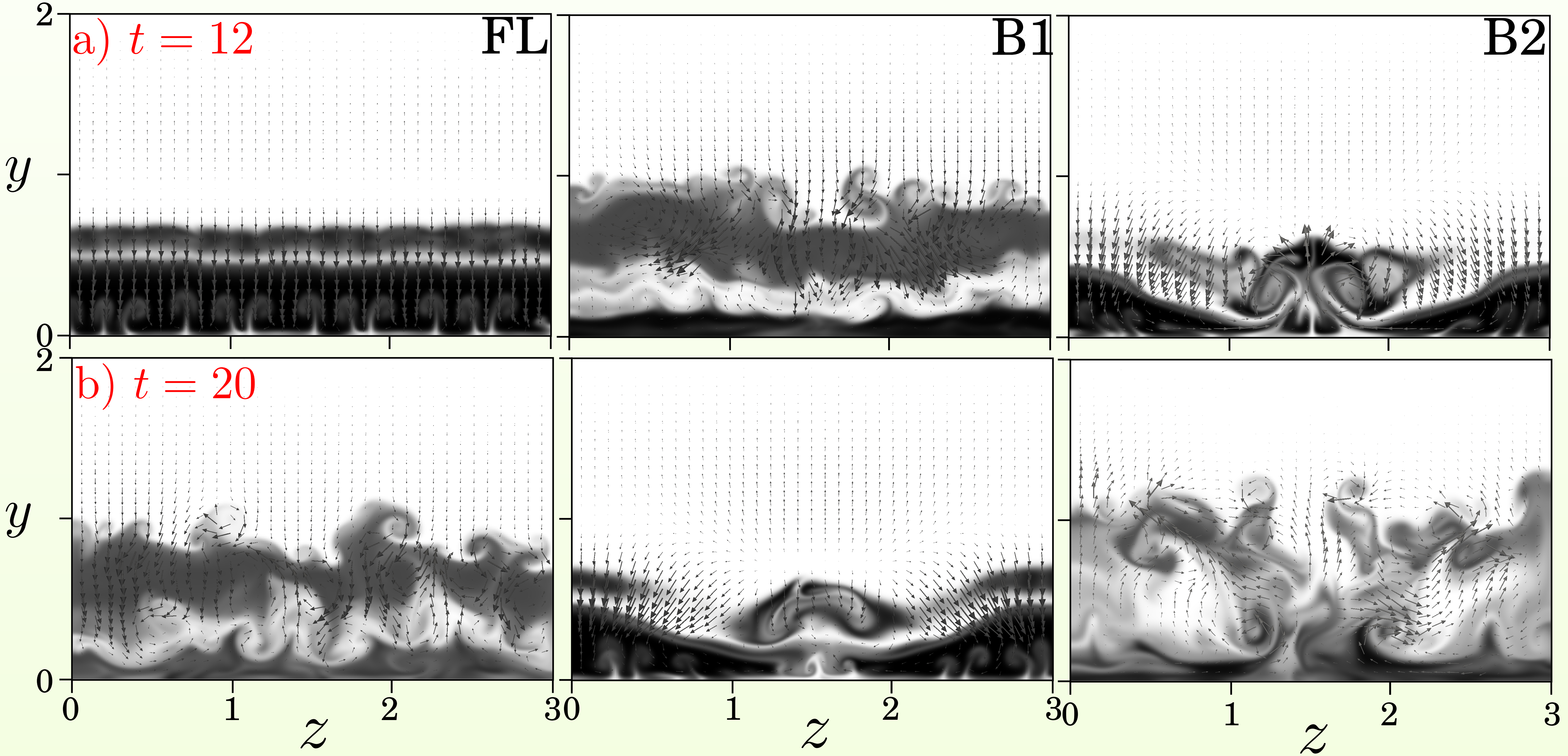

Mixing: Interstitial fluid

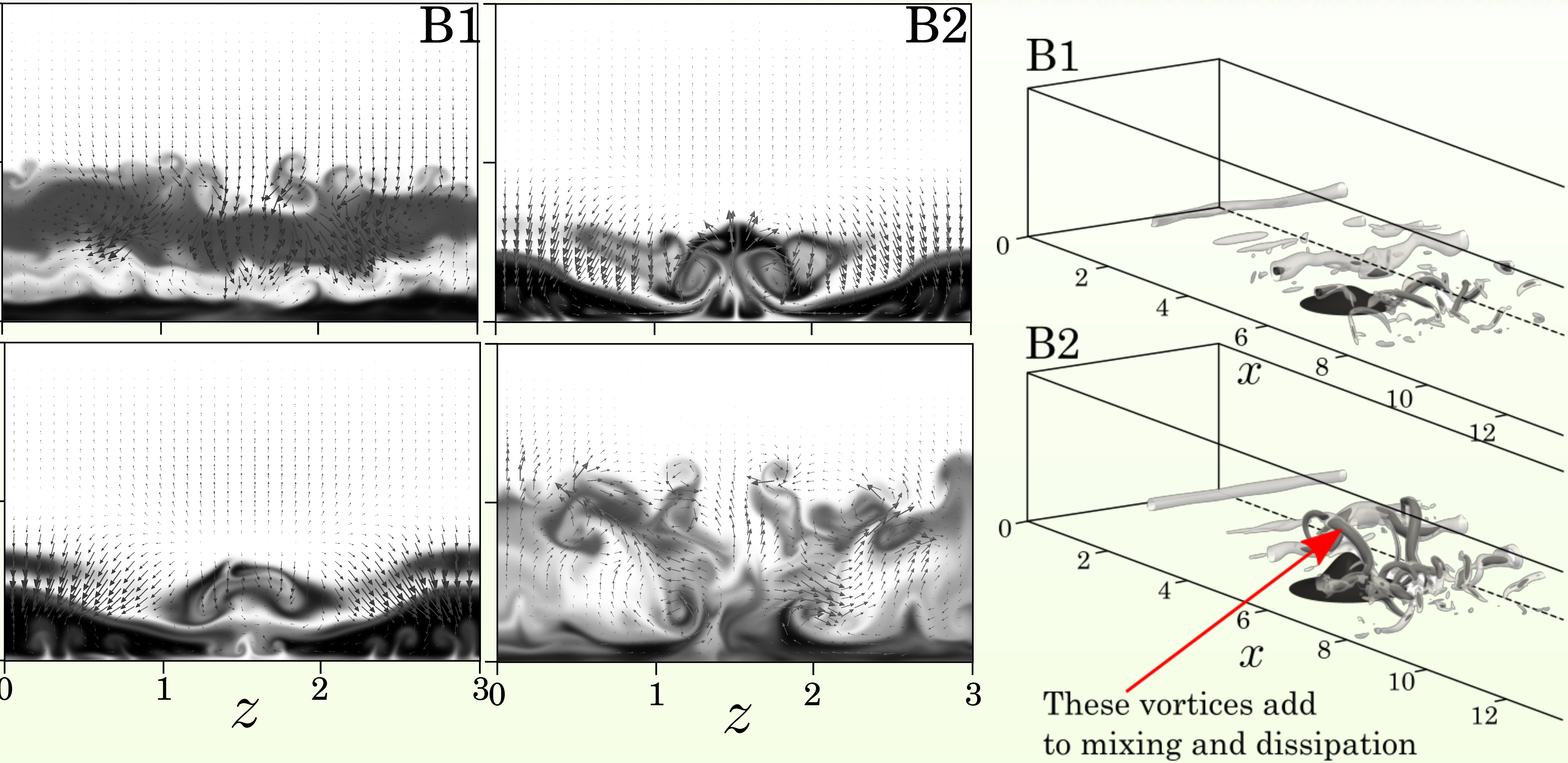

Mixing: Interstitial fluid

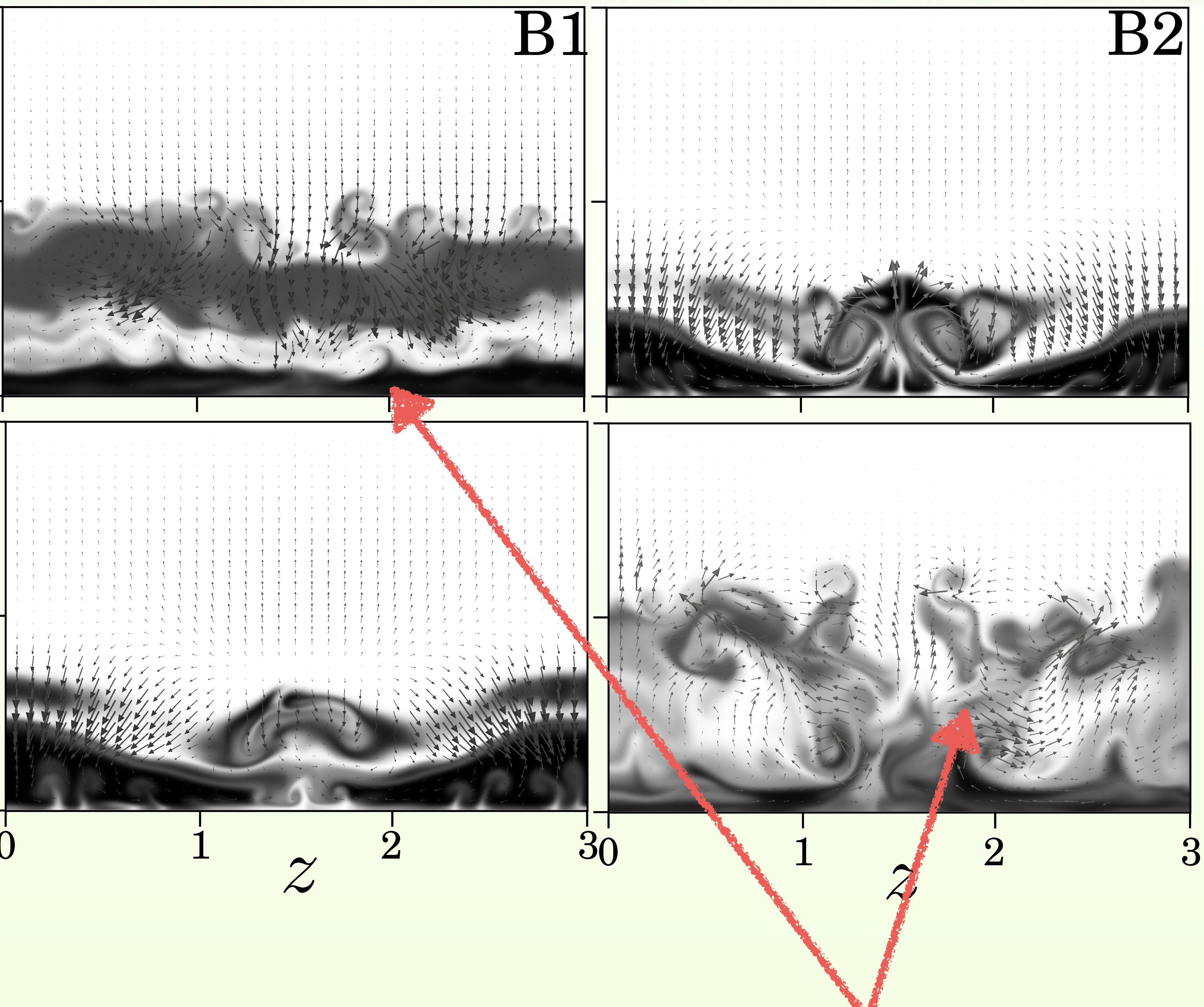

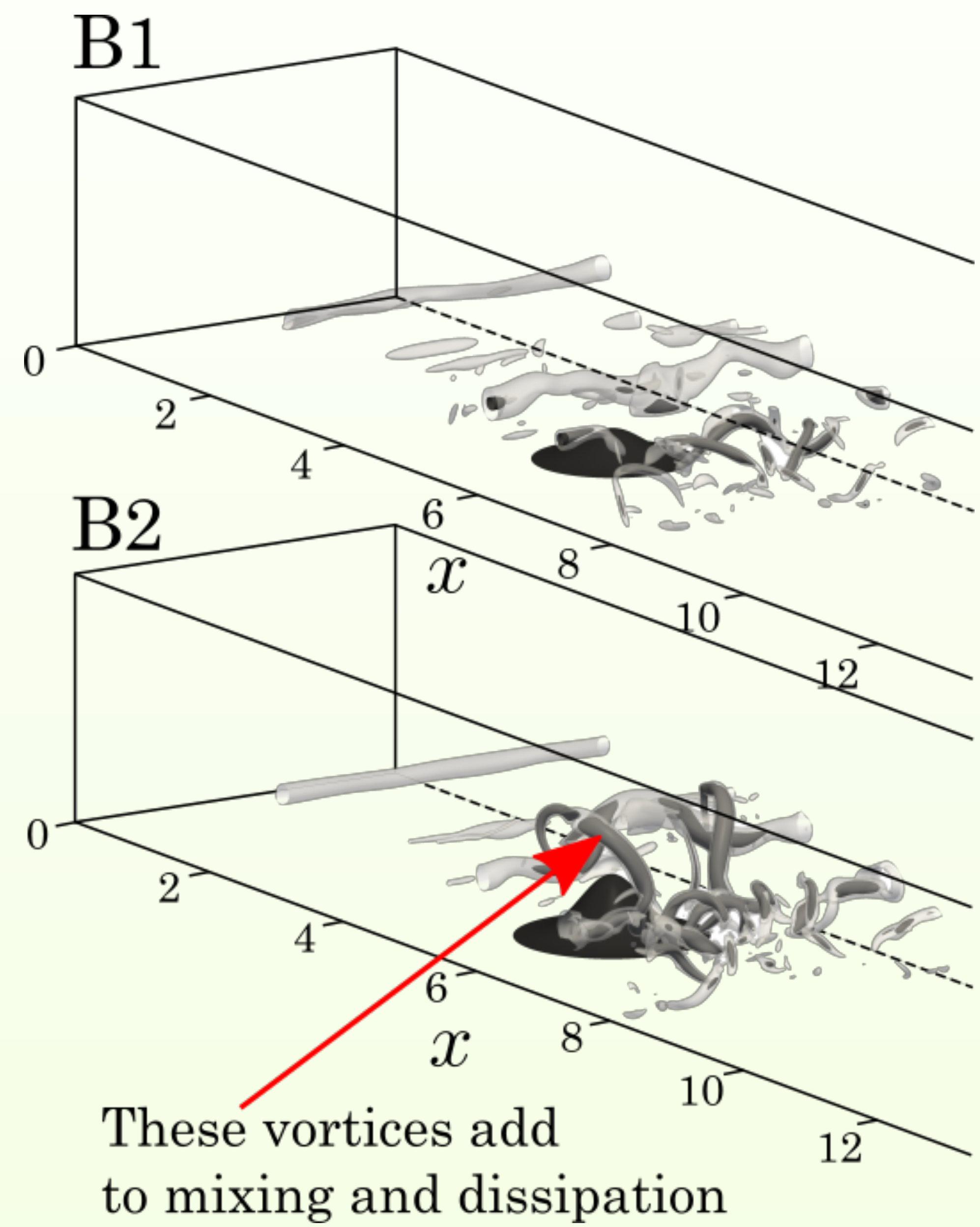

Layered structure disappears in the case with the tallest bump

Mixing: Interstitial fluid

Streamwise vorticity components at two different locations

Downstream of the bump (vicinity)

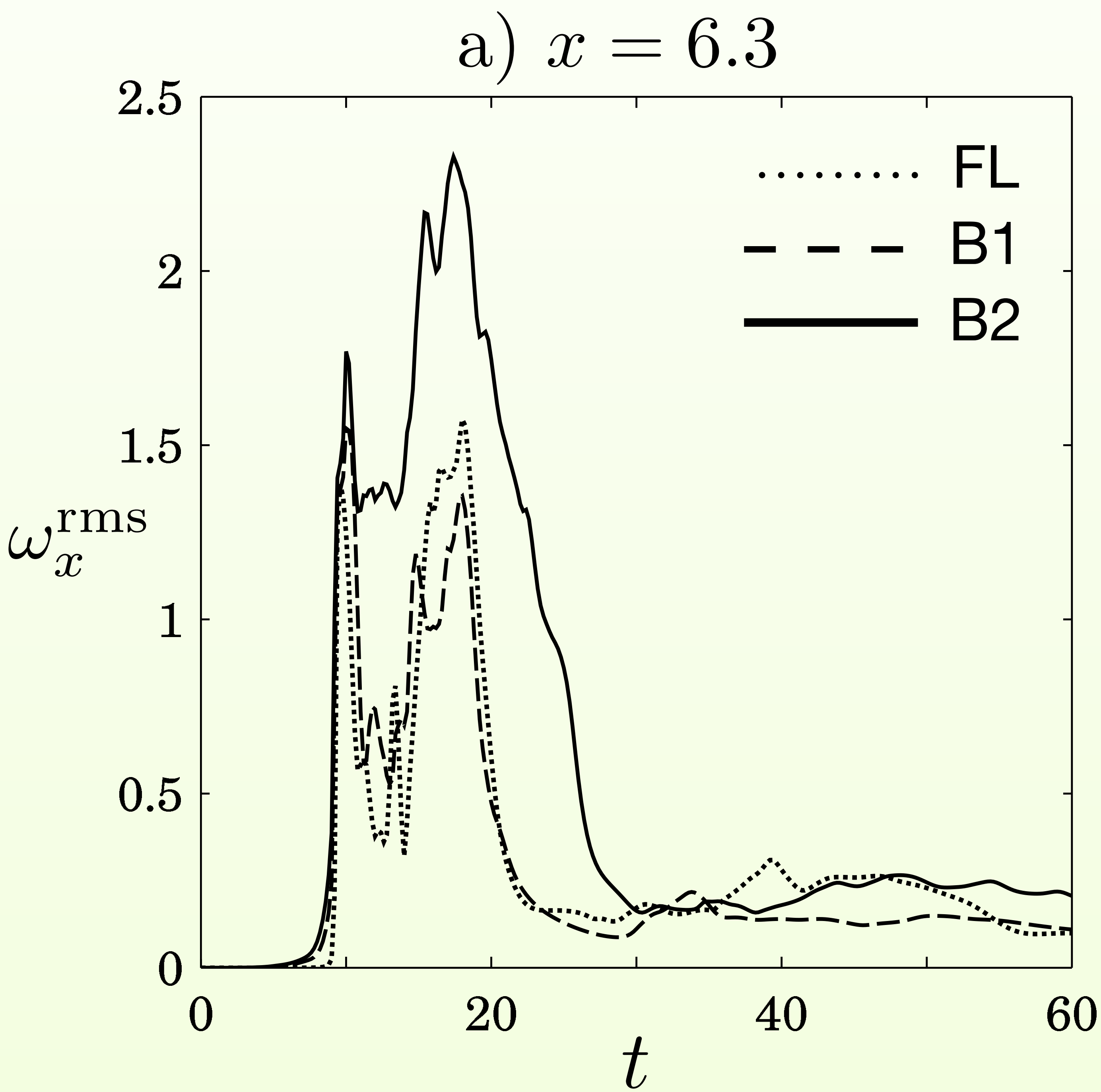

Far downstream of the bump

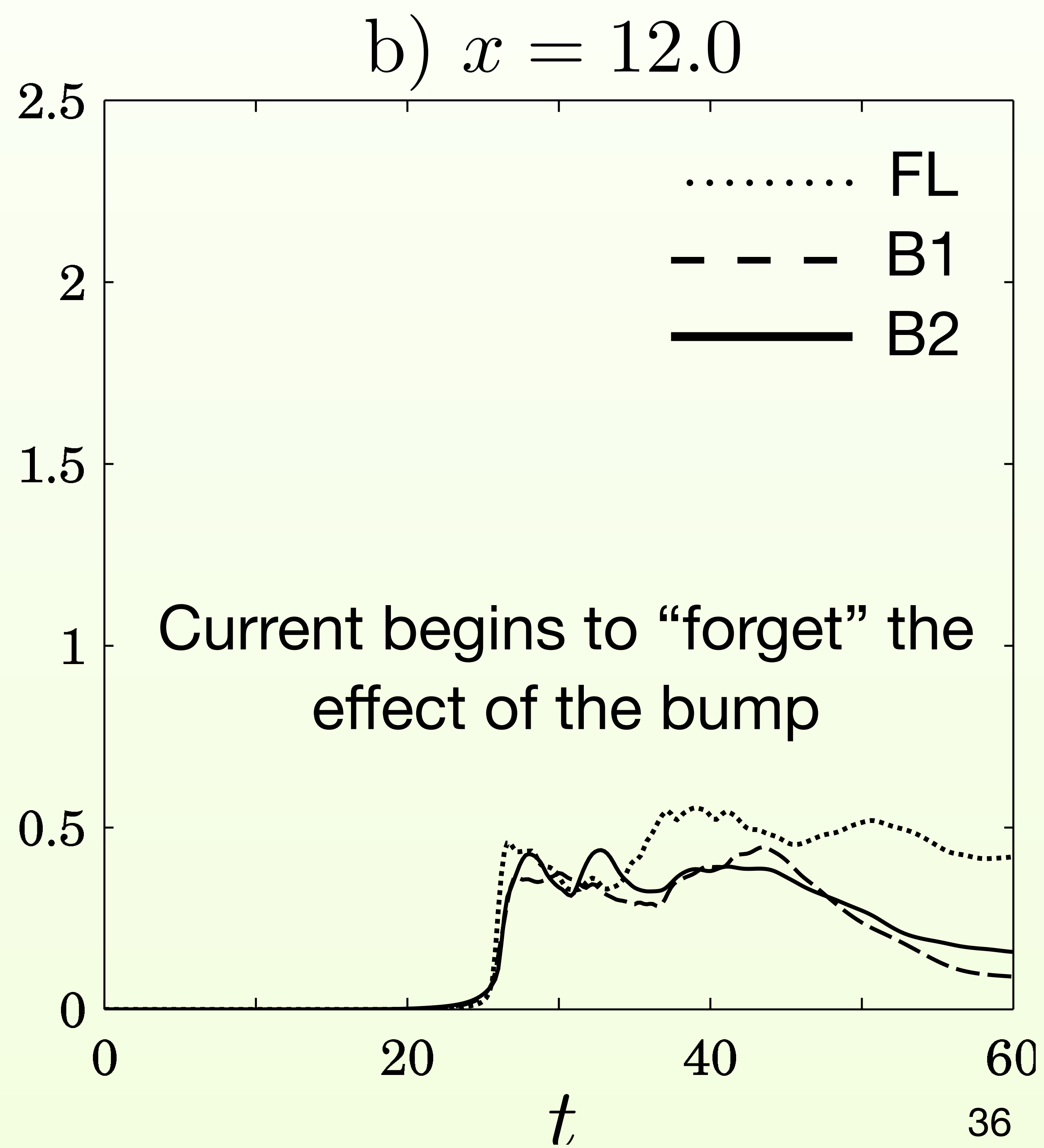

Mixing: Interstitial fluid

- Lock-fluid (interstitial fluid) is tracked via a continuous concentration field:

$$c_l(x, y, z, t)$$

- It is advocated along the fluid velocity (We set *Sc* = 6)

$$\Phi^\theta = \underbrace{\frac{1}{H \times L_s \times W}}_{\text{Lock volume}} \int_V G(c_l; c_\theta)\ \mathrm{d}V$$

- With

$$G(c_l; c_\theta) = \begin{cases} 1 & \text{if} \quad c_l \geq c_\theta \\ 0 & \text{if} \quad c_l < c_\theta \end{cases}$$

c_θ: Mixing concentration threshold

Mixing: Interstitial fluid

Intermediate bump height

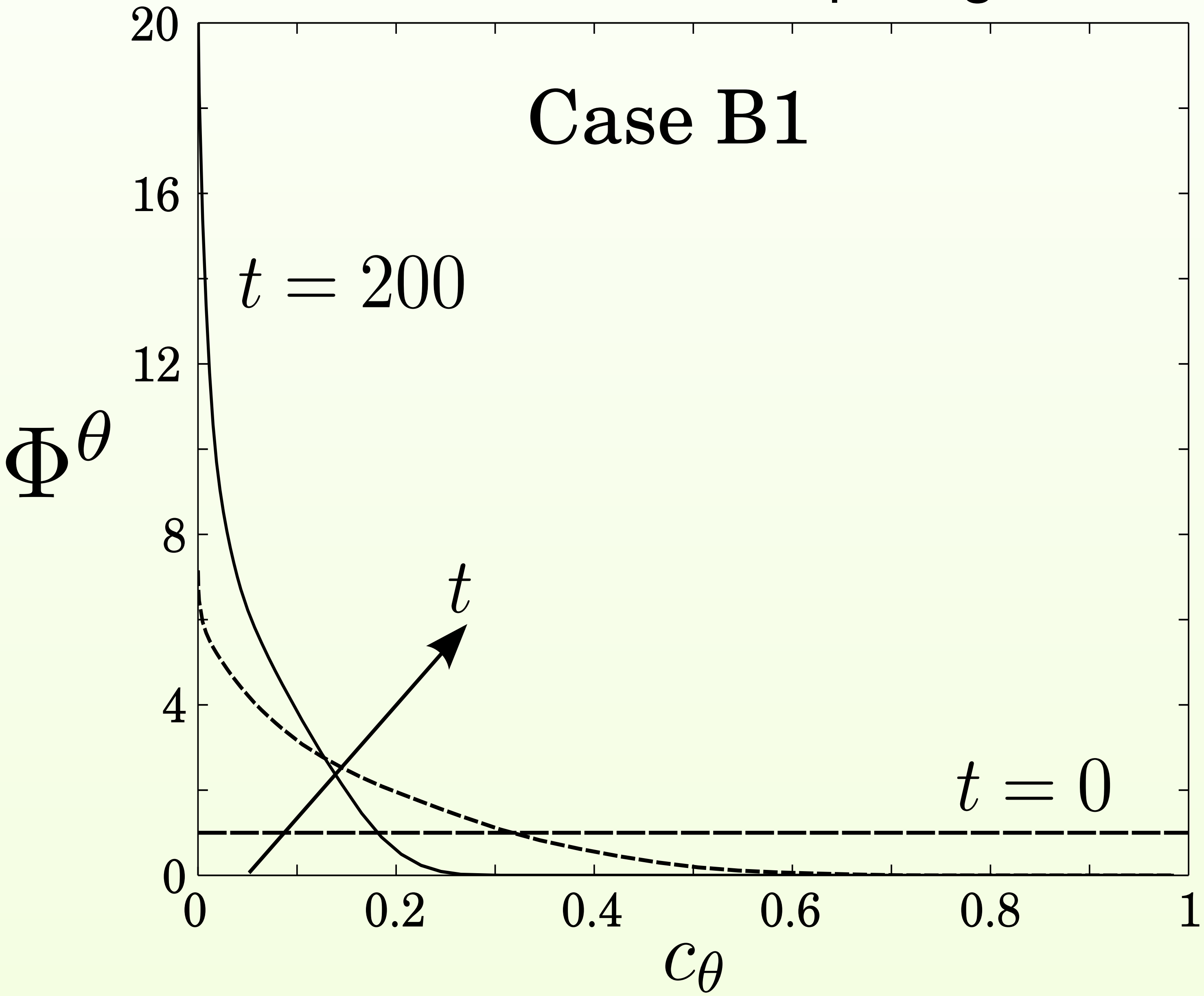

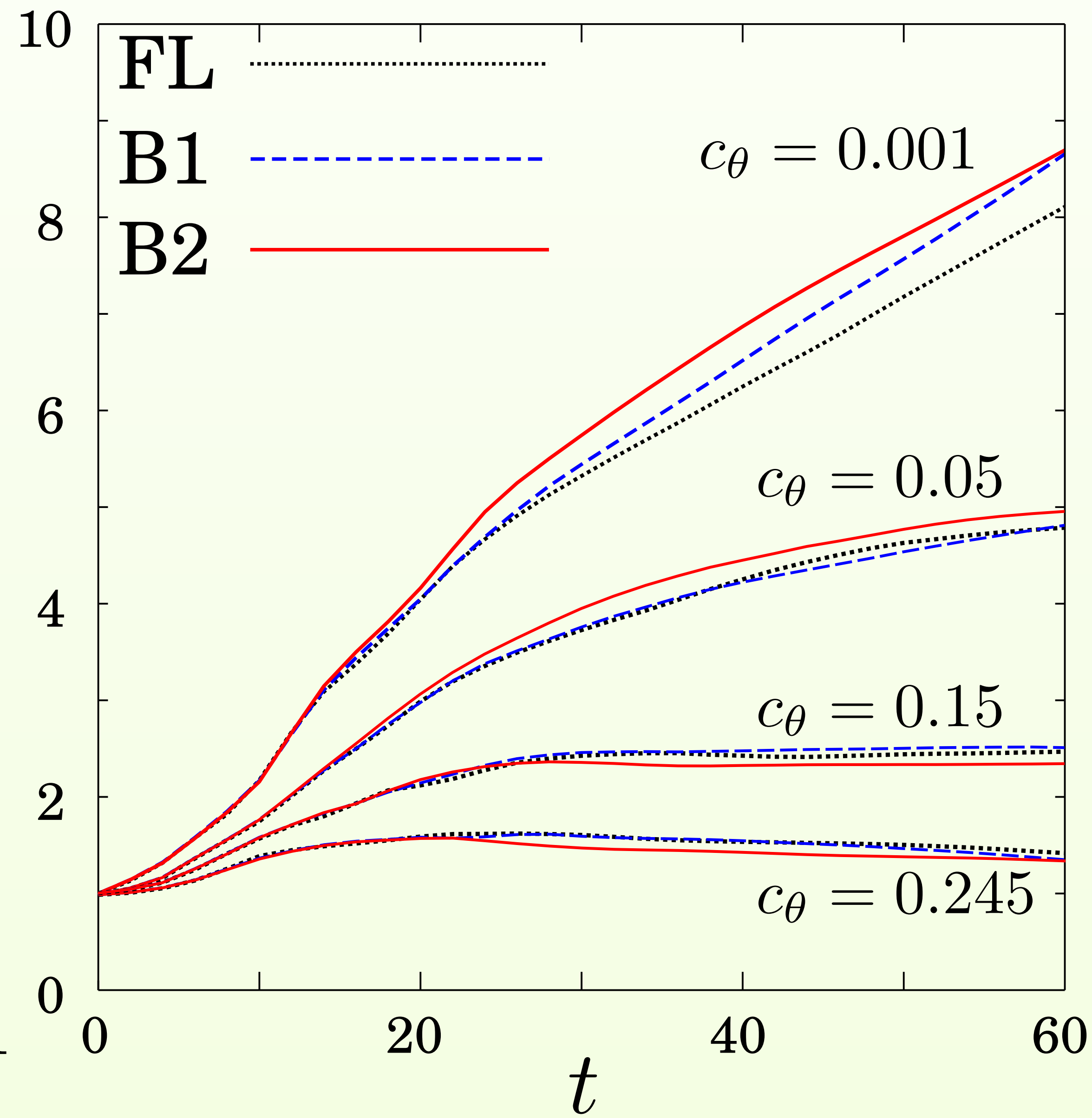

Mixing: Interstitial fluid

Mixing identified: entrainment of ambient fluid into lock-fluid

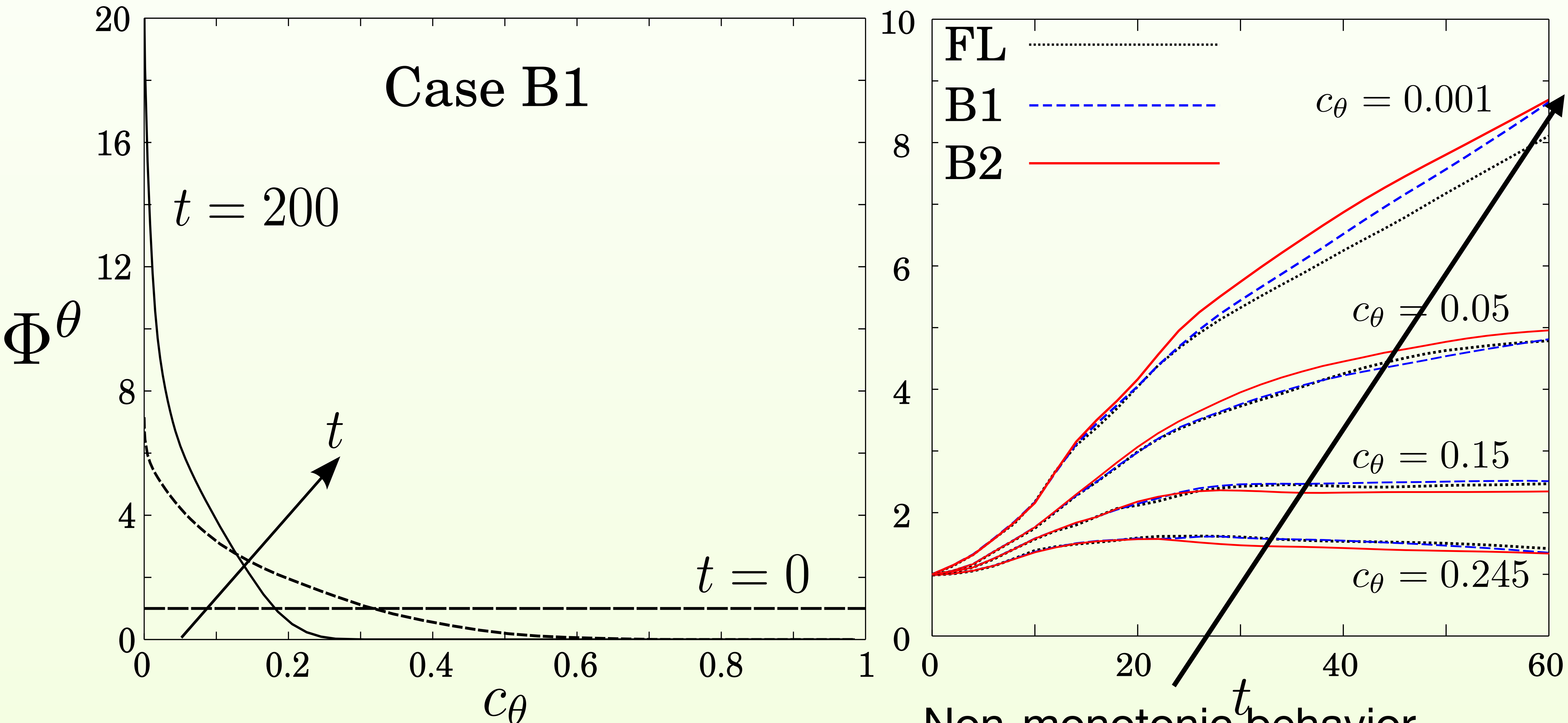

Non-monotonic behavior

Influence of settling velocity

B2-GC: Similar to case B2, settling velocity set to zero

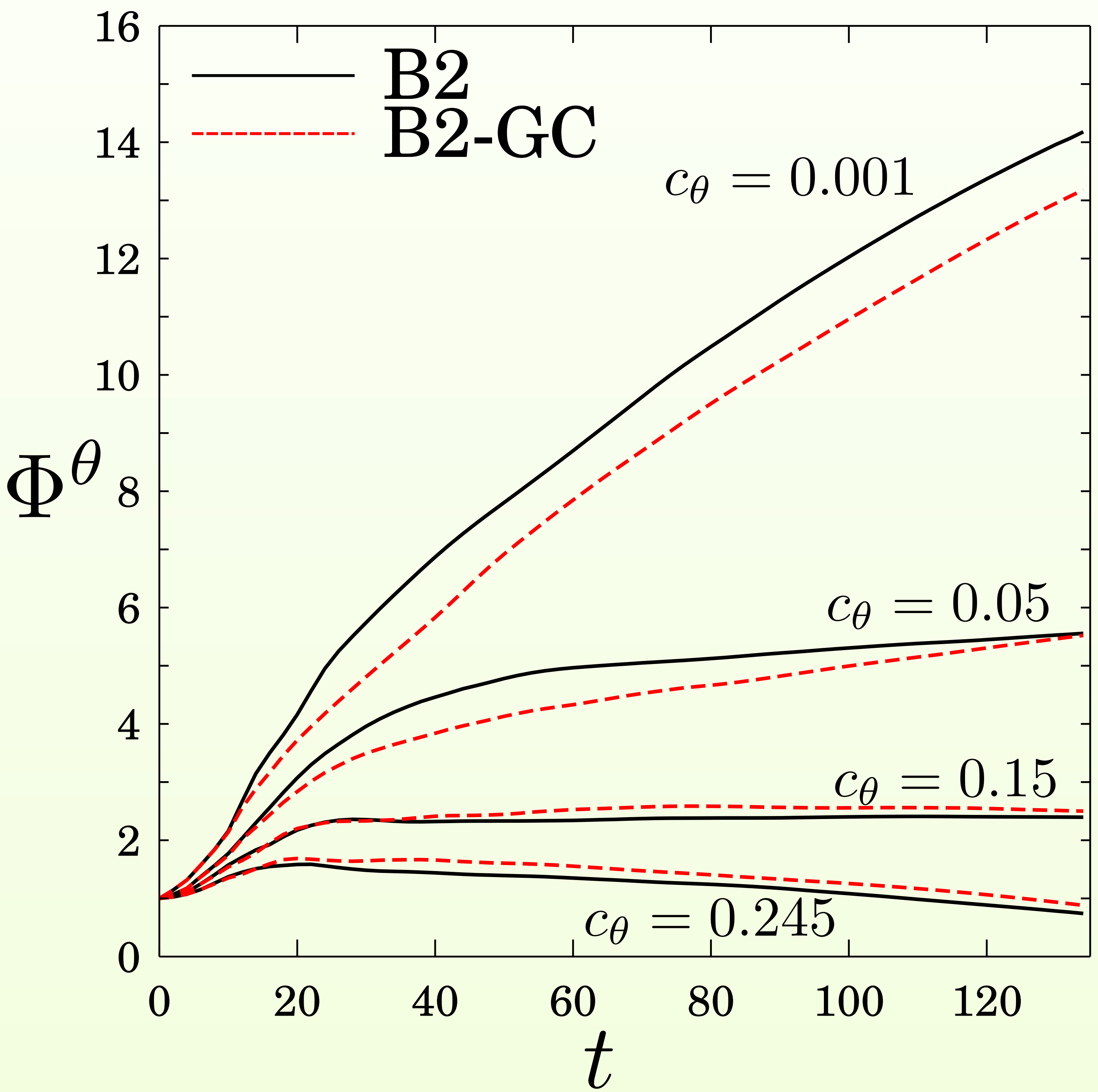

Influence of settling velocity

B2-GC: Similar to case B2, settling velocity set to zero

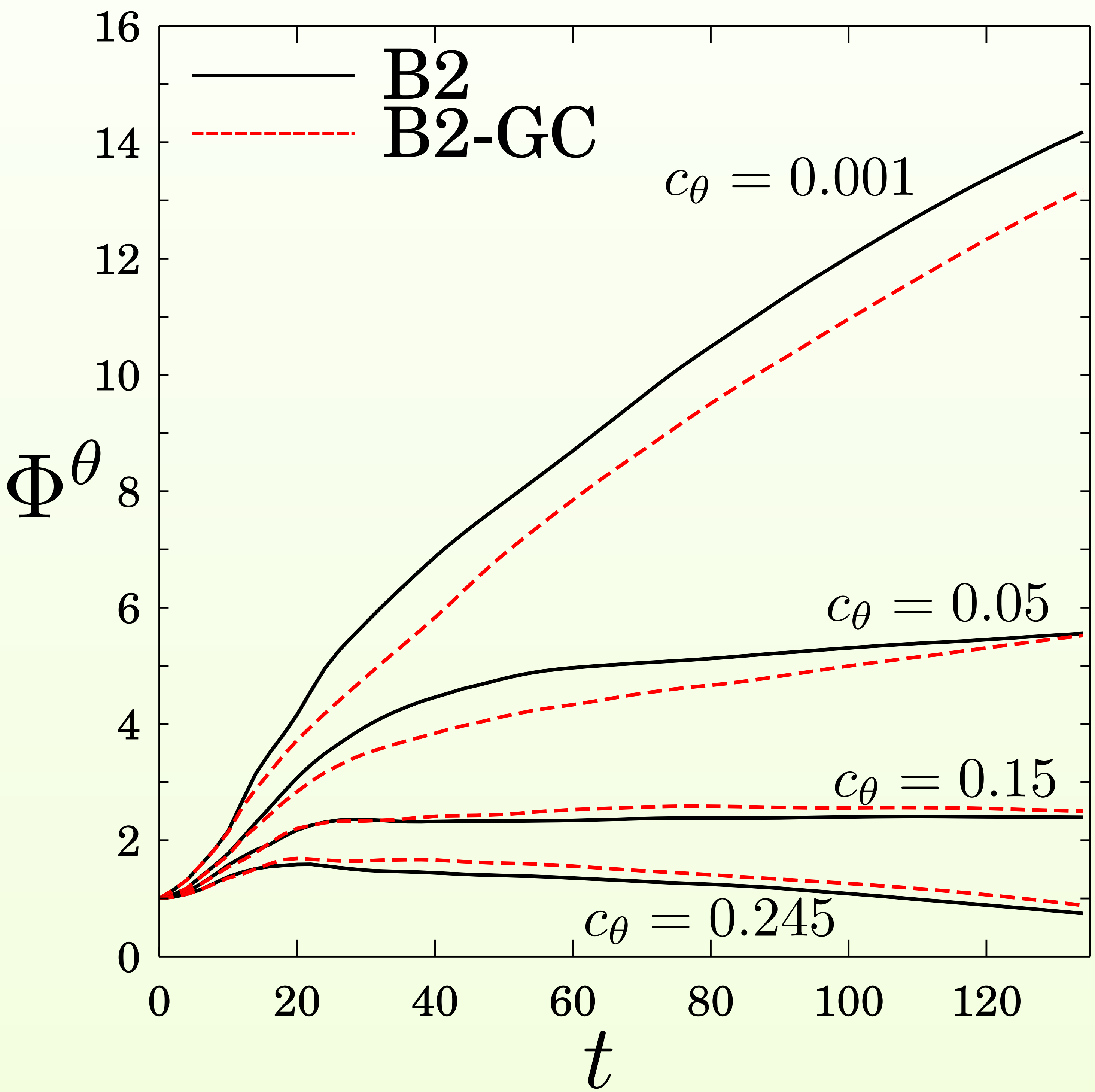

Front location

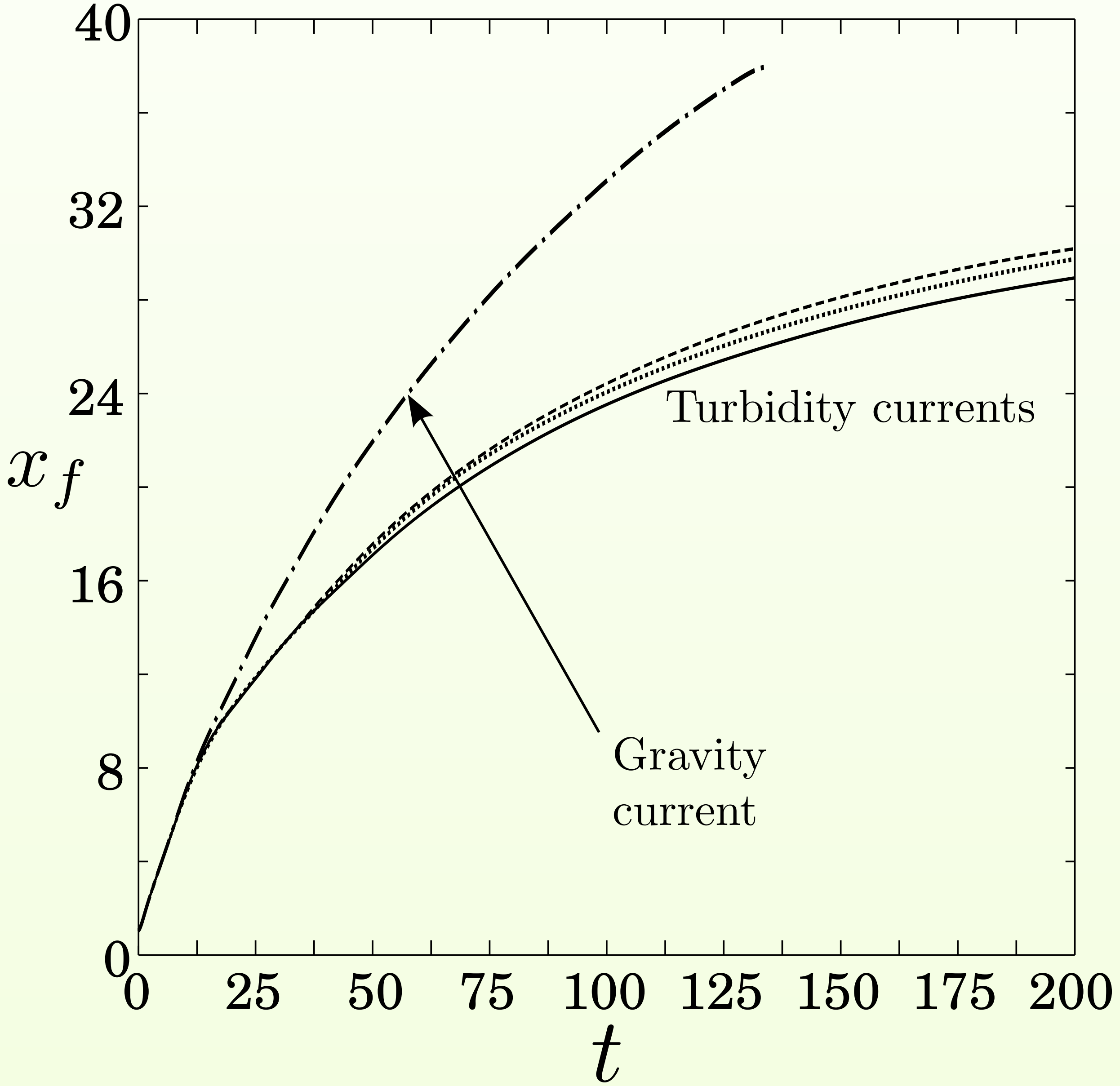

Influence of settling velocity

B2-GC: Similar to case B2, settling velocity set to zero

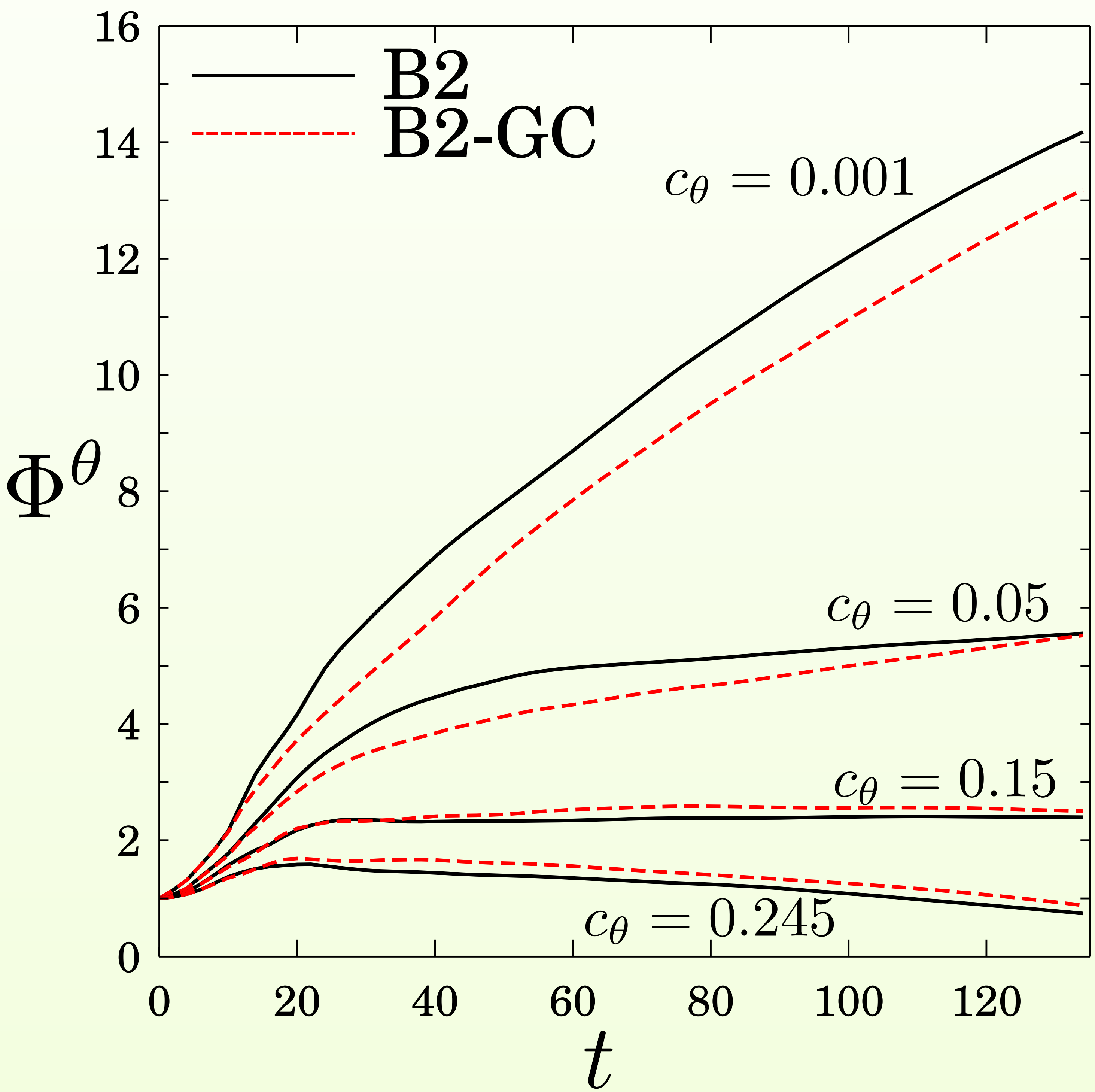

Despite traveling slower than B2-GC, dilute mixing is more pronounced in turbidity current (case B2)?

Influence of settling velocity

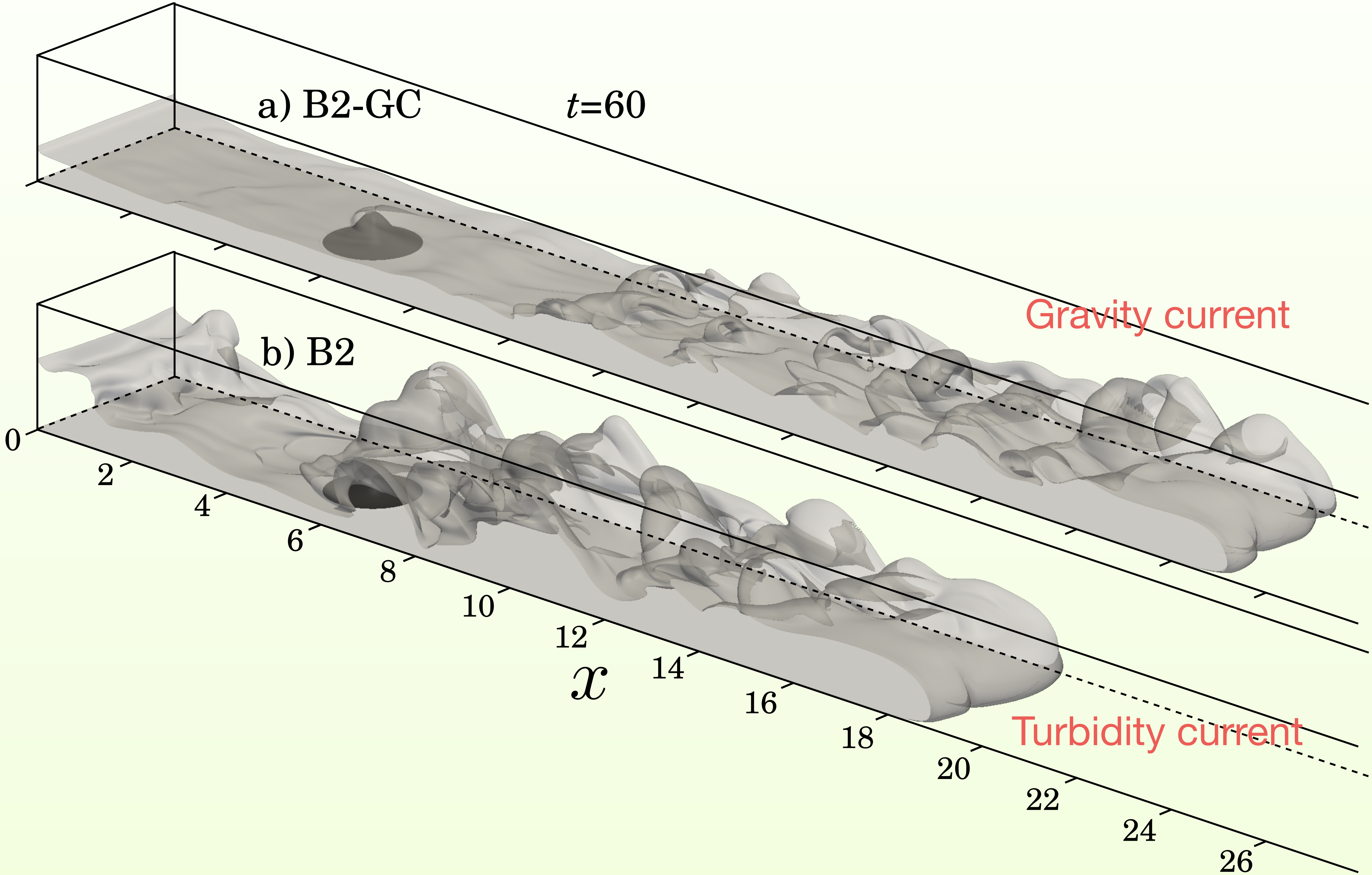

Mixing at the interfacial region

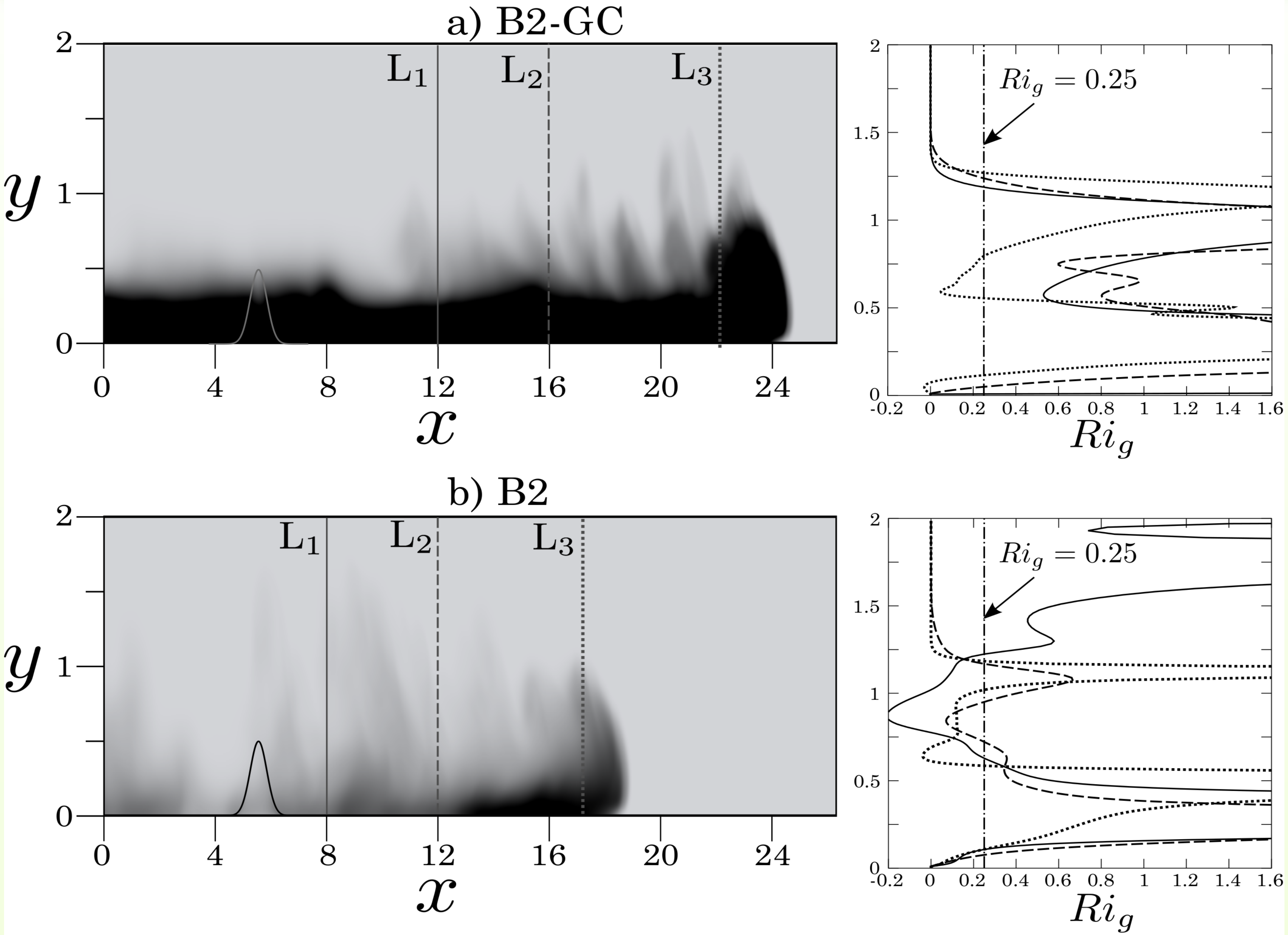

Mixing at the interfacial region

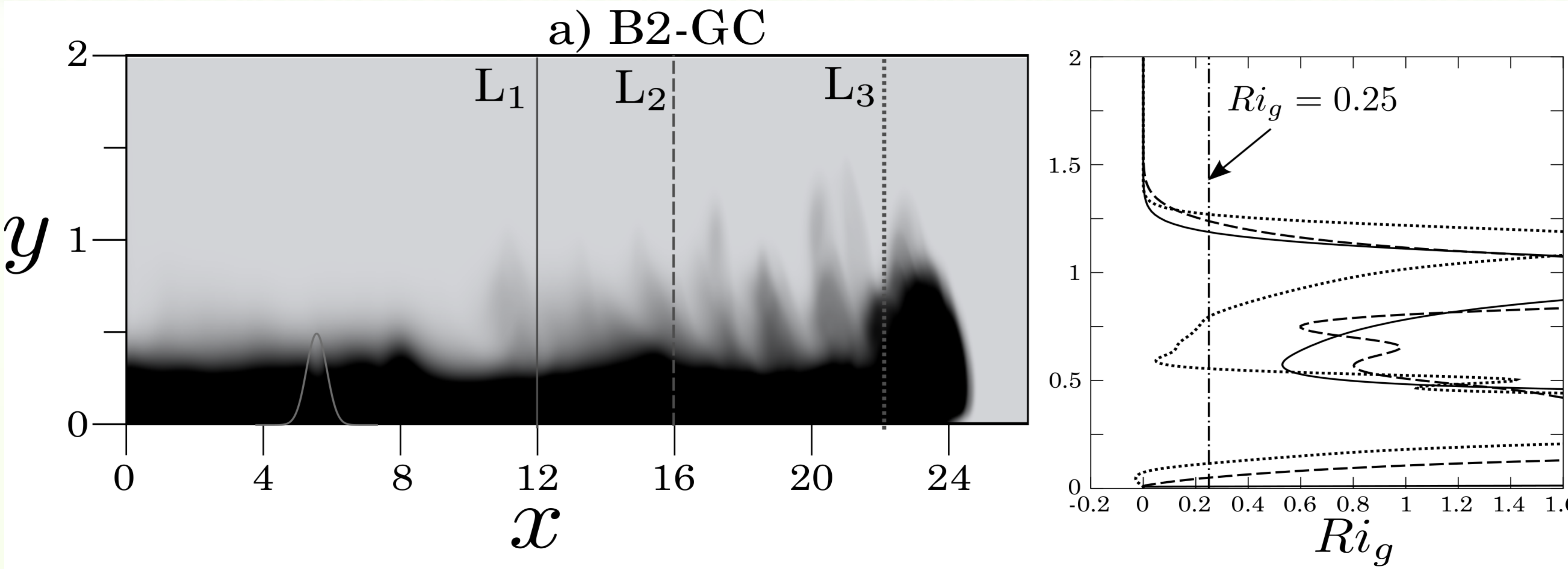

Gravity current: Demonstrate a stable interface everywhere (Ri > 0.25)
(exception: behind the nose region)

Mixing at the interfacial region

Turbidity current: Production of strong K-H instabilities. Causes the upper interface to become unstable and mixed (*Ri* < 0.25)

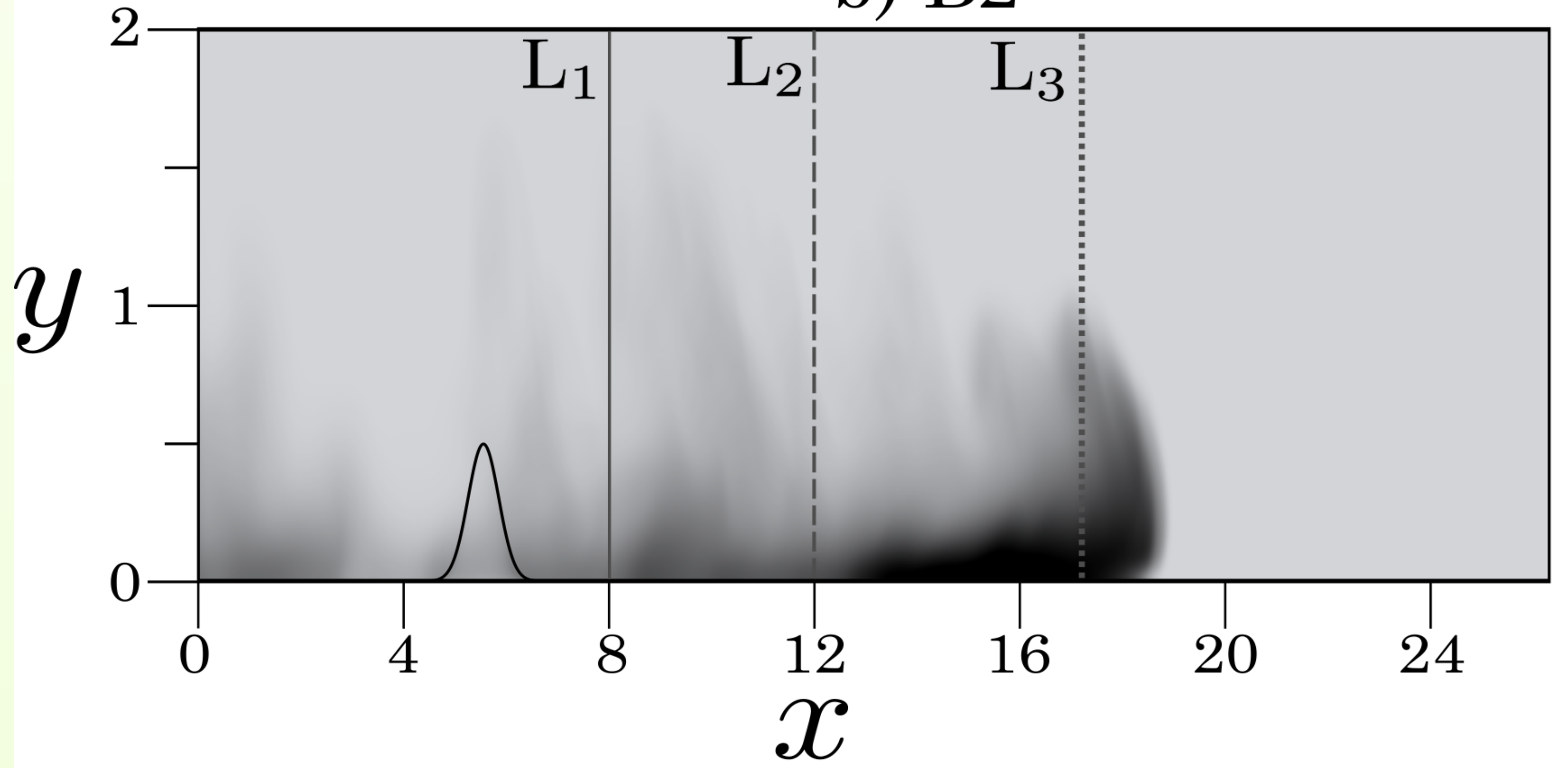

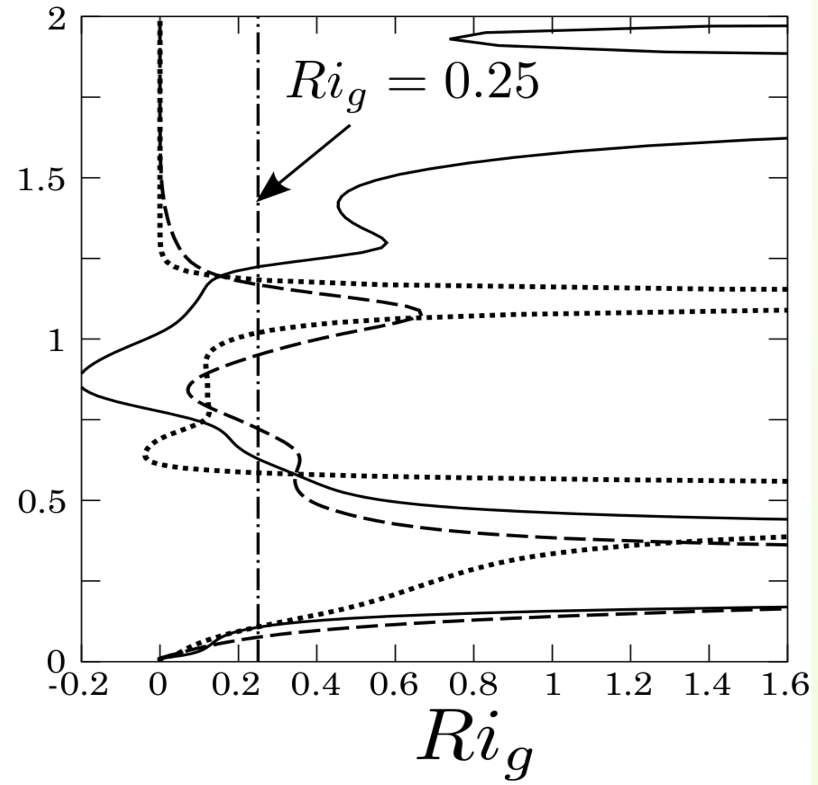

Mixing at the interfacial region

Doubly-averaged (in spanwise and streamwise directions) interstitial fluid

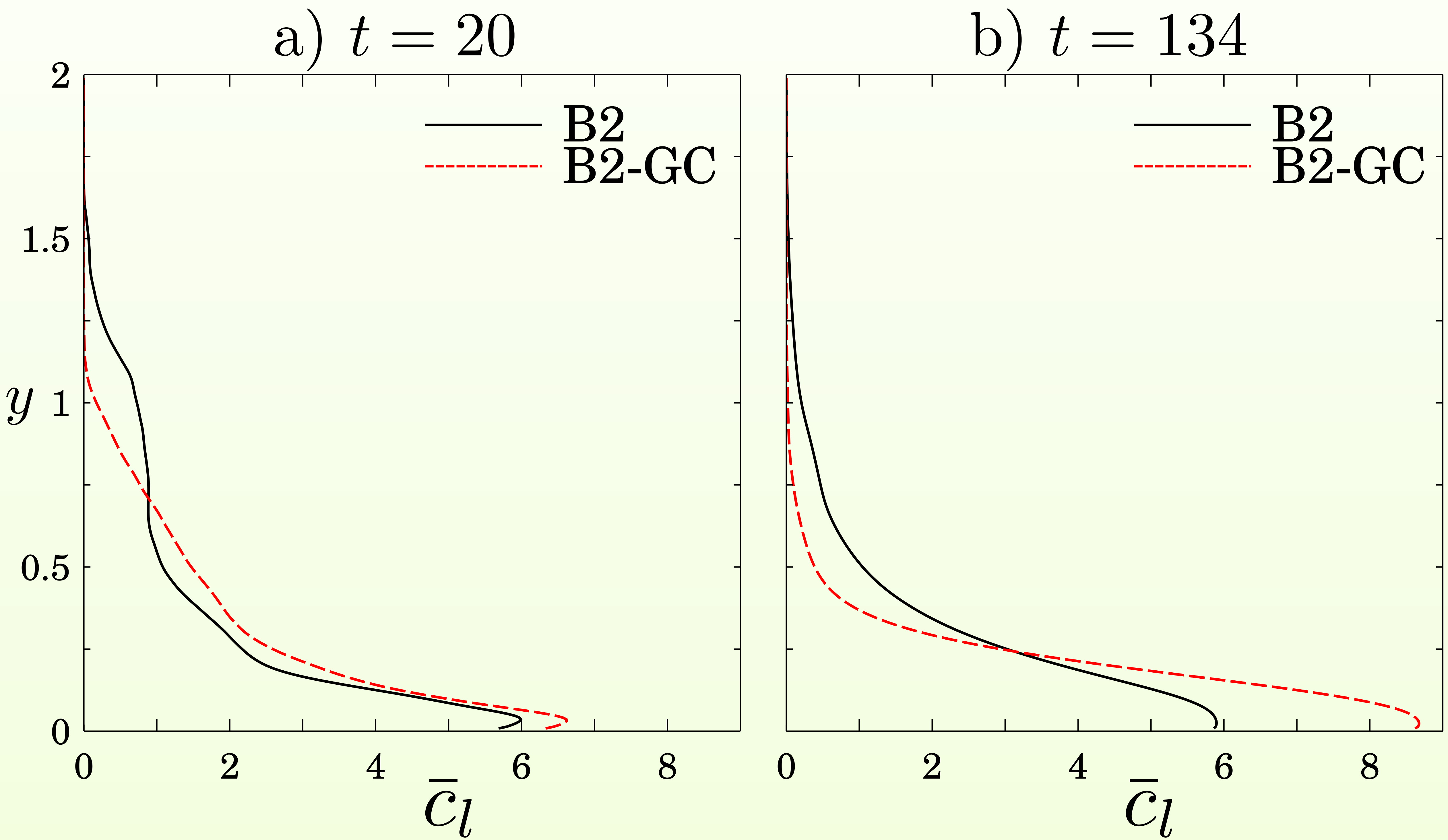

Mixing at the interfacial region

Doubly-averaged (in spanwise and streamwise directions) interstitial fluid

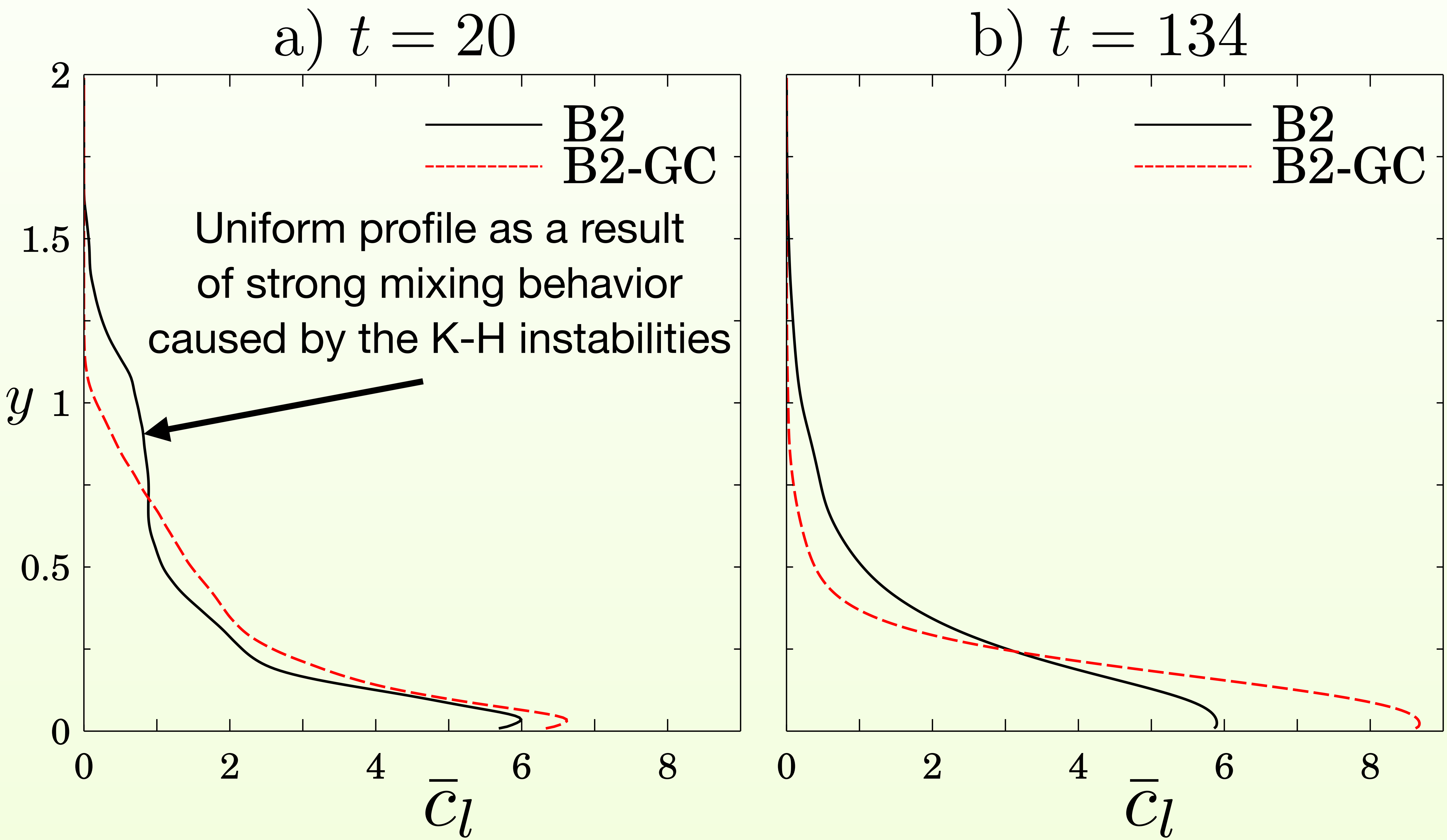

LONG-RANGE SEDIMENT TRANSPORT IN THE WORLD'S OCEANS BY STABLY STRATIFIED TURBIDITY CURRENTS

Benjamin Kneller*[1], Mohamad Nasr-Azadani[2], Senthil Radhakrishnan[2] and Eckart Meiburg[2]

[1]School of Geosciences, University of Aberdeen, UK
[2]Department of Mechanical Engineering, University of California at Santa Barbara, USA

Much of the sediment generated by erosion of the continents is delivered to the deep ocean, forming submarine fans that may extend thousands of kilometers across the continental slope and rise ([1]). A majority of the sediment supplied to the outer parts of submarine fans is carried by turbidity currents flowing through submarine channels (e.g. [2]). The persistence of these flows over long distances with gradients that may be 10^{-4} or less, while maintaining sediment in suspension, is enigmatic. The widely-held view of

In preparation: B. Kneller, M. M. Nasr-Azadani, S. Radhakrishnan, and E. Meiburg

Mixing at the interfacial region

Could suppression of turbulence at the interfacial region (in this example, for a gravity current with zero settling velocity) be a reason for the enigmatic existence of long range turbidity currents observed in nature?

Table 1: Parameter ranges reported for distal regions of three large submarine fans

	Congo	Amazon	Bengal
Gradient of distal channel reaches	$0.11°$ [16]	$0.11°$ [27]	$0.05°$ [2]
Length of channel	1,100 km [28]	900 km [27]	2,500 km [2]
Median sediment grain-size*	125-250 μm [29]	125-250 μm [27]	20-62 μm [30]
Approximate height of distal levees	70m [16]	50m [27]	30m [2]
Velocity	0.7 m/s [16]	1.2 m/s [27]	

*: 31-62 μm dominant on levees; silt dominates suspended load high in flow [16] [27].

In preparation: B. Kneller, M. M. Nasr-Azadani, S. Radhakrishnan, and E. Meiburg

Part I: Influence of bottom slope

Inlet Fr = 0.78

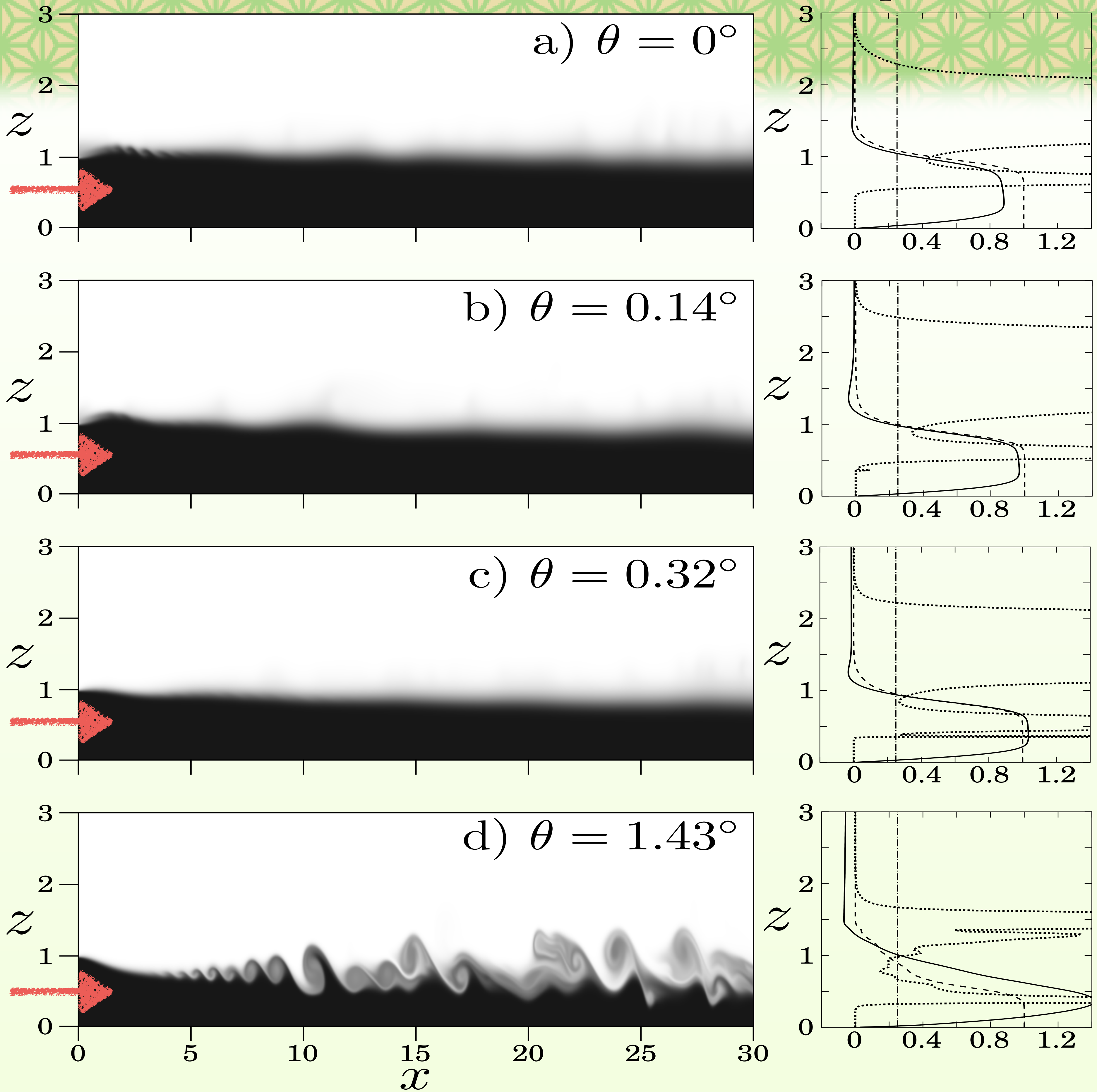

Part I: Influence of bottom slope

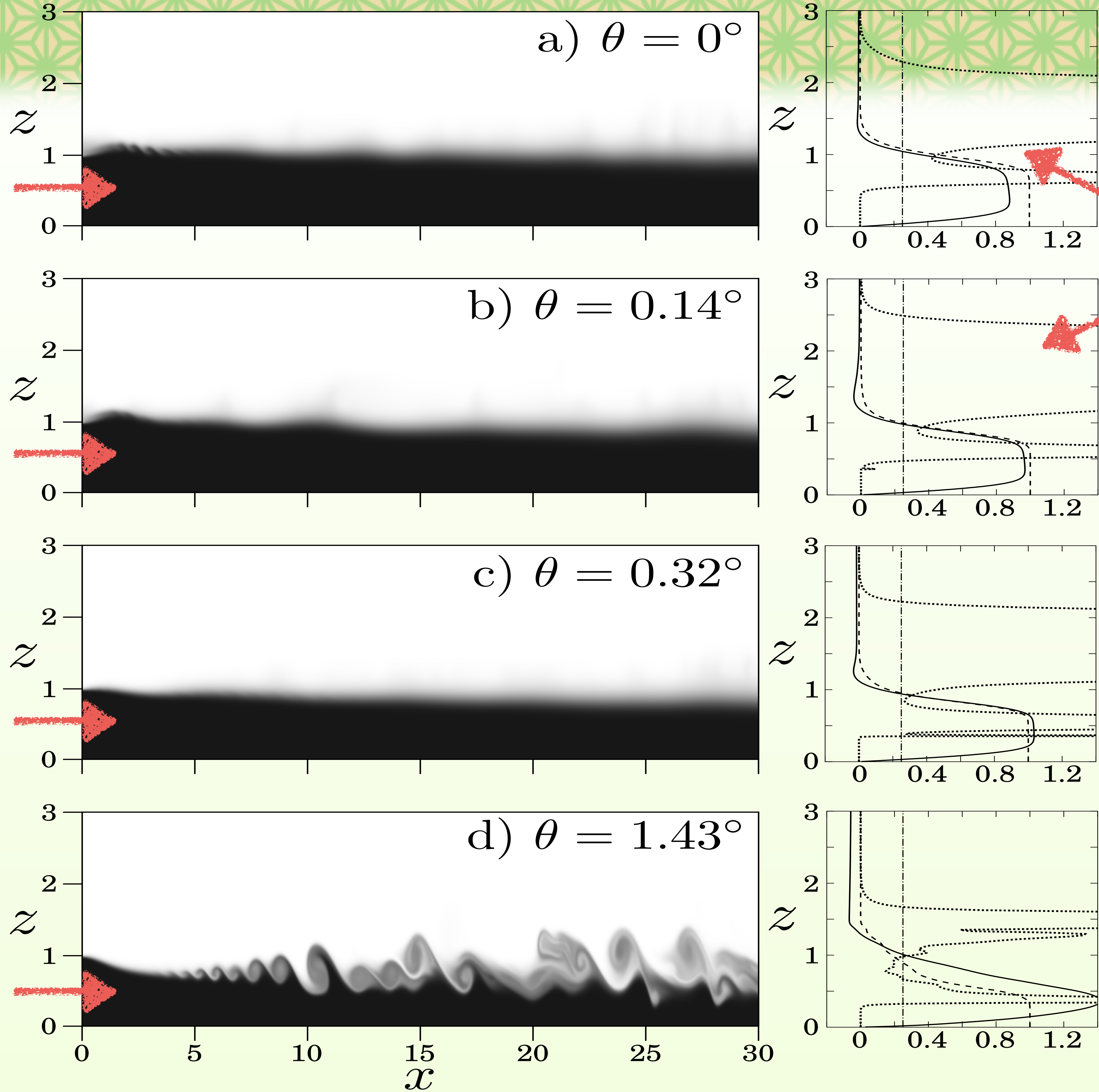

Inlet Fr = 0.78

Suppression of
K-H instabilities
at the upper interface
Ri < 0.25

Part I: Influence of bottom slope

Inlet Fr = 0.78

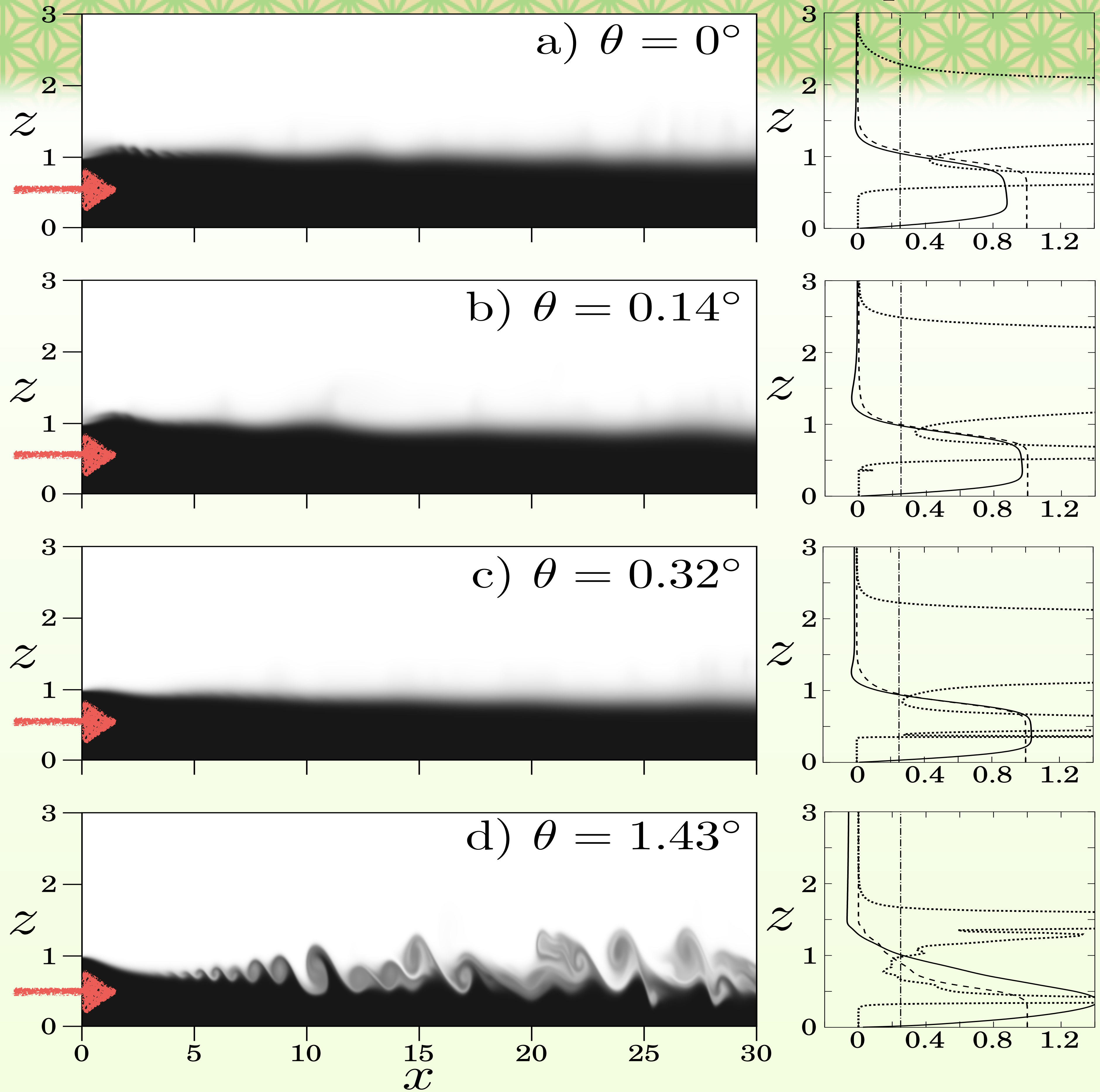

Velocity profile:
very different behavior

Part II: Influence of particle settling velocity

Inlet Fr = 0.78

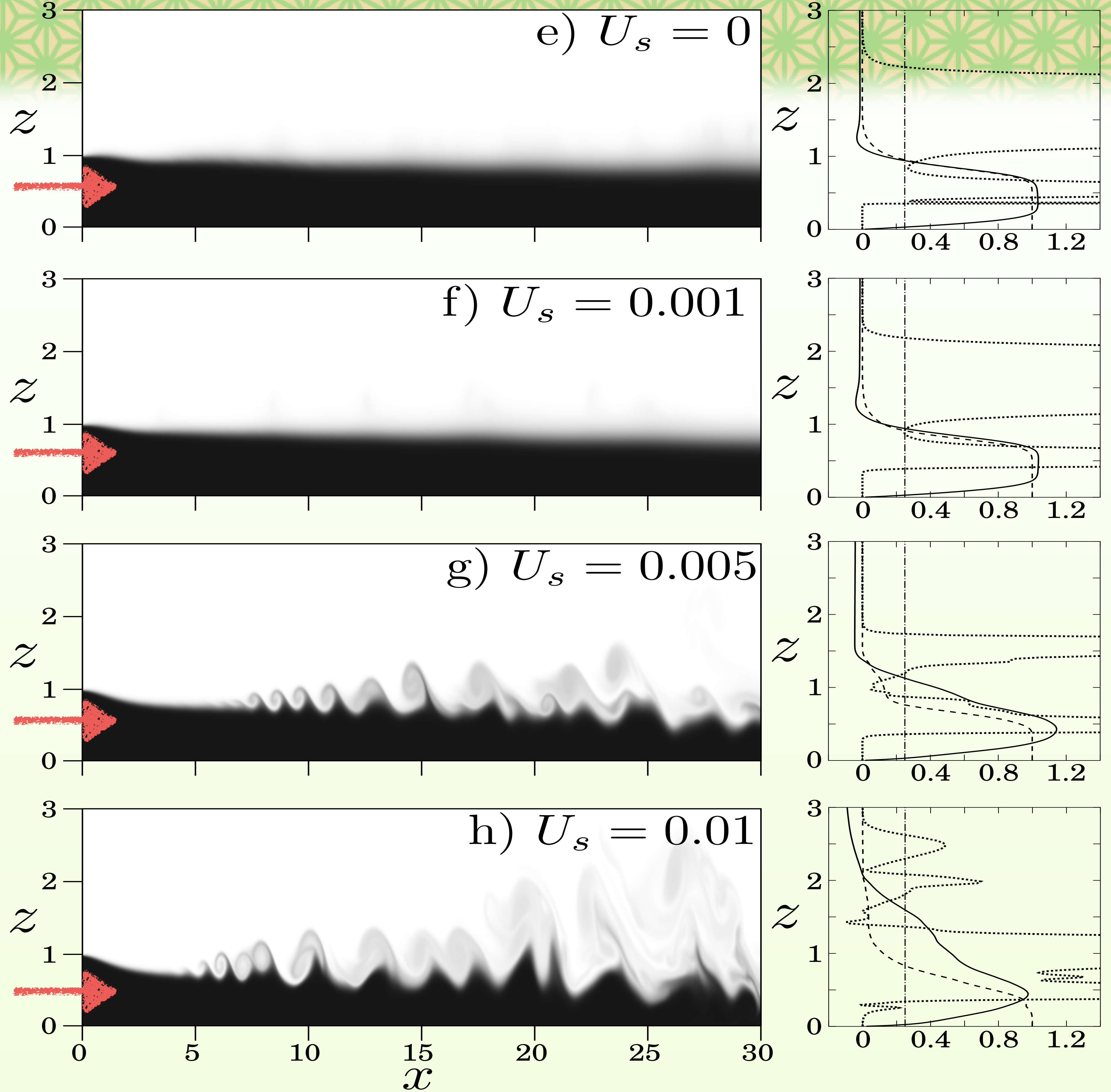

Inlet Fr = 0.78

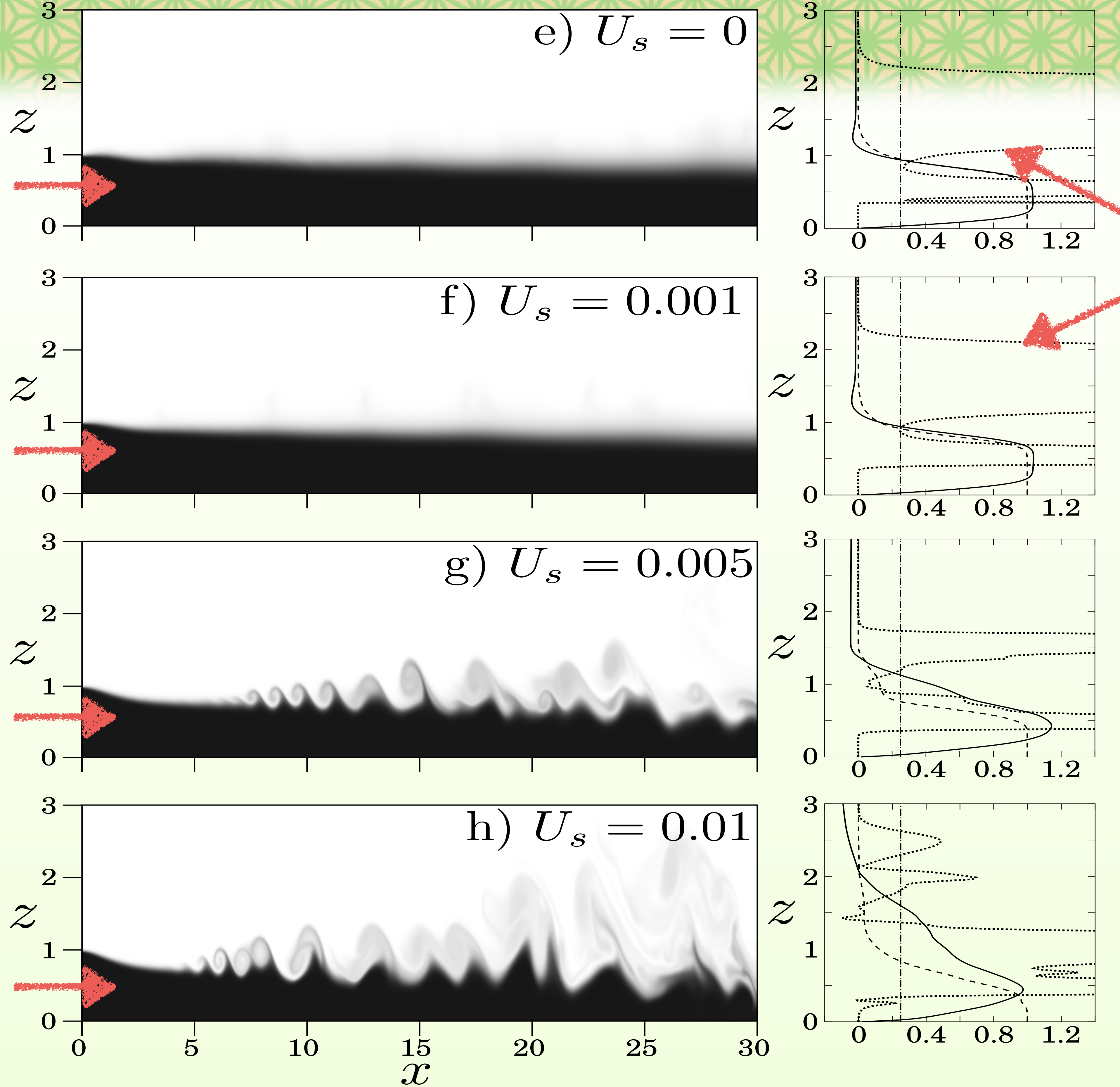

Suppression of K-H instabilities (and turbulence) at the upper interface: $Ri < 0.25$

Three-dimensional simulations: LES

Lock-exchange configuration

Gravity current
Reynolds: 100,000
Us=0

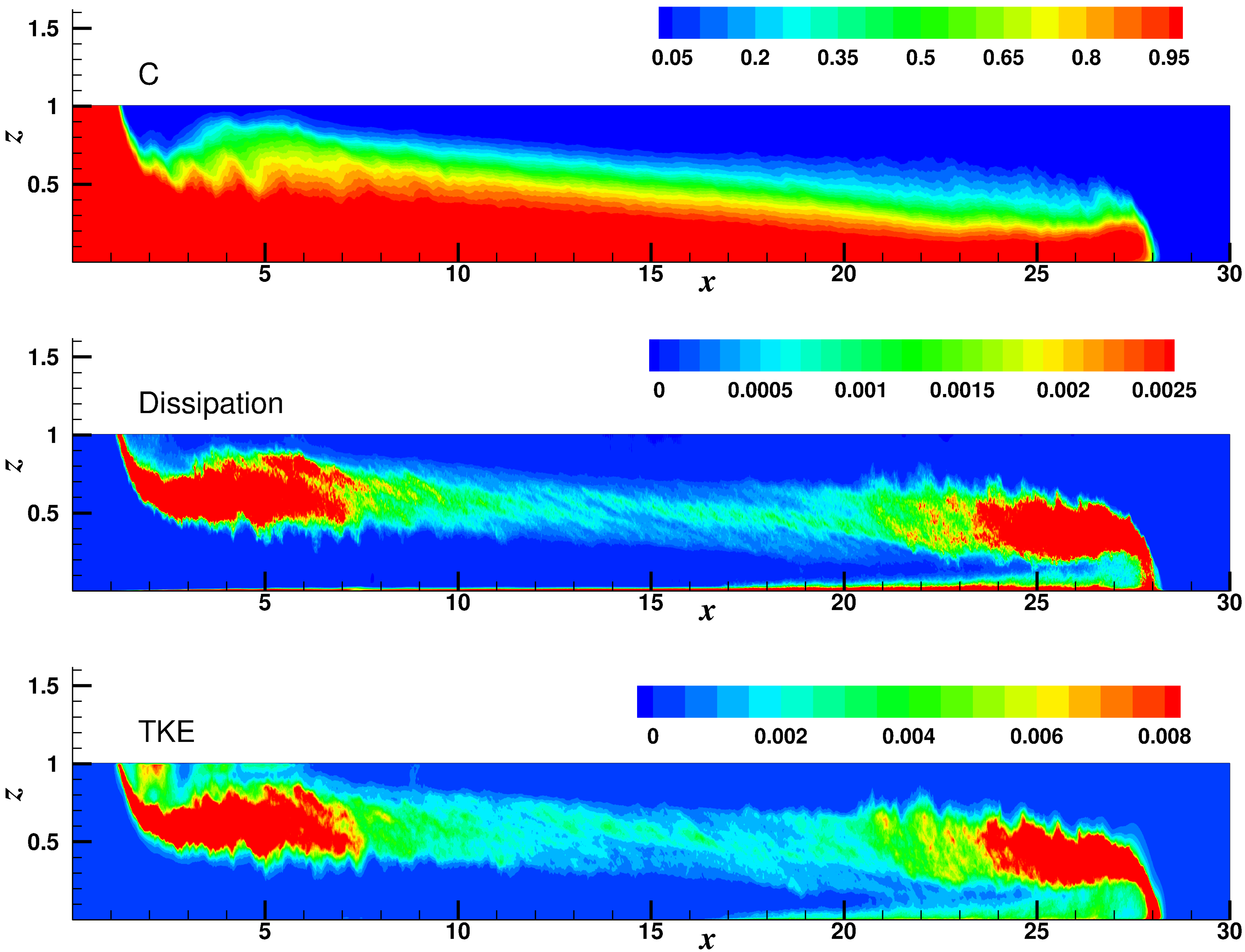

Three-dimensional simulations: LES

Lock-exchange configuration

Turbidity current
Reynolds: 100,000
Us = 0.02

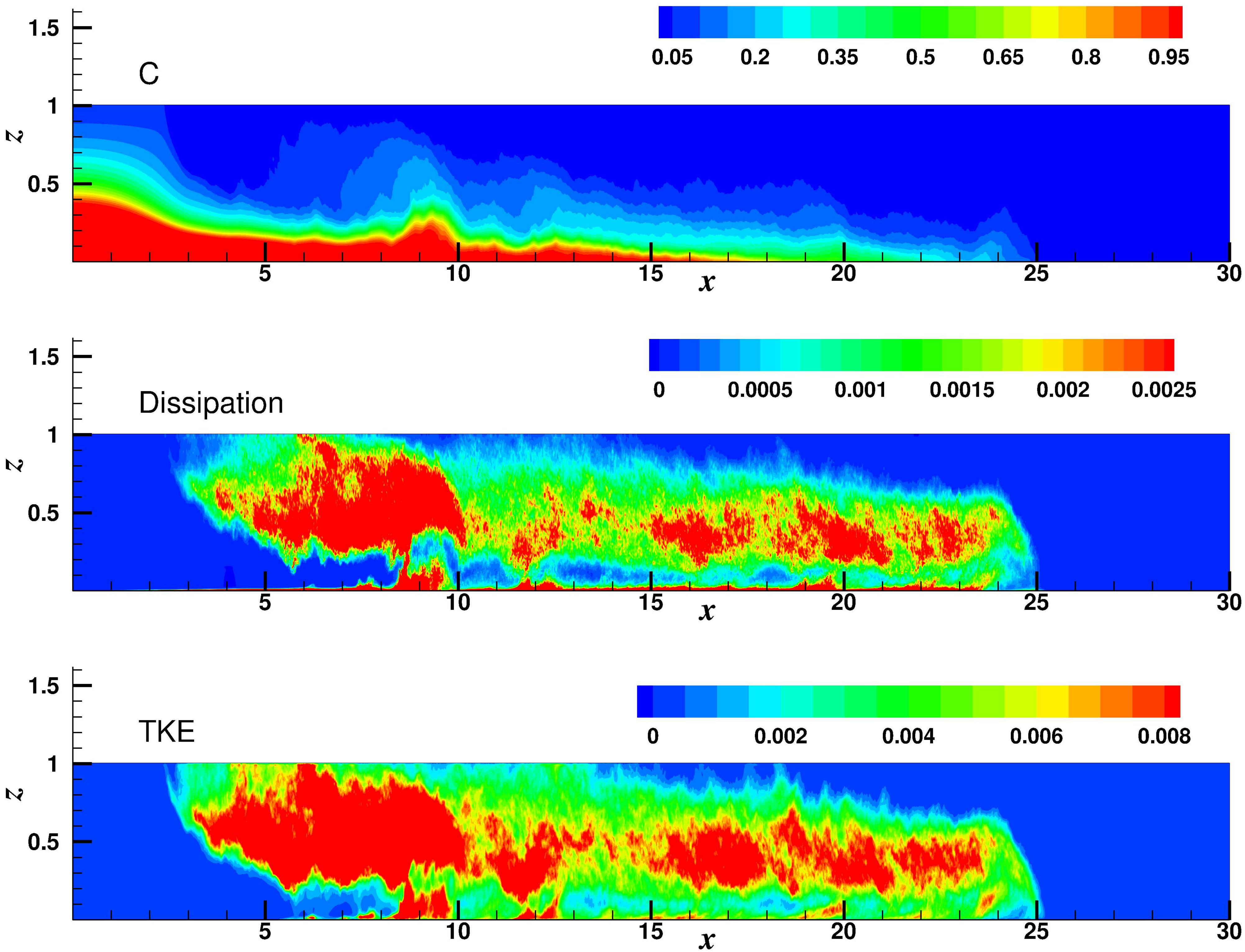

Three-dimensional simulations: LES

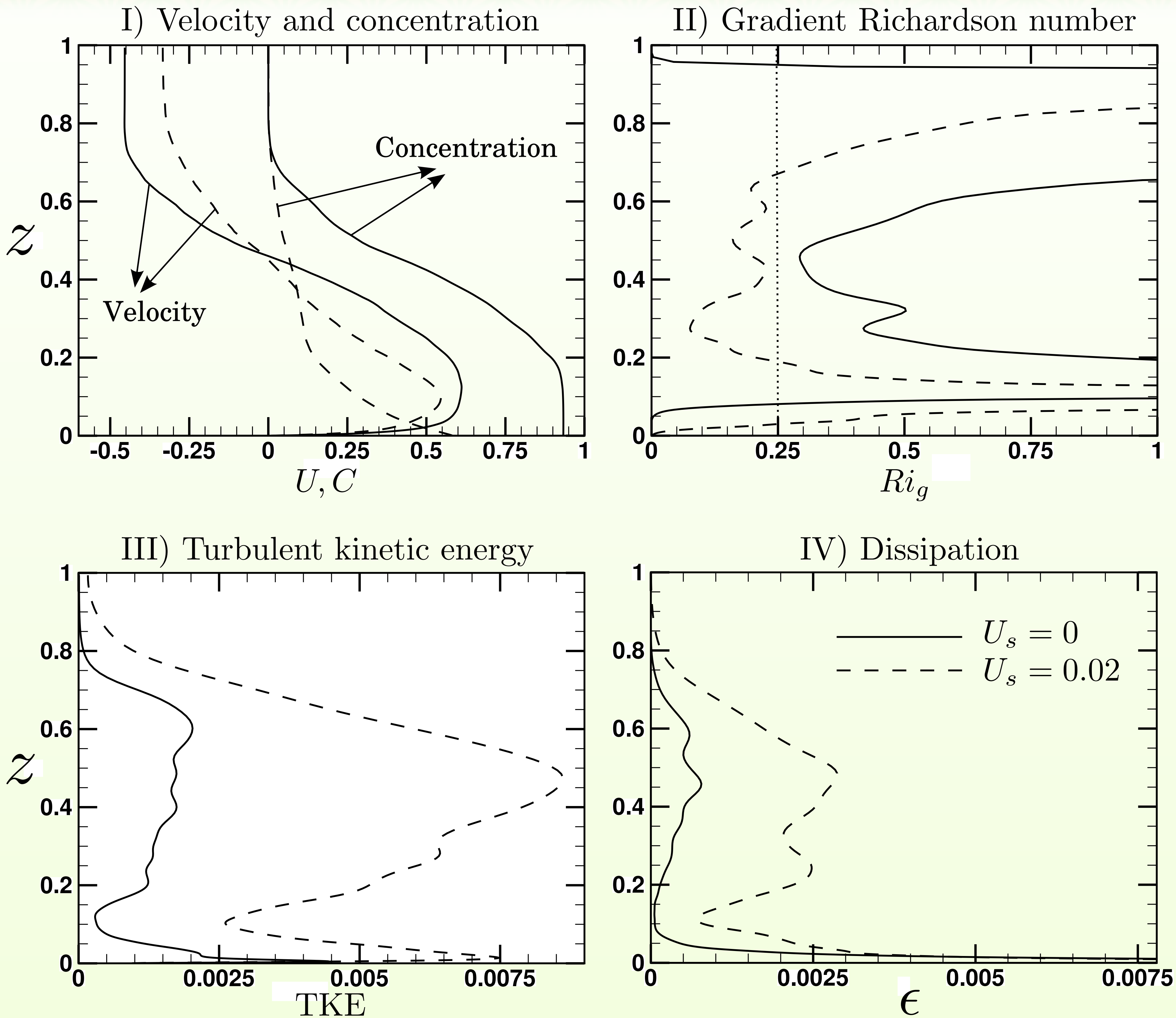

Three-dimensional simulations: LES

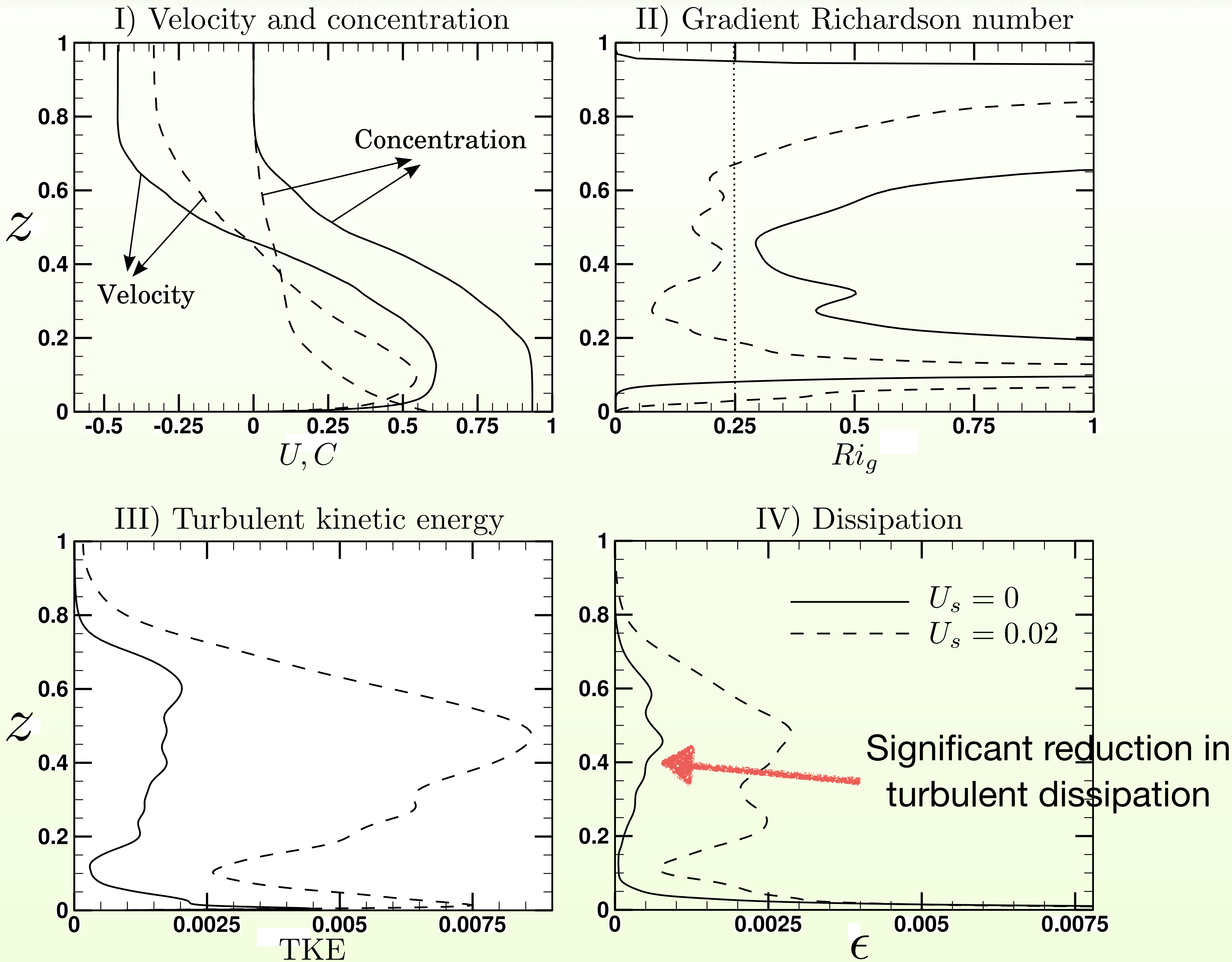

Sub-summary:

- Stability of upper interface in a gravity/turbidity current may play an important role in energy dissipation and, ultimately, the runout length of turbidity currents
- Unlike status quo definitions, i.e. utilizing bulk Froude/Richardson number for sub- vs. super-critical turbidity currents, it may be versatile to use gradient Richardson number as a way of identifying the behavior for these currents

Problem setup

Sim.	h	(x_b, z_b)	Re	(L_x, L_y, L_z)
FL	0.0	N/A	2000	(38,2,3)
B1	0.25	(5.5,1.5)	2000	(38,2,3)
B2	0.5	(5.5,1.5)	2000	(38,2,3)

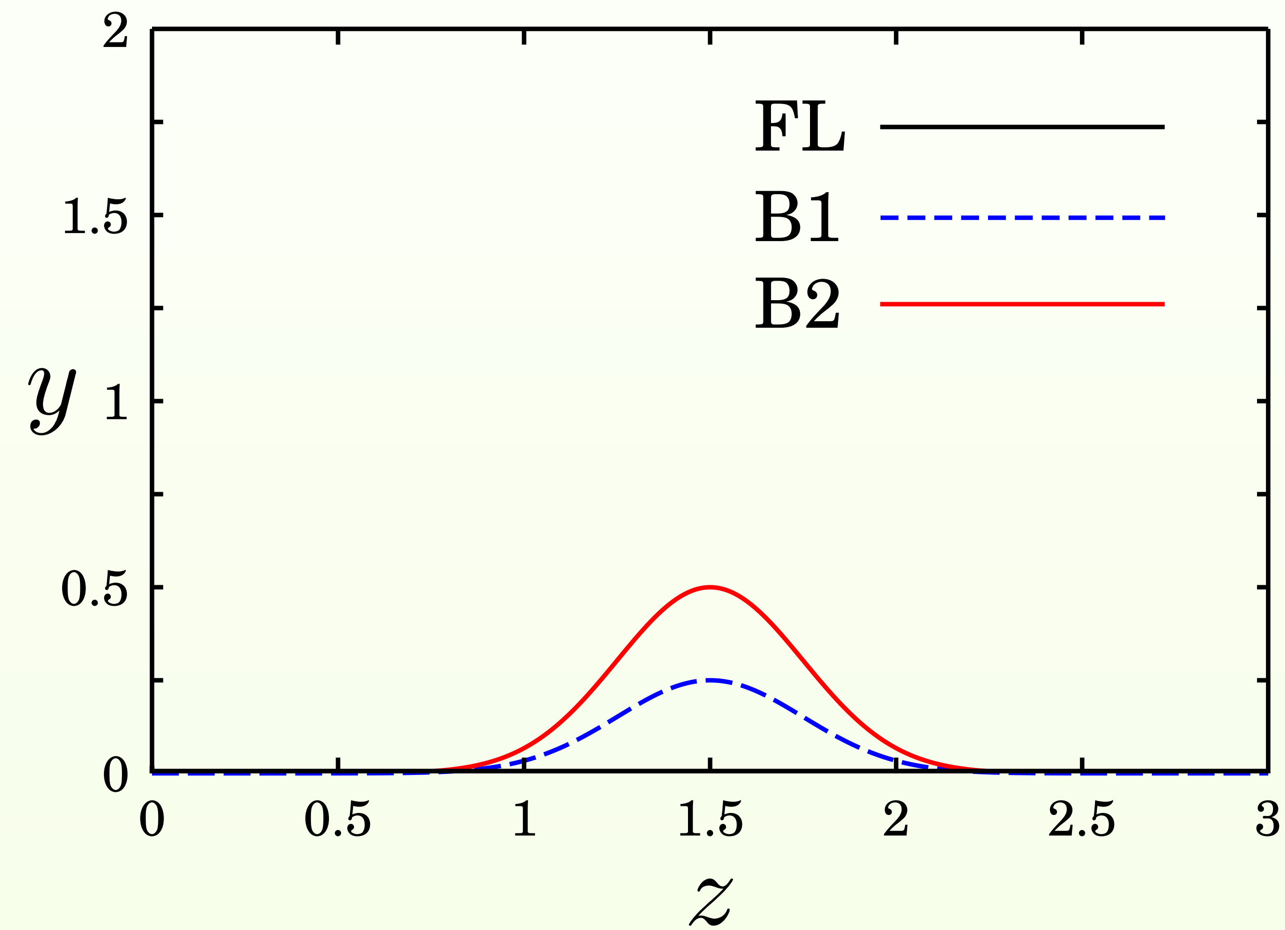

Two particle sizes:

1. Coarse particles (50%):

$$u_s^c = 0.03$$

2. Fine particles (50%):

$$u_s^f = 0.006$$

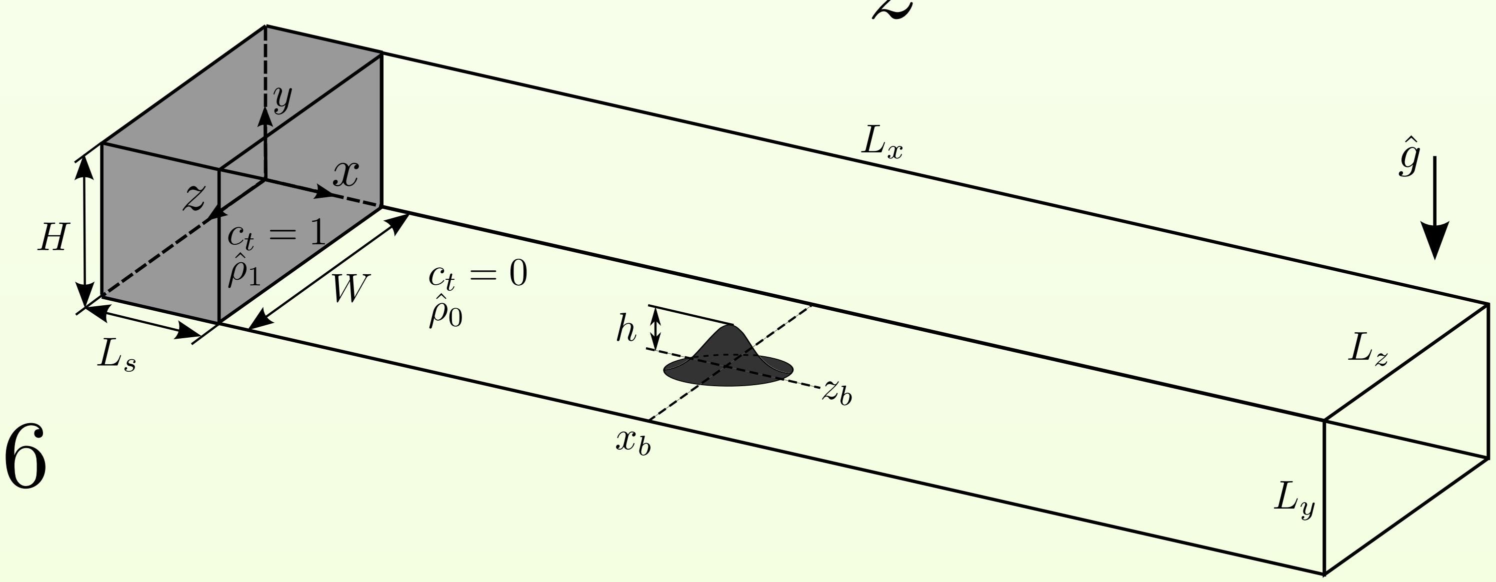

Influence of Reynolds number

Case B2-GC: Re=2000 & Re=5000

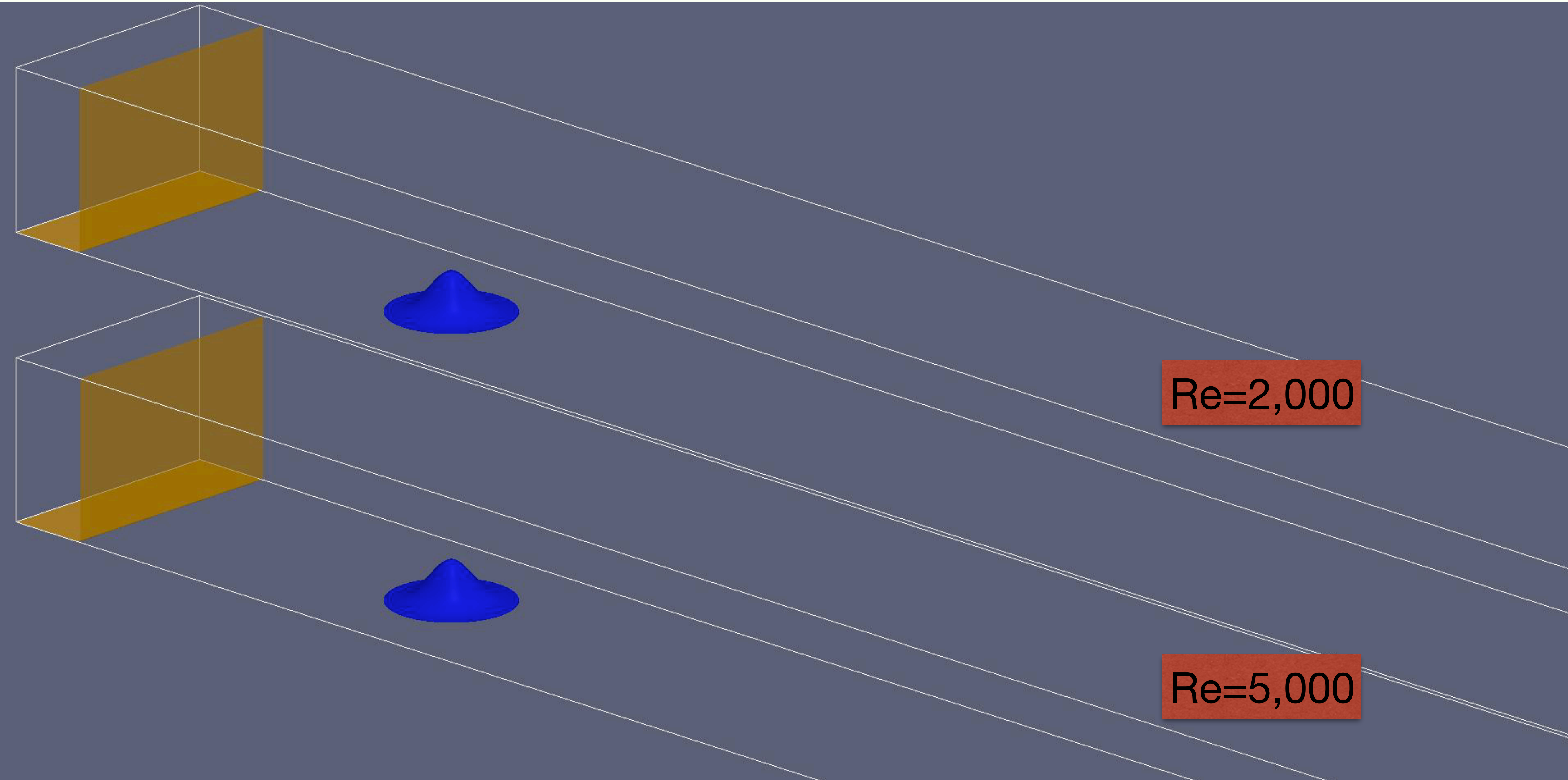

Influence of Reynolds number

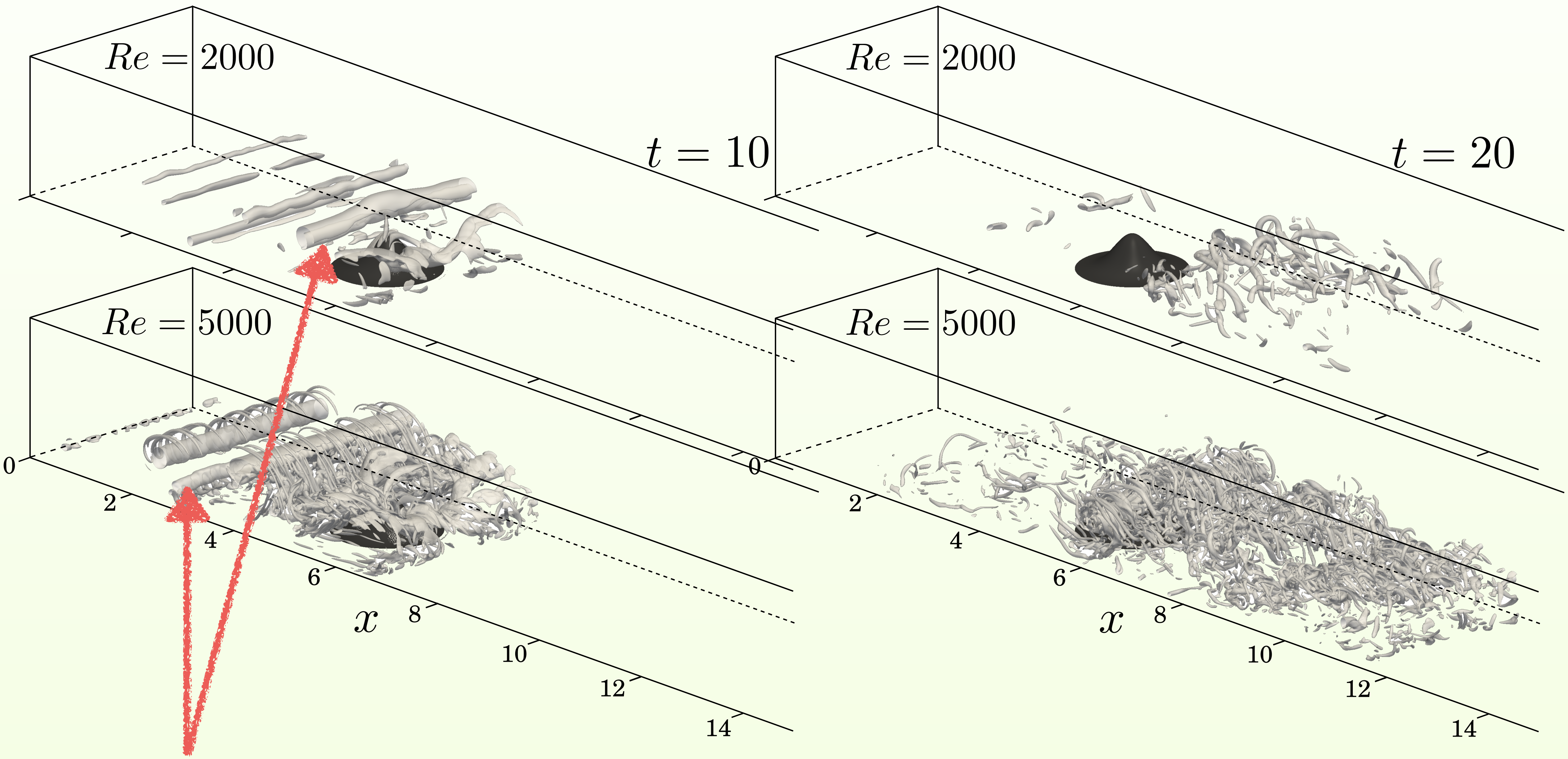

B2-GC case at Re = 2, 000 and Re = 5, 000.

Initial 2D-structures demonstrate similar behavior

Influence of Reynolds number

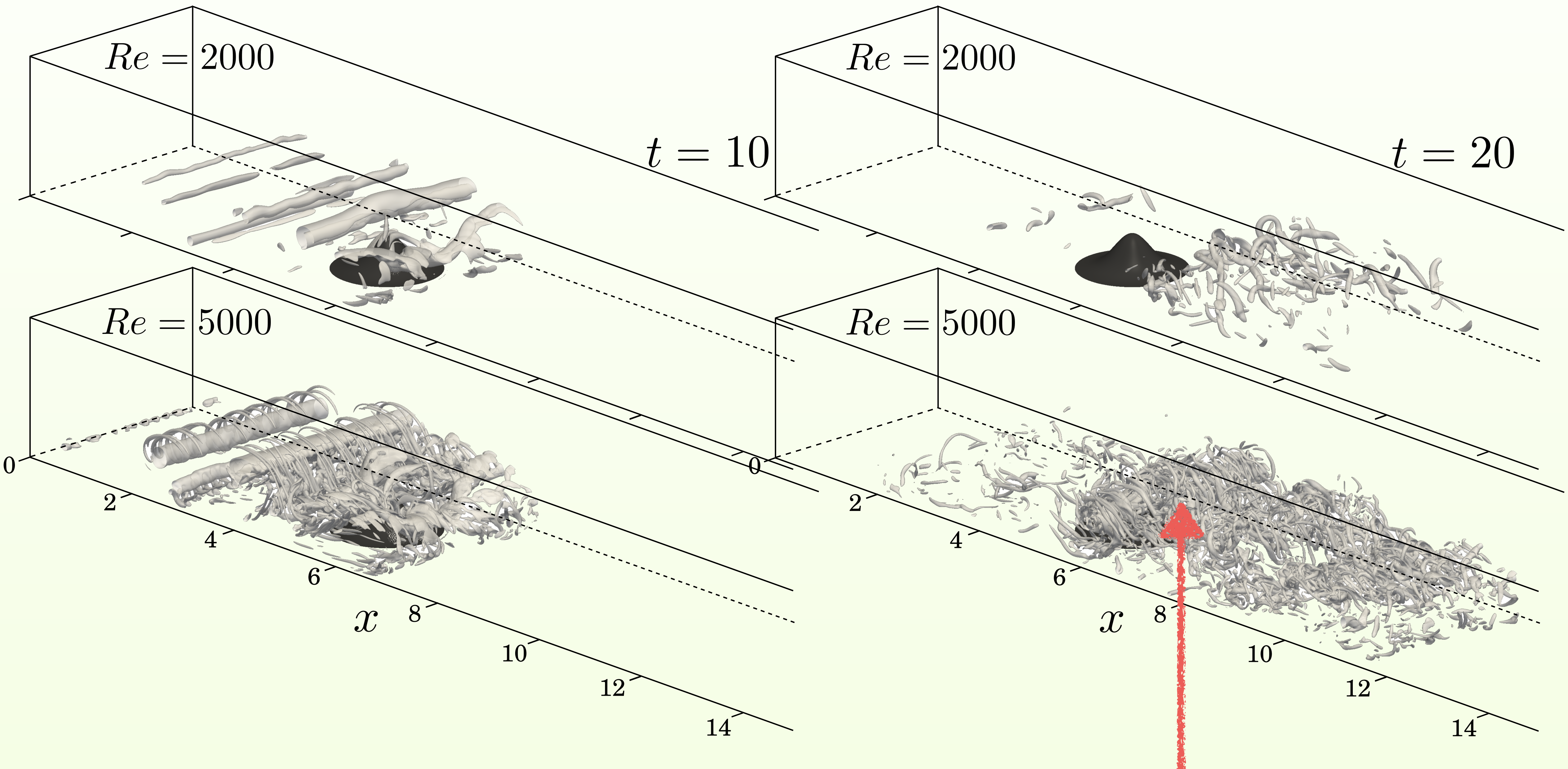

B2-GC case at Re = 2, 000 and Re = 5, 000.

Production of fine scales after the interaction of the current with the bump

Lobe-and-cleft structures

B2-GC: Gravity current

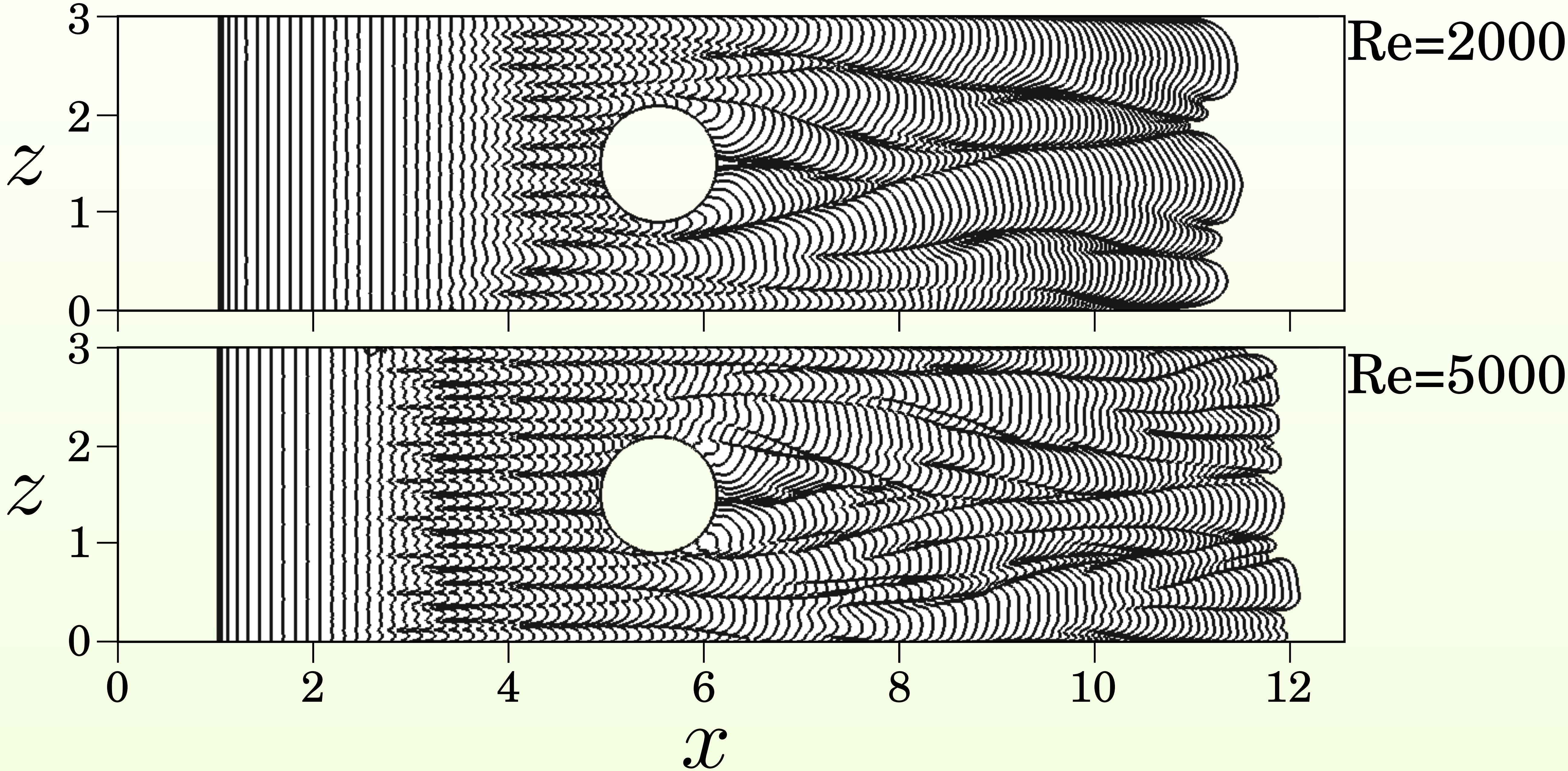

Very good agreement observed with predictions made by linear-stability analysis

Härtel *et al.* (2000), ***J. Fluid Mechanics***.

Mixing: Interstitial fluid

B2-GC: Gravity current

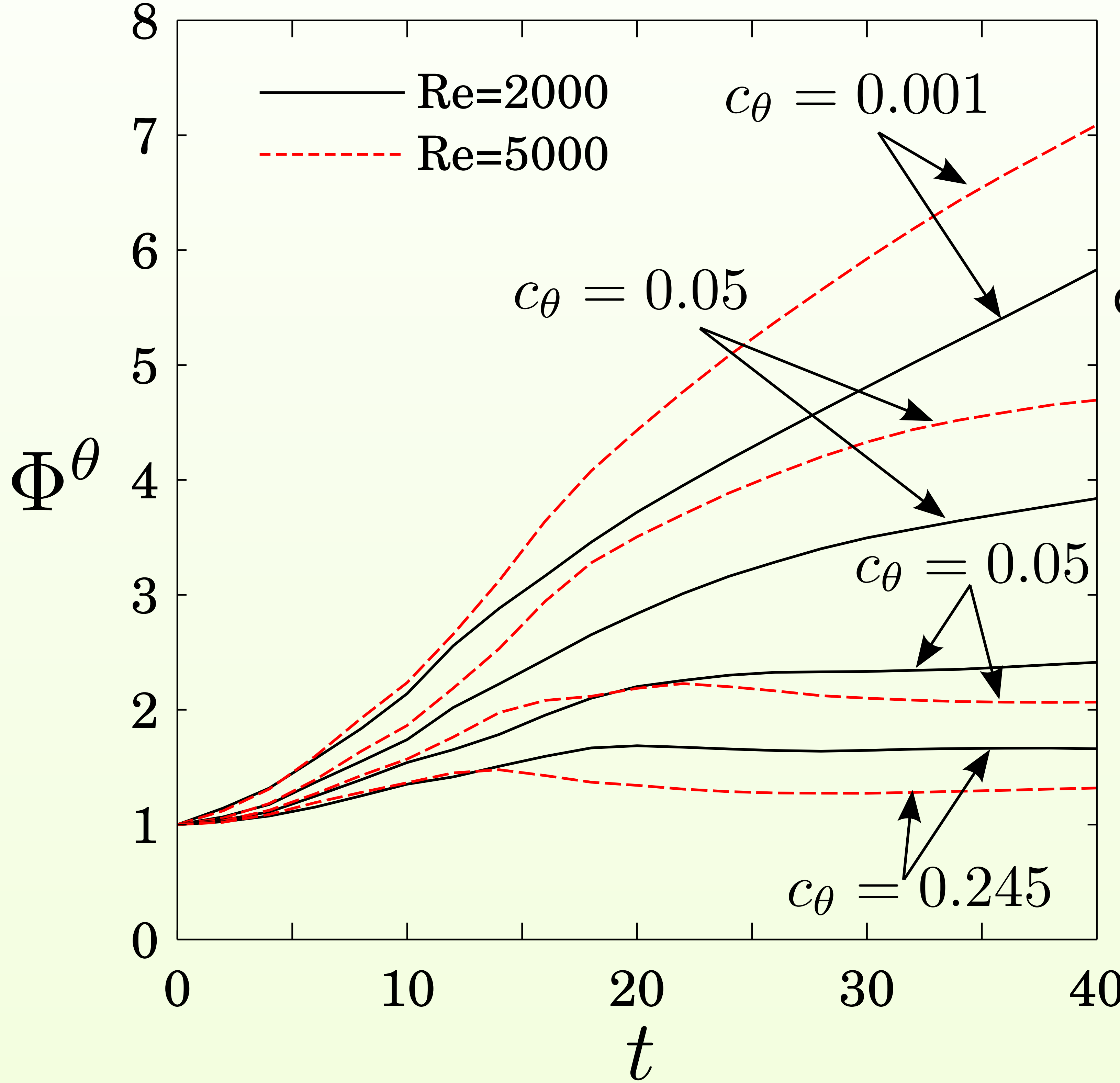

Enhanced dilute mixing

A closer look: Vicinity of the bump

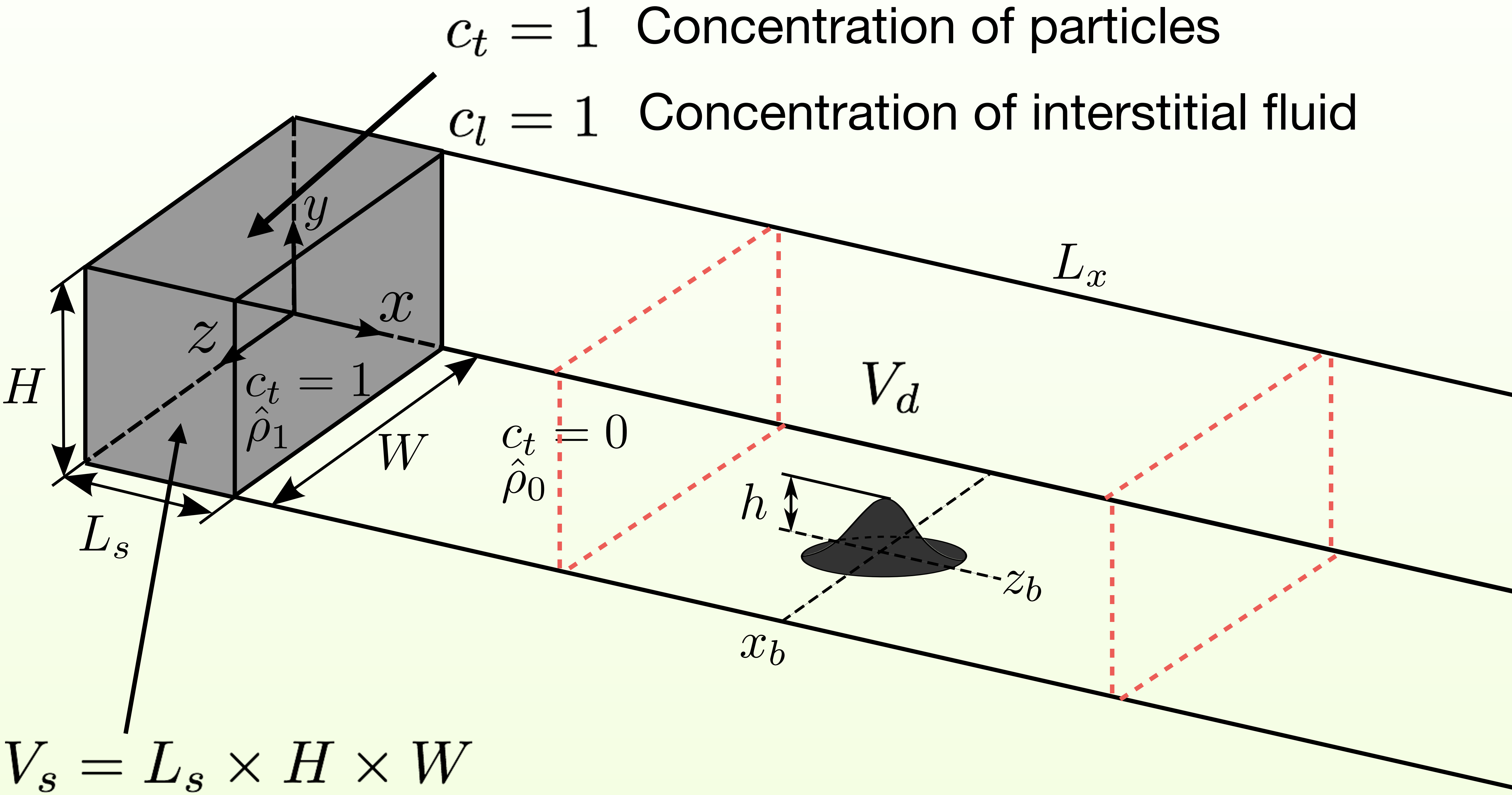

Mixing & unmixing

Mixing of ambient fluid with particles

$$\Theta = \frac{1}{V_s(V_d - V_s)/V_d} \int_{V_d} c_t(1 - c_l)\ \mathrm{d}V$$

Mixing of ambient fluid with interstitial fluid

$$\Phi = \frac{1}{V_s(V_d - V_s)/V_d} \int_{V_d} c_l(1 - c_l)\ \mathrm{d}V$$

Unmixing of particles and interstitial fluid

$$\Lambda = \frac{1}{V_s} \int_{V_d} (1 - c_t)c_l\ \mathrm{d}V$$

Mixing and unmixing

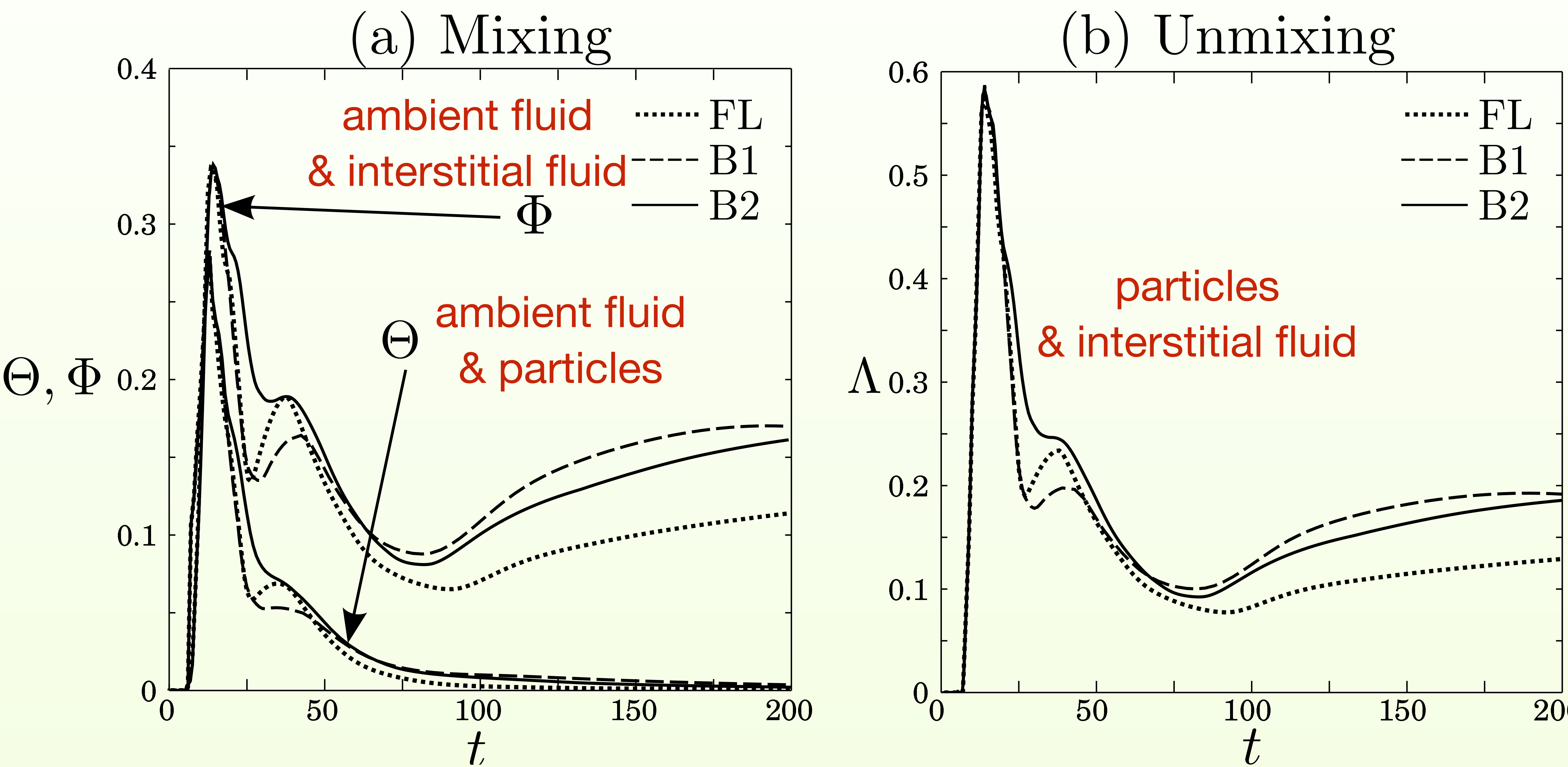

Summary

- High resolution DNS simulations of turbidity currents interacting with seafloor topography
- Investigated the effect of bump height on front location, vortical structures, and resulting mixing/unmixing behavior

Nasr-Azadani, M.M., & Meiburg, E. (2013). Influence of seafloor topography on the depositional behavior of bi-disperse turbidity currents: A three-dimensional, depth-resolved numerical investigation. ***Envi. Fluid Mechanics***.

Nasr-Azadani, M.M., & Meiburg, E. (2015). Turbidity currents interacting with three-dimensional seafloor topography. ***J. Fluid Mechanics***.

Nasr-Azadani, M.M., & Meiburg, E. (2016). Mixing dynamics of turbidity currents interacting with complex topographies. (Under review).

Mixing and entrainment at the interface of lock-release gravity currents: a comparison between laboratory experiments, Large Eddy Simulations and Direct Numerical Simulations

C. Cenedese[5], K. Bhaganagar[1], R. Nokes[2] , J. Hyatt[3] , M. M. Nasr-Azadani[4], M. Nayamatullah[1] , and E. Meiburg[4]

[1] University of Texas at San Antonio, [2] University of Canterbury, [3] Massachusetts Maritime Academy,
[4] University of California at Santa Barbara, [5] Woods Hole Oceanographic Institute

Entrainment in dense currents

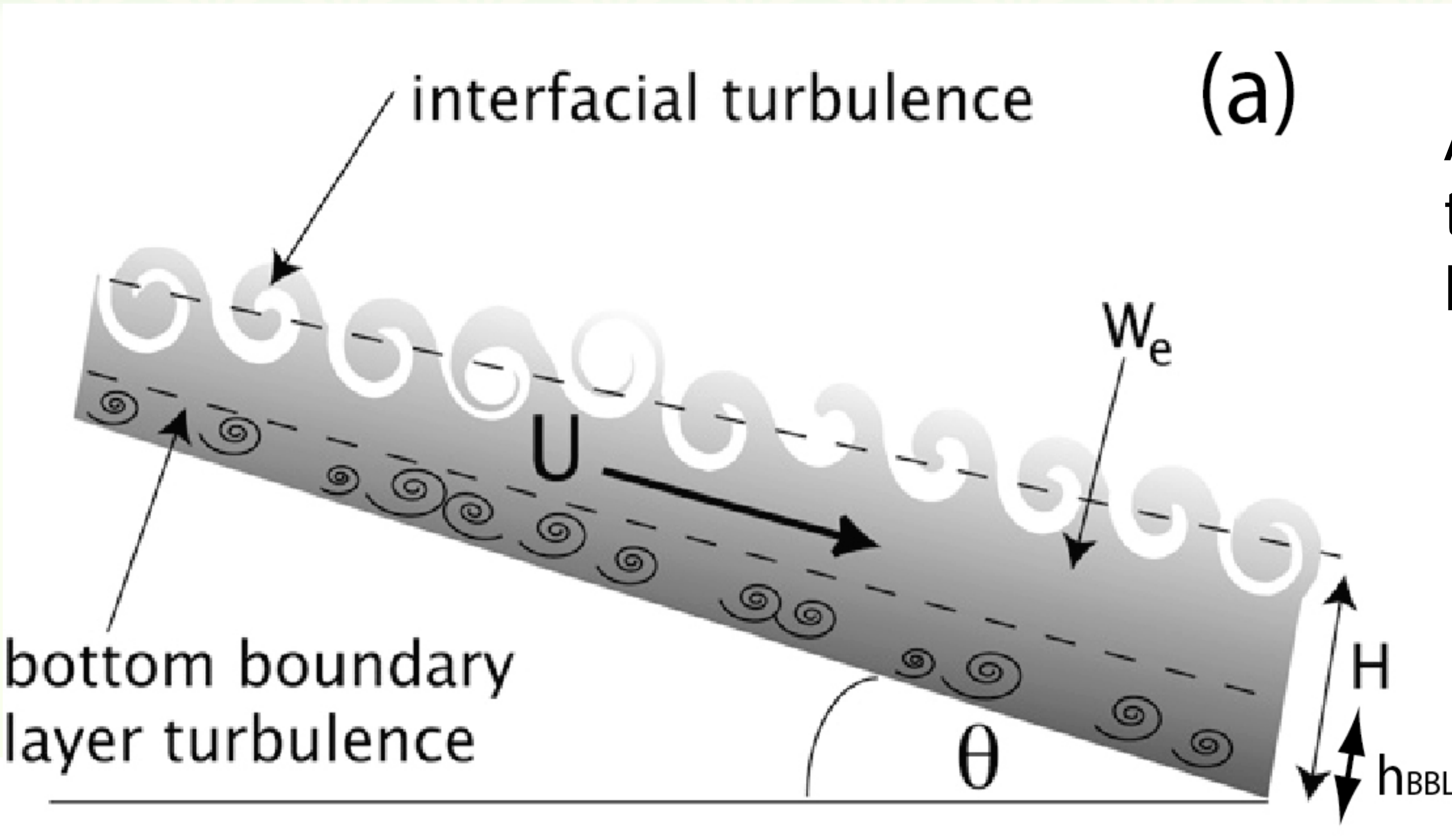

Assume entrainment is confined at the interface of the current, i.e. bottom drag does not influence entrainment.

Wells, Cenedese & Caulfield, JPO 2010

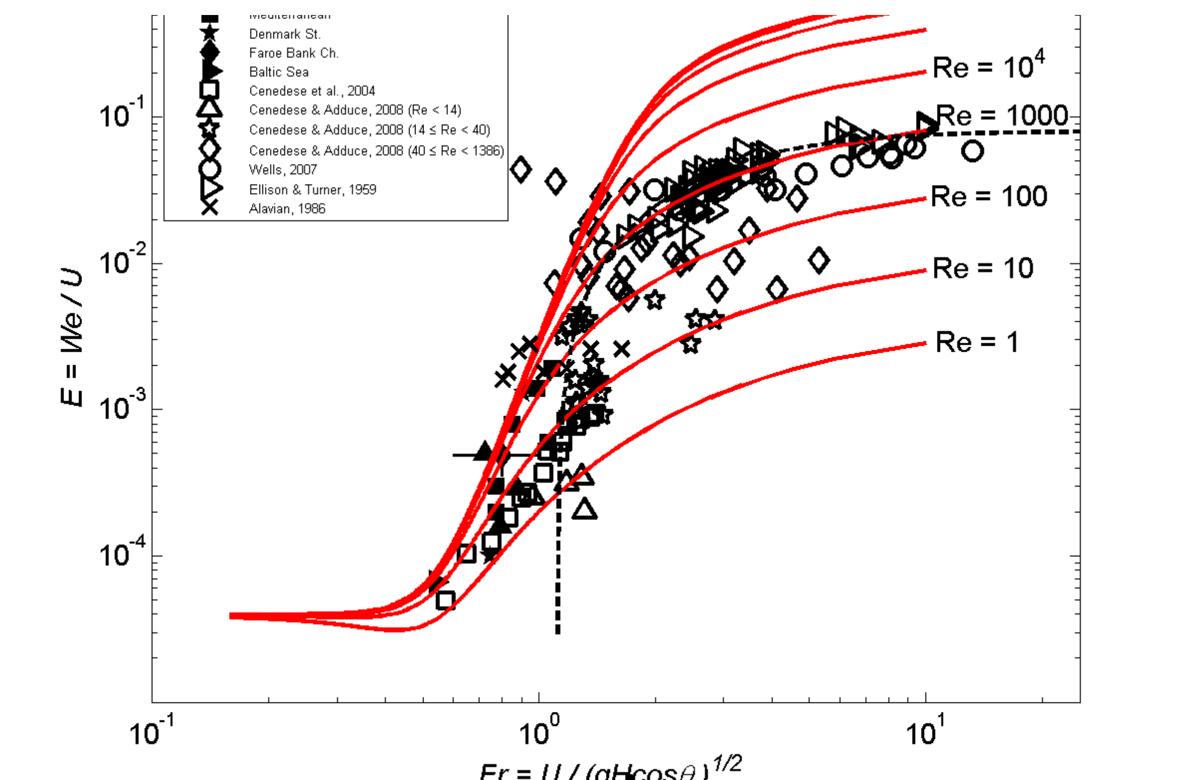

$$E_{new} = \frac{\mathrm{Min} + A Fr^{\alpha}}{1 + A C_{\inf} (Fr + Fr_0)^{\alpha}}$$

where :

$$A = 3.4\,10^{-3} \qquad \alpha = 7.18 \qquad Fr_0 = 0.51$$

$$C_{\inf} = \frac{1}{\mathrm{Max}} + \left(\frac{243.52}{\mathrm{Re}^{0.5}}\right)$$

$$\mathrm{Min} = 4\,10^{-5} \qquad \mathrm{Max} = 1$$

Entrainment in dense currents

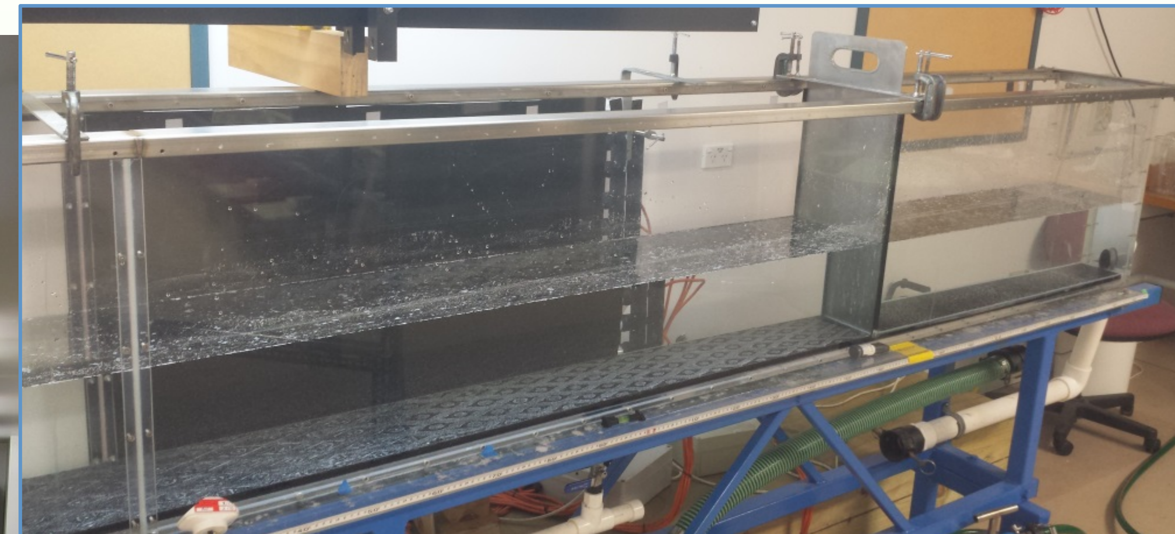

UC UNIVERSITY OF CANTERBURY
Te Whare Wānanga o Waitaha
CHRISTCHURCH NEW ZEALAND

Gravity current: Experiment

Channel height: 20 cm
Reynolds number: ~9,000

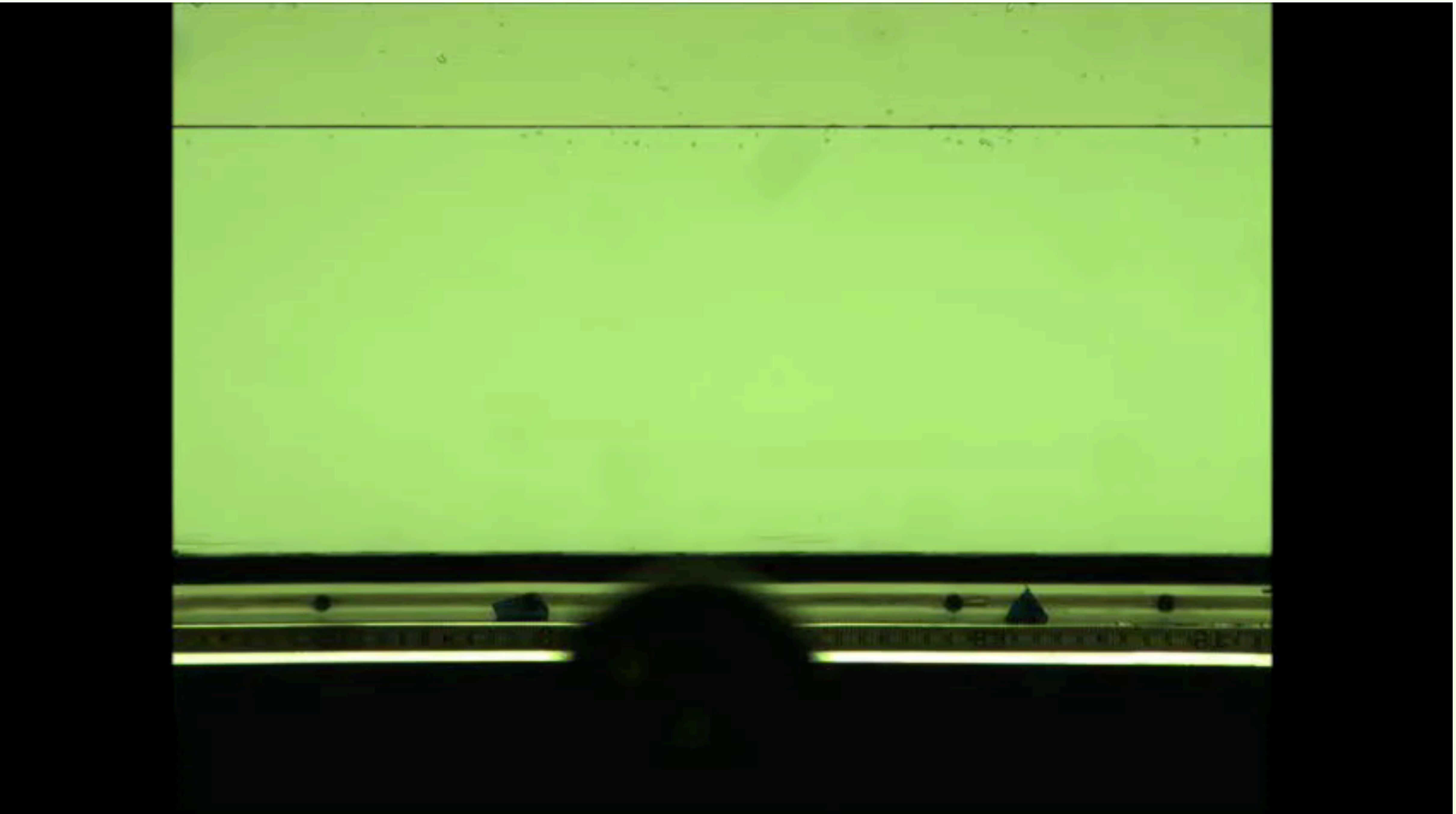

Spanwise-averaged density field

Channel height: 20 cm
Reynolds number: ~9,000

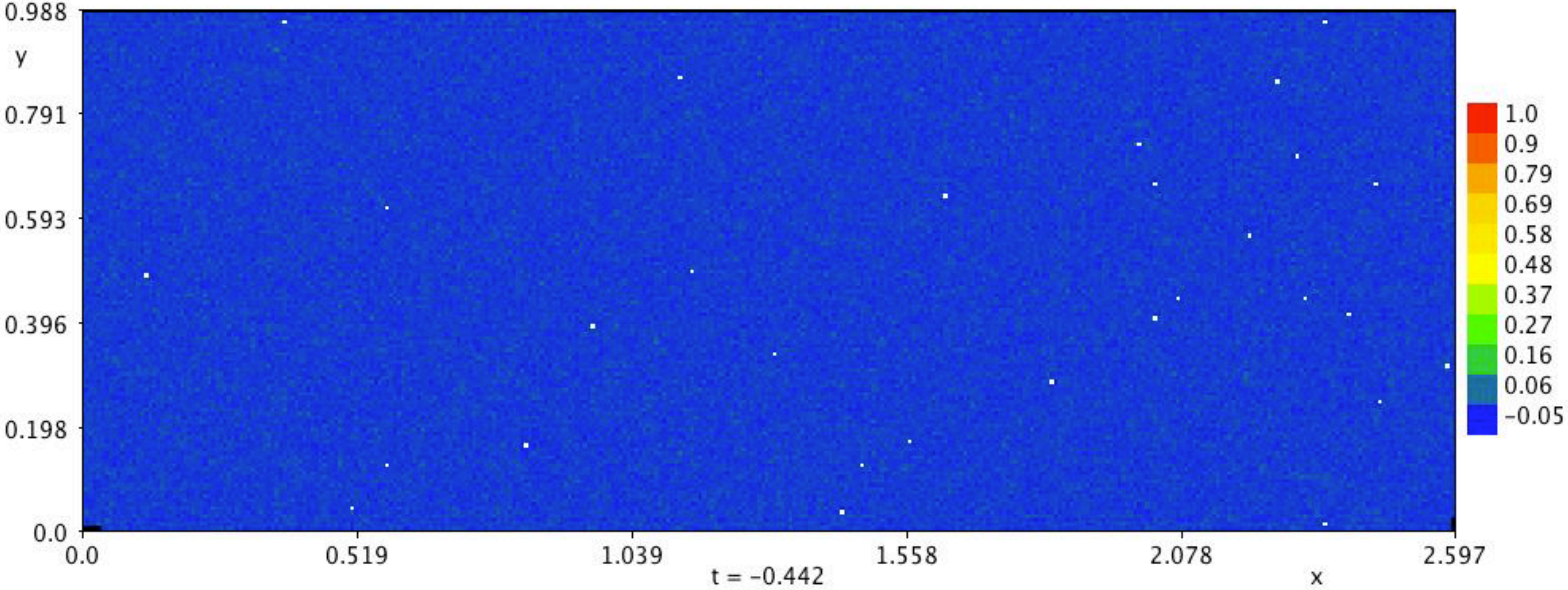

DNS: Spanwise-averaged density field

Reynolds number: ~2,200

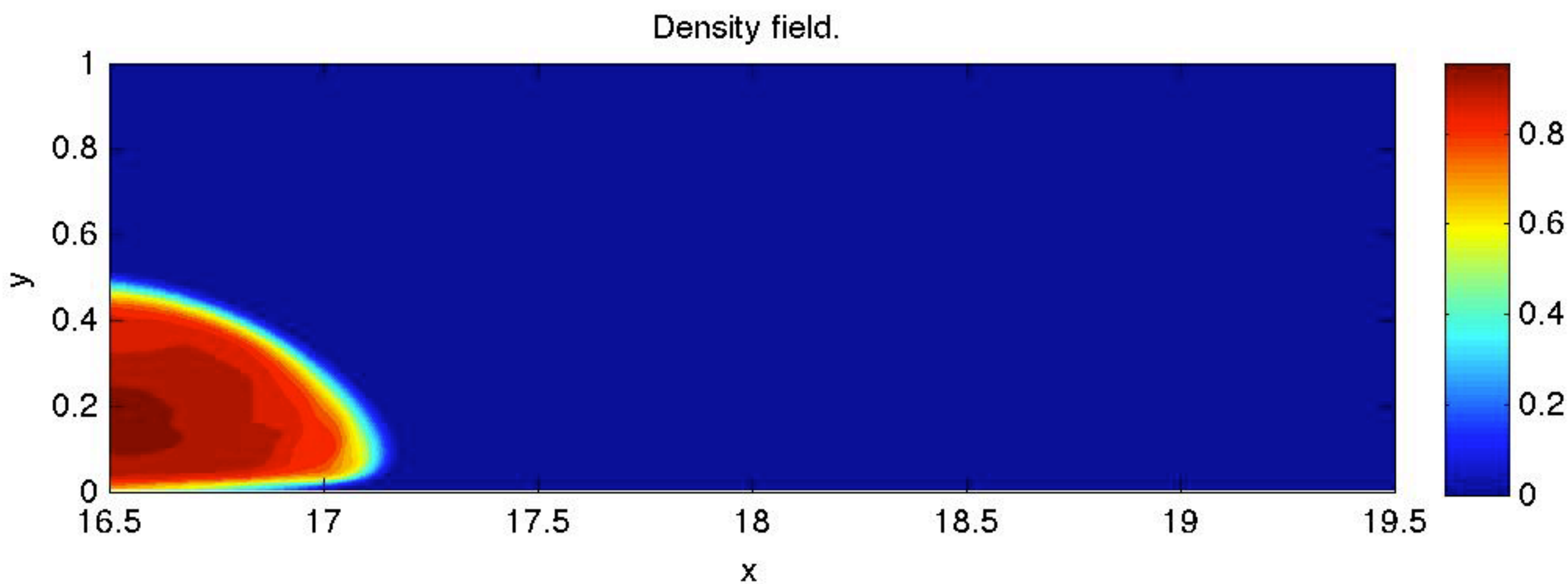

DNS

Reynolds number: ~2,200

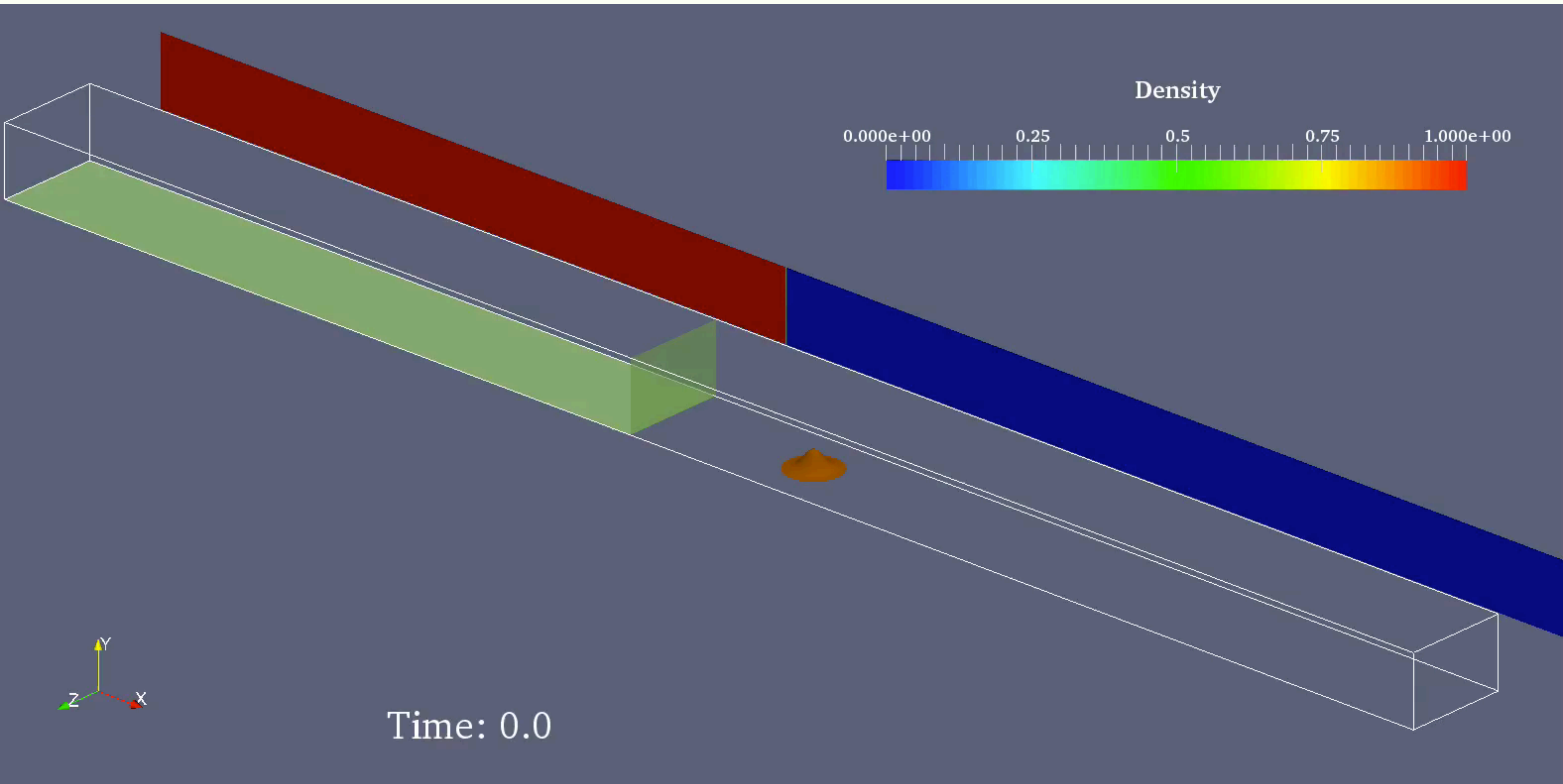

Density field: Experiments

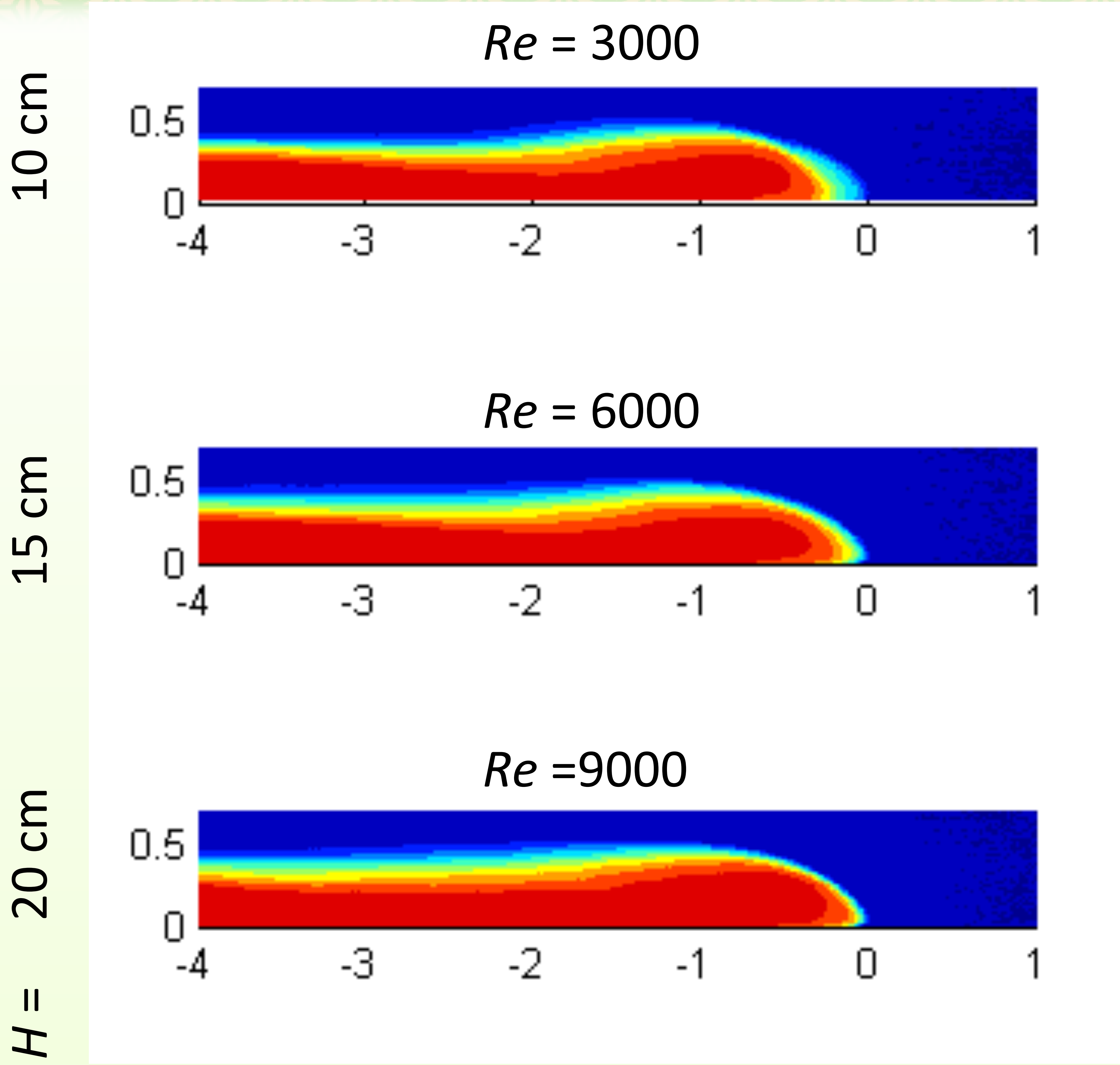

Horizontal velocity field

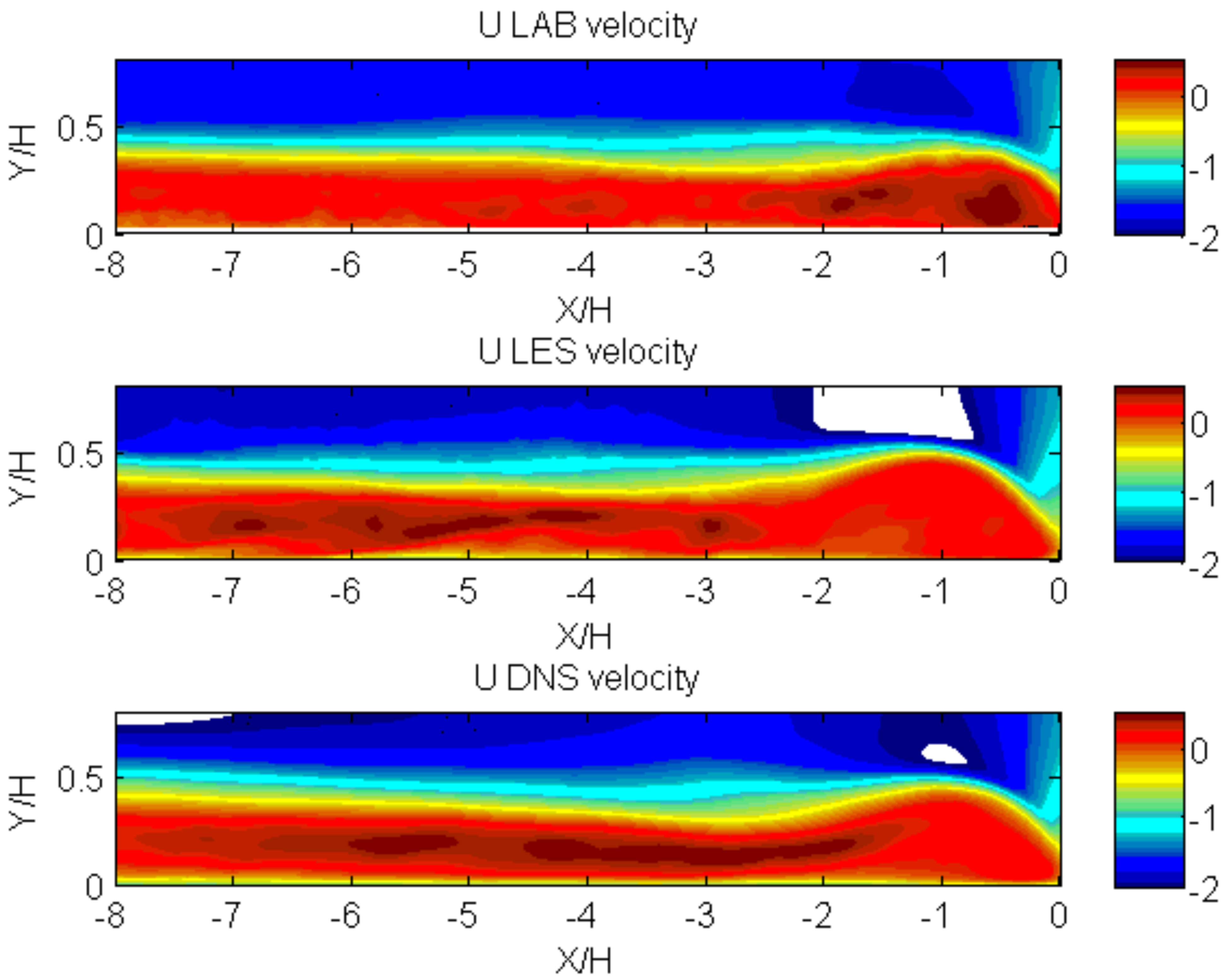

Vertical velocity field

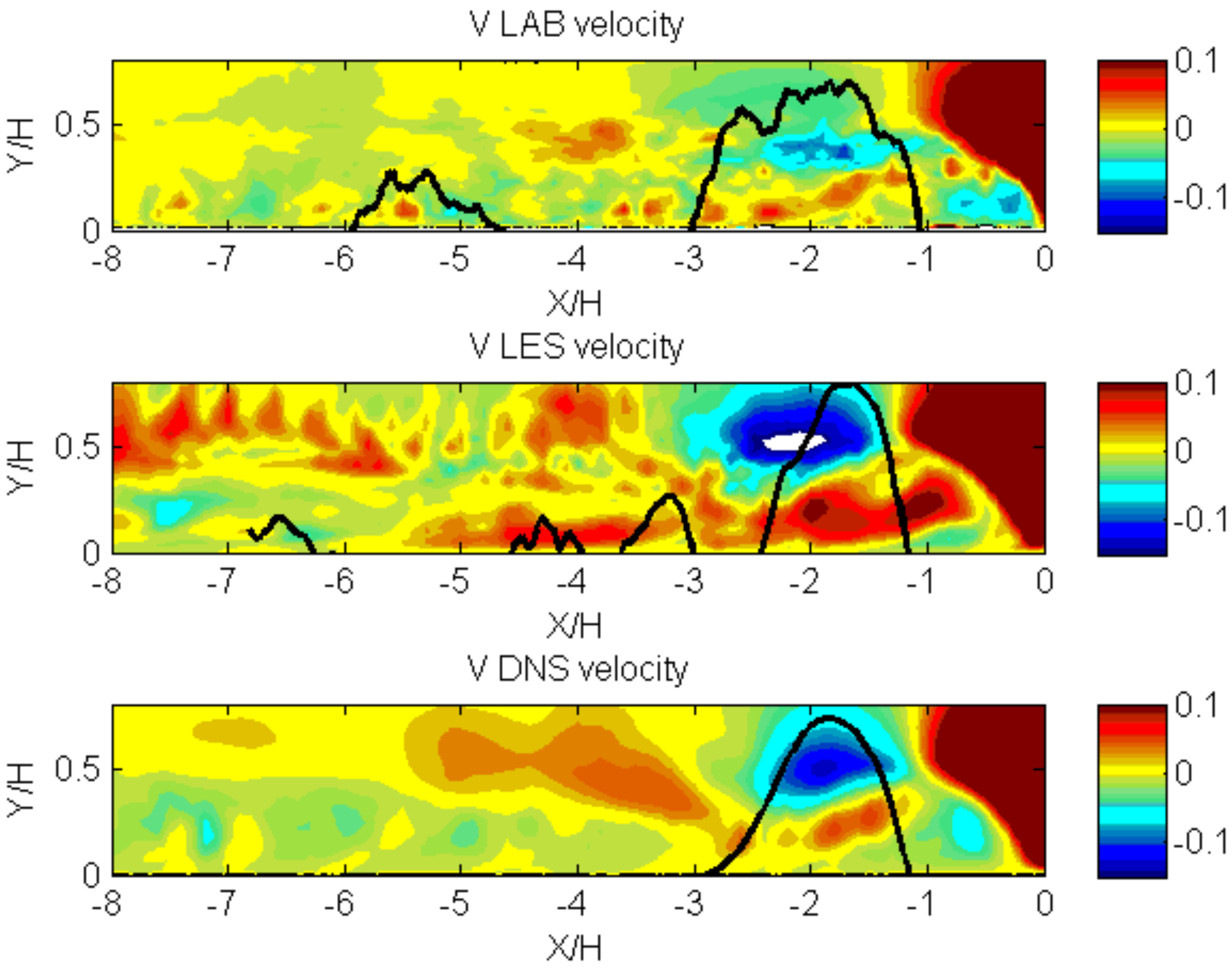

Vertical velocity field

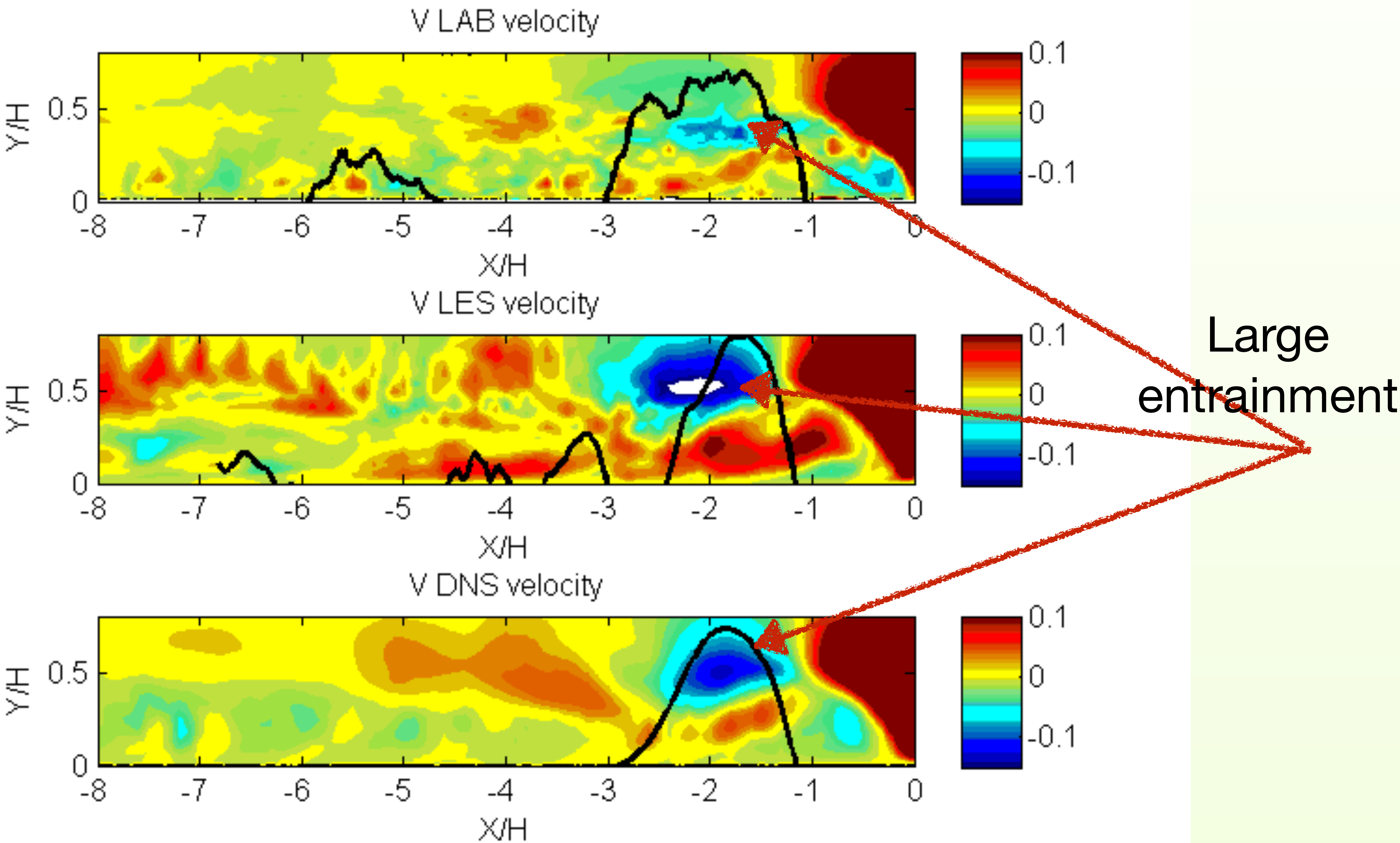

Average velocity

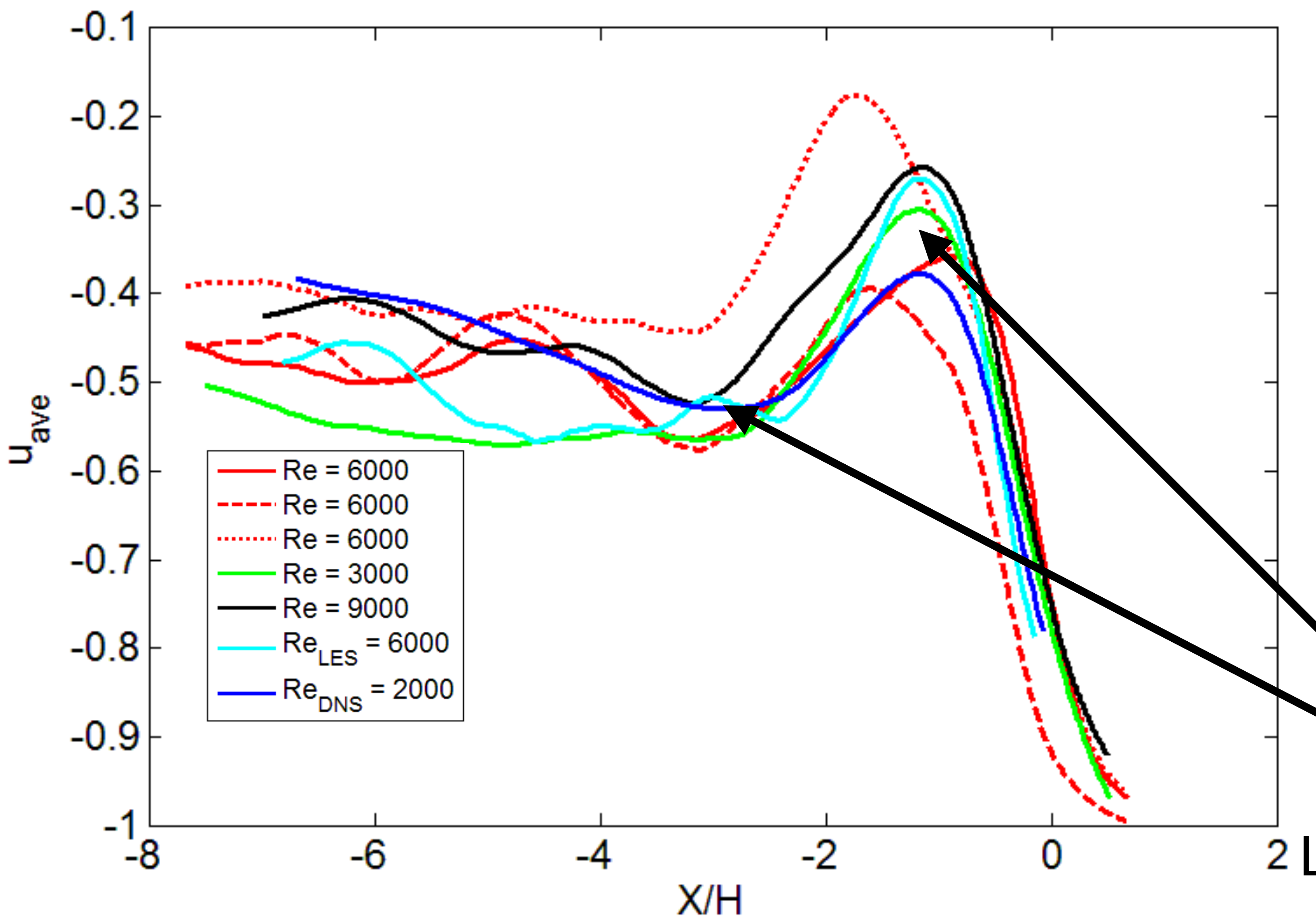

Locations: do not seem to depend strongly on Reynolds number

Entrainment coefficient

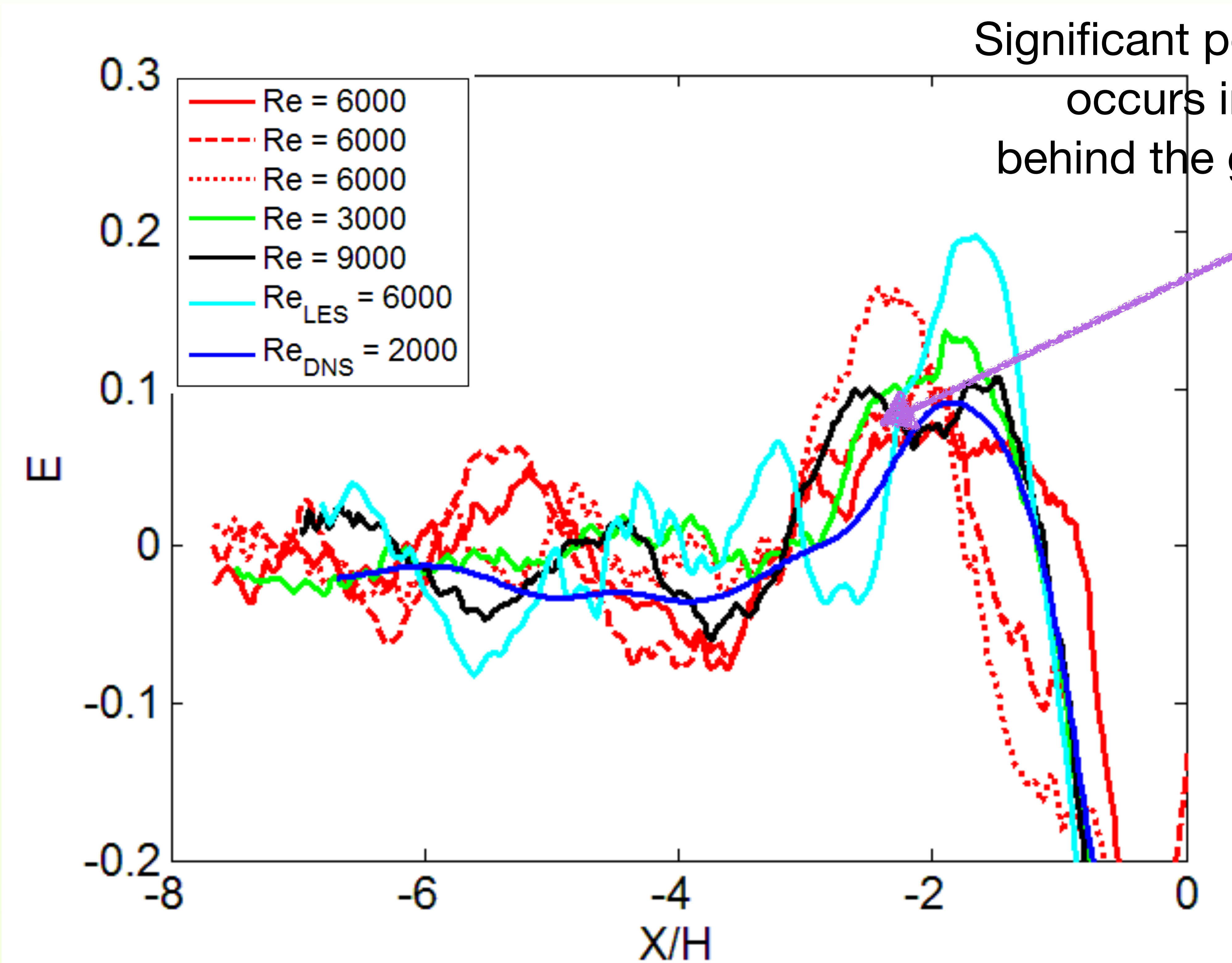

Significant portion of entrainment occurs in this region, i.e. behind the gravity current head

Summary

- Non-uniform entrainment behavior into gravity current body
- It does not depend strongly on Reynolds number
- Strong entrainment behind the gravity current head: O(5) gravity current height
- Good agreement observed: DNS, LES and experiments

Acknowledgment

- Community Surface Dynamics Modeling Systems (CSDMS): Beach HPC
- Janus supercomputing facility: National Science Foundation (award number CNS-0821794) and the University of Colorado at Boulder and is a joint effort of the University of Colorado Boulder, the University of Colorado Denver and the National Centre for Atmospheric Research
- The Epic@iVec supercomputing facility is part of the Pawsey Centre project of the iVec Institute, Australia

Mike Hollingsheads, http://stormandsky.com/